Bi-specific Aptamers mediating Tumour Cell Lysis

Vom Fachbereich Chemie der Technischen Universität Darmstadt
zur Erlangung des akademischen Grades eines
Doctor rerum naturalium (Dr. rer. nat.)
genehmigte

Dissertation

vorgelegt von
M.Sc. Molekulare Biotechnologie
Achim Boltz
aus Gießen

Referent:	Professor Dr. Harald Kolmar
Korreferenten:	Professor Dr. H. Ulrich Göringer
	Professor Dr. Günter Mayer
Tag der Einreichung:	27. Januar 2011
Tag der mündlichen Prüfung:	12. April 2011

Darmstadt 2011

D17

Die vorliegende Arbeit wurde unter der Leitung von Herrn Prof. Dr. Harald Kolmar am Clemens-Schöpf-Insitut für Organische Chemie und Biochemie der Technischen Universität Darmstadt sowie bei MerckSerono in Darmstadt von April 2008 bis Dezember 2010 angefertigt.

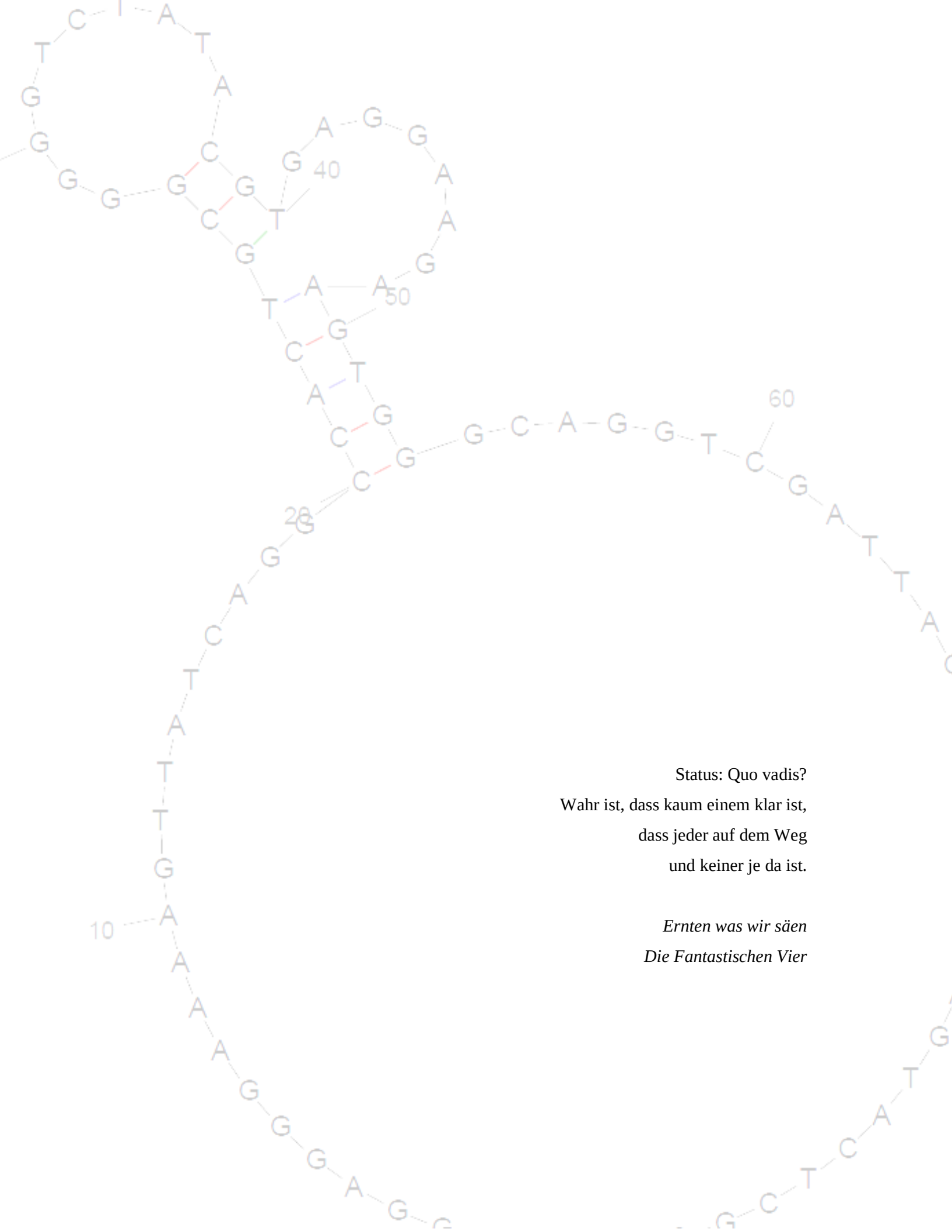

Status: Quo vadis?
Wahr ist, dass kaum einem klar ist,
dass jeder auf dem Weg
und keiner je da ist.

Ernten was wir säen
Die Fantastischen Vier

TABLE OF CONTENTS

1 ABSTRACT

1.1 Zusammenfassung

Das Ziel der vorliegenden Arbeit ist die Entwicklung bi-spezifischer DNA Aptamere, die den auf Tumorzellen überexprimierten Tyrosinkinase-Rezeptor c-Met sowie den auf Natürlichen Killerzellen exprimierten Fcγ-Rezeptor IIIα (CD16α) gleichzeitig binden und dadurch eine spezifische Lyse von diesen Tumorzellen vermitteln sollen. Vergleichbare Antikörper-vermittelte zelluläre Zytotoxizität (*antibody-dependent cellular cytotoxicity*, ADCC) stellt einen Wirkungsmechanismus Antiköper-basierter Tumortherapien dar. An Tumorzellen gebundene therapeutische Antikörper rekrutieren dabei Natürliche Killerzellen, die eine Lyse der Krebszellen auslösen. Vorteile von Aptameren im Vergleich zu therapeutischen monoklonalen Antikörpern können eine einfache Selektion, kostengünstige und uniforme Synthese sowie geringe oder keine Immunogenität sein.

Es wurden CD16α spezifische DNA Aptamere mittels SELEX (*systematic evolution of ligands by exponential enrichment*) isoliert, die spezifisch und mit hoher Affinität (6 – 195 nM) an rekombinantes und auf Natürlichen Killerzellen exprimiertes CD16α banden. Selektierte c-Met spezifische DNA Aptamere zeigten ebenfalls hohe Spezifität und Affinität (91 pM und 11 nM) zu rekombinantem und zellulär präsentiertem Zielprotein. Je zwei optimierte CD16α und c-Met spezifische Aptamere wurden mit Linkern unterschiedlicher Zusammensetzungen und Längen in 24 Varianten verknüpft. Die Erhaltung der ursprünglichen Bindungseigenschaften und eine gleichzeitige Bindung an beide Zielproteine konnte in biochemischen Assays belegt werden. Fünf bi-spezifische Aptamere vermittelten zelluläre Zytotoxizität, die abhängig von der Aptamerkonzentration und der Menge an Effektorzellen war. Verdrängung eines bi-spezifischen Aptamers durch den die CD16α-Bindung kompetierenden Antikörper 3G8 führte zum Rückgang der Aptamer-vermittelten Zelllyse und bestätigte damit den postulierten Wirkmechanismus. Ein bi-spezifisches Aptamer vermittelte Lyse von humanen GTL-16 Magen- und EBC-1 Lungen-Tumorzellen.

Die vorliegenden Ergebnisse zeigen zum ersten Mal die Erzeugung einer zusätzlichen Effektorfunktion durch Verknüpfung zweier unterschiedlicher Aptamere. Durch Austausch des Tumor-spezifischen Aptamers könnte dieses Konzept einfach und schnell zur Therapie von unterschiedlichen Tumoren verwendet werden.

1.2 Abstract

The aim of the work presented herein is the development of bi-specific DNA aptamers simultaneously binding to tumour cell overexpressed receptor tyrosine kinase c-Met and Fcγ receptor IIIα (CD16α) on Natural Killer (NK) cells to mediate specific tumour cell lysis. Comparable antibody-dependent cellular cytotoxicity (ADCC) plays a pivotal role in antibody-based tumour therapies. Tumour-bound therapeutic antibodies recruit Natural Killer cells via their Fc receptors and induce specific lysis of tumour cells. In comparison to therapeutic monoclonal antibodies, potential advantages of aptamers are a facile selection, cost-effective and uniform synthesis as well as no to low immunogenicity.

CD16α specific DNA aptamers were isolated by SELEX (systematic evolution of ligands by exponential enrichment) that bound with both high specificity and affinity (6 – 195 nM) to recombinant and NK cell expressed CD16α. Selected c-Met specific DNA aptamers showed high affinity (91 pM and 11 nM) and specificity to recombinant and cellular presented target protein as well. Two aptamers of each selection were optimised and coupled applying linkers of varying compositions and lengths to yield 24 constructs. Bi-specific aptamers that retained suitable binding properties and displayed simultaneous binding were applied in functional ADCC assays. Five bi-specific aptamers mediated cellular cytotoxicity dependent on aptamer- and effector cell concentration. Displacement of a bi-specific aptamer from CD16α by the competing antibody 3G8 reduced aptamer-dependent cytotoxicity and hence confirmed the proposed mode of action. A bi-specific aptamer mediated specific lysis of human gastric and lung tumour cells, GTL-16 and EBC-1, respectively.

These results represent the first gain of an effector function by coupling of two distinct aptamers to generate an anti-tumour effective molecule. A facile exchange of the tumour-specific aptamer to target other surface tumour markers could broaden the concept of aptamer-dependent cellular cytotoxicity to therapies of further tumour species.

2 INTRODUCTION

2.1 Aptamers

Aptamers (derived from aptus, *latin*: fitting, and meros, *greek*: area) are single stranded DNA or RNA oligonucleotides that bind to molecules of nearly all classes. Their well defined and rigid tertiary structure allows both a specific and high affinity molecular recognition (Figure 1). Reported aptamer targets range from inorganic components and small organic molecules, nucleic and amino acids to carbohydrates, peptides, proteins and even complex structures as tissues, spores or live parasites (Homann and Goringer, 1999; Stoltenburg *et al.*, 2007). Aptamers bind to their targets through a combination of factors including complementarity in shape, stacking interactions between aromatic compounds and the nucleobases of the aptamers, electrostatic interactions between charged groups, or hydrogen bondings (Patel *et al.*, 1997; Hermann and Patel, 2000). These interactions enable aptamers to disrupt protein-protein-interactions. Since many properties can be compared to their antibody analogues, aptamers are also called "chemical antibodies". They can vary from 15 to over 80 nucleotides in length resulting in apparent molecular mass of ca. 5 – 25 kDa. Aptamers can be produced by polymerase chain reaction (PCR; Mullis *et al.*, 1986) with subsequent strand separation for DNA or transcription for RNA aptamers, respectively, *in vivo* synthesis (Umekage and Kikuchi, 2006; Suzuki *et al.*, 2010) or usually by well established and cost-effective solid phase synthesis.

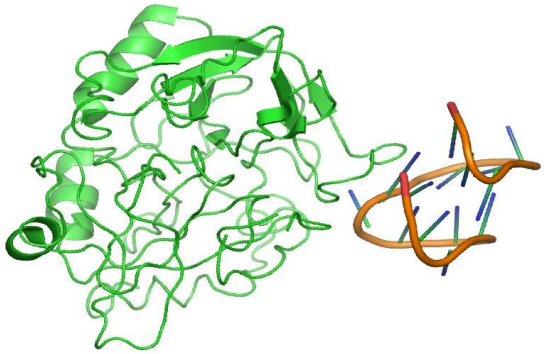

Figure 1: Crystal structure of a DNA aptamer bound to thrombin.

A DNA aptamer (backbone orange, nucleobases green-blue) is specifically folded and binds to the target protein thrombin (green) among others by complementarity of shape. Modified from PDB entry 1HUT (Padmanabhan *et al.*, 1993).

Aptamers have been selected with high affinities and specificities to their targets, enabling the differentiation, for example, between caffeine and theophyllin or between ATP and AMP (Jenison *et al.*, 1994; Sazani *et al.*, 2004). Affinities are often comparable to those observed for antibodies: most K_D values are in the low nanomolar to picomolar range. Aptamers can be selected in the SELEX process (systematic evolution of ligands by exponential enrichment, described in more detail in chapter 2.4.2), and in contrast to most poly- or monoclonal

antibodies selection methods, SELEX is an *in vitro* process independent of animals or cell lines (Tuerk and Gold, 1990). Thus, SELEX can be applied under non-physiological conditions and selection of aptamers against toxic target molecules or non-immunogenic molecules is possible. Furthermore, SELEX can be successfully applied to the isolation of aptamers that address complex structures such as cells or whole tissues without proper knowledge of target structures (Shamah *et al.*, 2008). The multitude of different targets used in SELEX experiments (Stoltenburg *et al.*, 2007) indicates that the selection of aptamers is possible for virtually any target. However, published aptamer work also reveals certain limitations of aptamers and some general prerequisites for a potential target to successfully select aptamers (Klussmann, 2006). Target molecules should be present in sufficient amount and with high purity. Target features that improve chances for successful aptamer selection are positively charged groups, the presence of hydrogen bond donors and acceptors and aromatic compounds (Rimmele, 2003). The aptamer selection is more difficult for targets with largely hydrophobic character and for negatively charged molecules (e.g. containing phosphate groups or a low isoelectric point). Aptamers are relatively unstable in biological fluids, but different strategies such as chemical modifications (Keefe and Cload, 2008; chapters 2.3 and 2.4.1) can lead to significantly improved stabilities. Finally, high-affinity aptamers were not, until now, as widely available as antibodies, but taking into account the time investment in antibody research as compared to aptamers, it seems as if this area is catching up rapidly.

2.2 Bi-valent aptamers

Aptamers are mainly selected to bind in a monovalent manner to their respective target. Applications vary from specific detection of targets for diagnostic purposes (Baldrich *et al.*, 2004) to molecular alteration of target functions such as competitive or allosteric enzyme inhibition (Bock *et al.*, 1992). A few studies have engaged in creation of bi- or oligo-valent aptamers mostly to enhance their affinity by avidity. Müller and colleagues fused two thrombin aptamers binding different epitopes via a 15dA-nucleotide linker resulting in a ~10-fold higher affinity and increased enzyme inhibition (Muller *et al.*, 2007; Muller *et al.*, 2008). This effect was also independently demonstrated using phosphoramidite spacers (Kim *et al.*, 2008) or with hybridisation-ligation-based multivalent circular aptamers (Di Giusto and King, 2004). Similarily, aptamers with up to four binding entities showed improved anticoagulant activitiy due to increased stability and avidity (Di Giusto *et al.*, 2006). Moreover, a group of

related DNA aptamers inhibiting HIV-1 reverse transcriptase (RT) were combined via either a single nucleotide or a hexaethylene glycol linker and inhibited primate RT with low nano-molar IC_{50} values (Michalowski *et al.*, 2008). In addition, bi-specific aptamers have been developed to capture different ligands in diagnostic applications (Tahiri-Alaoui *et al.*, 2002).

An interesting example of converting a single receptor binding aptamer into a receptor agonist by hybridisation of two aptamer copies to a polyethylene glycol linked tandem oligo was shown by Dollins (2008). Systemic delivery of this bi-valent aptamer which binds OX40, a member of the TNF receptor family, induced various specific cellular activation responses. Hybridisation was also used by the same laboratory to create bi-valent aptamers that costimulated a $CD8^+$ T cell receptor resulting in tumour growth inhibition in mice (McNamara *et al.*, 2008). Even tetrameric aptamers were constructed that showed enhanced bioactivity (Santulli-Marotto *et al.*, 2003). While some studies state that constant regions in selected aptamers do not contribute to the tertiary structure (Cowperthwaite and Ellington, 2008) and hence would be available for hybridisation and dimerisation, other examples show that any part of the sequence can be critical and also extensions can alter aptamer folding and properties (Li *et al.*, 2009). Taken together, coupling approaches require exact characterisation of the tolerance of additional or endogenous hybridisation sequences for each aptamer. Not only can two aptamers be coupled but Mallikaratchy and colleagues added a functional group to a cell-surface specific aptamer for stimulated release of chemical effector molecules at the cell surface (Mallikaratchy *et al.*, 2009).

2.3 Aptamers as therapeutic agents

As the view of regulatory mechanisms in cells has broadened to include not only interactions of proteins to proteins but also to nucleic acids, oligonucleotides have emerged as a promising class of binding molecules for analytical purposes and as biopharmaceuticals (Burke and Nickens, 2002). Some approaches to target a disease at the genetic level are antisense technology, RNAi, ribozymes, immunostimulatory nucleotides via CpG-motifs as well as aptamers (Kaur and Roy, 2008). For the latter one, several applications can be considered: inside the cell, aptamers can affect gene-regulation (Sen, 2008); by binding to cell surfaces, they can specifically modulate target activity and trigger activation or inhibition signals, making therapeutic applications feasible (Cullen and Greene, 1989; Burmeister *et al.*, 2006; Que-Gewirth and Sullenger, 2007; Scherer *et al.*, 2007; McNamara *et al.*, 2008); finally, aptamers can be applied in ligand-based targeted therapies to specifically deliver cytotoxic

payloads to tumour cells. Several tumour specific aptamers exist that could be utilised in such a way (reviewed in Das *et al.*, 2009; Ferreira *et al.*, 2009; Orava *et al.*, 2010). An interesting variant of this concept is the aptamer-mediated delivery of nucleotide based effector molecules: one folded aptamer domain is coupled to a siRNA in one single oligonucleotide strand that can induce internalisation and subsequent downregulation of essential proteins (Chu *et al.*, 2006; McNamara *et al.*, 2006; Cerchia *et al.*, 2009; Dassie *et al.*, 2009; Zhou *et al.*, 2009b). Since the whole molecule comprises nucleic acids only, no to low immunogenicity can be anticipated. Aptamers directed to targets of therapeutic interest are reviewed by Keefe *et. al.*, 2010. Another area of research that is being actively pursued and decribed in more detail elsewhere is the application of aptamers for *in vivo* diagnostics and imaging (Hicke *et al.*, 2006; Tavitian *et al.*, 2009 ; Kim *et al.*, 2010).

On the therapeutic front, aptamers have made tremendous progress leading to the first approved drug Macugen (pegaptanib sodium) in 2007 (Que-Gewirth *et al.*, 2007). Many promising approaches are persued in pre-clinical development (Cerchia *et al.*, 2002; Nimjee *et al.*, 2005; Burmeister *et al.*, 2006; Lee *et al.*, 2006; Scherer *et al.*, 2007; Ferreira *et al.*, 2008; Shaw *et al.*, 2008) and many are already in clinical trials only a few years after the inception of the technology (Bates *et al.*, 2009; Keefe *et al.*, 2010). Several characteristics of aptamers render them a suitable molecule class for therapeutical approaches, offering specific competitive advantages over antibodies and other protein-based formats. One major advantage is a high probability of an absence of immunogenicity. Aptamers display low to no immunogenicity when administered in preclinical doses 1000-fold greater than doses used in animal and human therapeutic applications (White *et al.*, 2000). Microarray studies found only mild transcriptional responses of unintended effects upon the cellular innate immune response (Di Giusto *et al.*, 2006). Immune responses to oligonucleotide-based therapeutics could be triggered intrinsically merely by activation of Toll-like receptor 9 (TLR9) that is localised only intracellularly and recognises non-methylated CpG sequences of double-stranded DNA (Ulevitch, 2004). Other TLRs (such as TLR3, TLR7, and TLR8) are involved in recognition of double- and single-stranded RNAs that is putatively decreased when modified nucleotides are applied. TLR activation can trigger the release of IFN-α and other cytokines that can result in either systemic side effects or an eligible local inflammation (Ulevitch, 2004). Whereas the efficacy of many monoclonal antibodies can be severely limited by immune responses against the administered antibodies, it is difficult to elicit neutralising antibodies to aptamers (Pendergrast *et al.*, 2005). Although the immune response to DNA aptamers in humans remains to be determined in more detail major immunogenicity

of aptamers is not anticipated. In addition, high affinity and selectivity is achievable; aptamers are chemically robust; after denaturing by heat or denaturants, they intrinsically regenerate easily within minutes and can be stored for up to one year at room temperature as lyophilized powders, thus exhibiting a very long shelf-life.

Natural nucleic acids exhibit poor pharmacokinetics, primarily due to nuclease degradation and renal clearance. Both limitations can be overcome by appropriate chemical modifications: Unmodified aptamers are degraded in serum by a combination of endonucleases, 5'-3' and 3'-5'exonucleases whose activity can be blocked by chemical modifications such as 2'-hydroxy-, 2'-methoxy- and/or 2'fluoro-substitutions (Zinnen *et al.*, 2002). 3'-3'- (Shaw *et al.*, 1991; Kasahara *et al.*, 2010) or 5'-caps such as polyethylene glycol (PEG) as well as cyclisation (Di Giusto *et al.*, 2004) prevent exonuclease degradation, but even then aptamers must have molecular weights greater than approximately 60 kDa to avoid renal clearance. While several strategies such as protein-aptamer complexation, tagging with cholesterol or attachment to liposomes have been applied, most work concentrated on PEGylation. When PEG is covalently attached the aptamer half-life in animals is extended from minutes to up to 12 hours in monkeys (Healy *et al.*, 2004; Pendergrast *et al.*, 2005).

Aptamers can be administered by either intravenous or subcutaneous injection. With high solubility (>150 mg/ml) and comparatively low molecular weight (aptamer with 5 – 25 kDa to antibody with 150 kDa), a weekly dose of aptamer can be delivered by injection in a volume of less than 0.5 ml. Aptamer bioavailability via subcutaneous administration is greater than 80 % in monkey studies (Tucker et al., 1999). There is also evidence that nucleic acid-based therapeutics can be dosed topically and via pulmonary administration (Pendergrast *et al.*, 2005).

Aptamers can be produced by chemical synthesis with high accuracy and reproducibility so that no variation between different production batches is anticipated (Kawazoe et al., 1996). They are purified by stringent denaturing conditions ensuring very high purity. While the capital cost of a large-scale protein production plant is enormous, a single large-scale synthesizer can produce upwards of 100 kg of oligonucleotide per year and requires a relatively modest initial investment. The cost of goods for DNA aptamer synthesis at the kilogram scale is estimated at $500/g, comparable to that for highly optimised antibodies (Pendergrast *et al.*, 2005).

Finally, folded aptamers can be inactivated by disrupting their structure with the addition of short complementary antisense sequences that can be easily produced. When aptamers are applied as therapeutic agents these antisense antidotes can safely and selectively control the drug activity (Rusconi *et al.*, 2002; Rimmele, 2003; Que-Gewirth *et al.*, 2007). For example, since it is important that the effects of anticoagulants be reversible, using aptamers could improve the safety of these widely used drugs (Oney *et al.*, 2007; Muller *et al.*, 2008; Chan *et al.*, 2008).

Although these factors could be beneficial in drug development, there are potential risks as well. Half life extension technology is currently limited to PEGylation, oral application is currently not achievable, and there is no experience with slow release formulations in an aptamer context.

2.4 Aptamer selection

The SELEX process (systematic evolution of ligands by exponential enrichment) aims to select for rare nucleic acid sequences with unique properties from very large random sequence oligonucleotide libraries and was first described in 1990 (Tuerk *et al.*, 1990; Robertson and Joyce, 1990; Ellington and Szostak, 1990). SELEX is based upon an iterative process of *in vitro* selection and amplification (Figures 2 and 3).

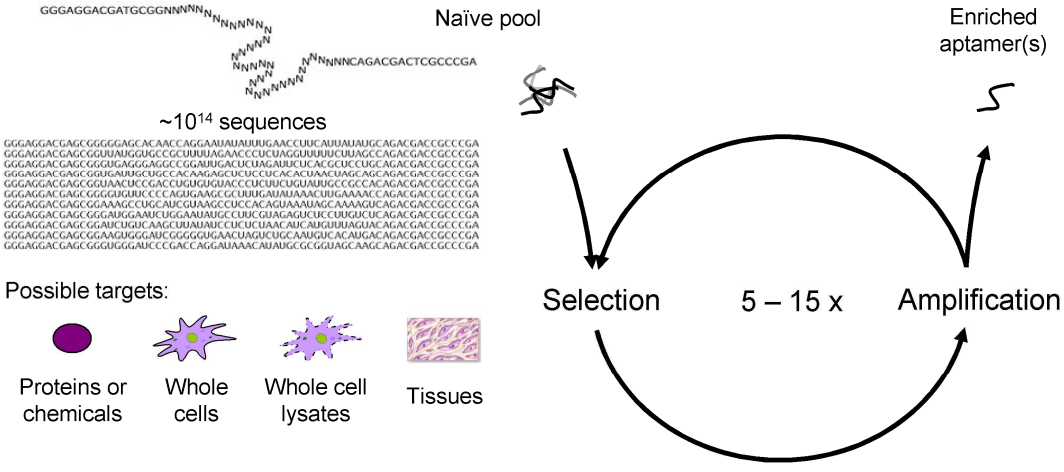

Figure 2: Scheme of the SELEX procedure.

Aptamers are selected from libraries of up to ~10^{14} unique sequences targeting essentially all molecule classes up to complex samples such as tissues. SELEX is carried out in an iterative process of selection and amplification of bound aptamers: A naive pool is allowed to bind target molecules, unbound aptamers are removed and bound sequences are amplified by PCR. After reconverting PCR products to single stranded aptamers, the pre-selected pool is again used for selection. After several rounds of SELEX, pools are sequenced and enriched aptamers are characterised for specific binding and additional criteria of interest. Modified from Shamah *et al.*, 2008.

Combinatorial libraries based on replicable biopolymers such as nucleic acids offer the convenience of iterative molecules' amplification, making the screening process fast and easy. There are currently hundreds of publications about the selection of aptamers and their applications, which reflect the great interest for this research field and its enormous potential for pharmaceuticals as well as research and diagnostic tools.

2.4.1 Aptamer pools and compositions

The SELEX process begins with a random sequence library obtained from combinatorial chemical synthesis of DNA. Template molecules typically contain constant 5'- and 3'-terminal sequences that flank an internal region of 25 - 40 random nucleotides with each member in a library being a linear oligomer of a unique sequence. The complexity or the molecular diversity of a library is dependent on the number of randomised nucleotide positions. Theoretically, a library containing a 40-nucleotide random region is represented by $4^{40} = 1.2 \times 10^{24}$ individual sequences. However, in practice, a standard scale (1 μmole) synthesis followed by purification and PCR amplification will yield approximately 2×10^{14} individual template molecules. The success of finding unique and rare molecules that interact with a target equals the diversity of the libraries applied. The degree of molecular diversity present in random sequence oligonucleotide libraries supersedes that of other combinatorial libraries (except for ribosomal display) such as peptide libraries used for phage display, indicating that a complexity of 10^{14} is sufficient for most SELEX experiments (cf. Habicht and Siegemund, 2002 and Stoltenburg et al., 2007).

Natural nucleic acids can exhibit short serum half-lives due to nuclease degradation and rapid renal clearance that is dependent on their respective molecular masses (chapter 2.3). Nuclease degradation varies strongly (half lives were reported to be 0.5 - 42 h, Schmidt *et al.*, 2004; Peng and Damha, 2007) and depends on the primary sequence (Choi *et al.*, 2010), a rigid compact structure rather than exposed termini (Di Giusto *et al.*, 2004) and on nucleotide concentration (Shaw *et al.*, 1995). Degradation can be reduced by modifications to the 2'-hydroxyl position (Zinnen *et al.*, 2002), the nucleobase or the backbone of potential RNA substrates (reviewed in Mayer, 2009). SELEX is performed in this work using pools containing nucleotides with modifications at the 2'-position on the ribose (Keefe and Cload, 2008). In particular, the following pools containing their respective nucleotide chemistries could be used (next page):

DNA	all 2'-deoxynucleotides
dCmD	2'-deoxy-C, 2'O-methyl A, U, G
rRfY	2'-ribo A, G, 2'fluoro-C and U
rGmH	2'-ribo-G, 2'O-methyl A, U, C
mRfY	2'O-methyl A, G, 2'fluoro-C and U
MNA	all 2'-O-methyl

2.4.2 Systematic evolution of ligands by exponential enrichment

During SELEX, a random oligonucleotide library is incubated with a target of interest at a given temperature, usually 37 °C in selections for therapeutical binders. SELEX can be carried out against proteins or whole cells, even if the exact target is not exactly known (Figure 2). However, it must be noted that the probability of success in selection correlates with the quality of the applied target. During incubation of target and SELEX pool, a very small fraction of individual sequences interacts with the target and these sequences are separated from the rest of the library by means of different physical separation techniques. Typically, nitrocellulose filter partitioning is used with protein targets that are retained on nitrocellulose which captures the protein-aptamer complexes (Figure 3).

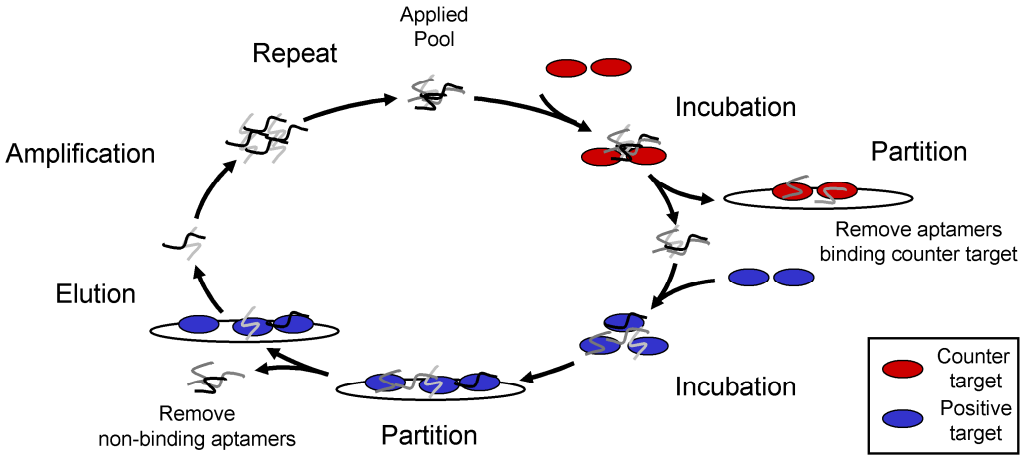

Figure 3: General iterative filter SELEX scheme.

A RNA or DNA aptamer library pool (top) is incubated with the counter target (red circle) and aptamers that do not bind to the counter target are partitioned from the bound molecules on a nitrocellulose filter (white circle). Remaining molecules are then incubated with the positive selection target (blue circle). Aptamer : target complexes are subsequently partitioned by immobilisation on another nitrocellulose filter following washing off non-binding aptamers. Bound molecules are eluted by heat and urea denaturation of target proteins and amplified by PCR. Multiple SELEX cycles can result in aptamers that have high affinity and specificity toward the target. Modified from Shamah *et al.*, 2008.

This method shares the advantage of selection with soluble target protein and was, for example, used in the initial rounds of SELEX against HER3 (Chen *et al.*, 2003). Similarily, magnetic beads can be used for separation purposes e.g. when aptamers bound to biotinylated

target proteins are removed from the solution applying streptavidin-coated beads that are subsequently captured in a magnetic field. In contrast, small molecular targets are generally immobilised on a solid support such as a microtiter plate and non-interacting sequences can be removed easily by a simple washing step. In addition, methods based on capillary electrophoresis, surface plasmon resonance, HPLC, and FACS (Mayer *et al.*, 2010) as well as automated processes have been developed for aptamer selections (Mayer, 2009). Plenty of SELEX procedure modifications have been developed, one of which is Counter-SELEX that generates aptamers that discriminate between closely related structures by introduction of a negative selection step to the related target thereby eliminating aptamers unable to distinguish between the related structures (Kulbachinskiy, 2007; Table 2 in Stoltenburg *et al.*, 2007; Shamah *et al.*, 2008).

If the desired target protein is not available in its soluble or correctly folded form or in the case of cancer tissue the target is unknown, SELEX can also be performed directly on whole cells (Blank *et al.*, 2001; Huang *et al.*, 2009). Since counterselection is mandatory if specific binders need to be enriched, related non-cancer cells or recombinant cell lines can serve for pre-selection to deplete unspecific cell binding aptamers. Library pools are initially incubated with a sufficient amount of related or parental cells to remove aptamers binding off-target. The supernatant is then applied to target-presenting cells and target-specific binders are separated by centrifugation of the cells. If cancer cells are applied directly, a related cell line has to be chosen for pre-selection (Sefah *et al.*, 2010). Separation of bound aptamers can be achieved by simple centrifugation of applied target cells as well as fluorescence-activated cell sorting using dye-labelled aptamer pools (Raddatz *et al.*, 2008). Commonly and independent of the separation method, bound aptamers are recovered by denaturation of the protein or cell-aptamer complexes at 95°C releasing conformation-dependent binding aptamers. Different partitioning methods can be applied sequentially to benefit from the respective advantages, e.g. a few initial rounds of filter selection under defined conditions followed by whole cell SELEX in later rounds for enrichment of binders specific to cellular presented target protein (Björn Hock, personal communication).

After selection and partitioning, the population of sequences bound to the target is amplified to obtain an enriched library to be used for the next selection cycle. Amplification is easily performed by PCR and the resulting double stranded DNA (dsDNA) can be reconstituted in high amounts with different methodologies for DNA or RNA. A dsDNA PCR product of a DNA aptamer already contains the desired aptamer strand, but must be prepared as a single

stranded oligonucleotide. Introduction of a pH-labile RNA base 3' of the 3'-primer enables an alkaline induced strand break and the aptamer can be separated by size in a subsequent electrophoresis. RNA aptamers can be transcribed from a dsDNA template that was elongated 5' by a T7 polymerase recognition site during PCR (Figure 4) (Keefe *et al.*, 2008).

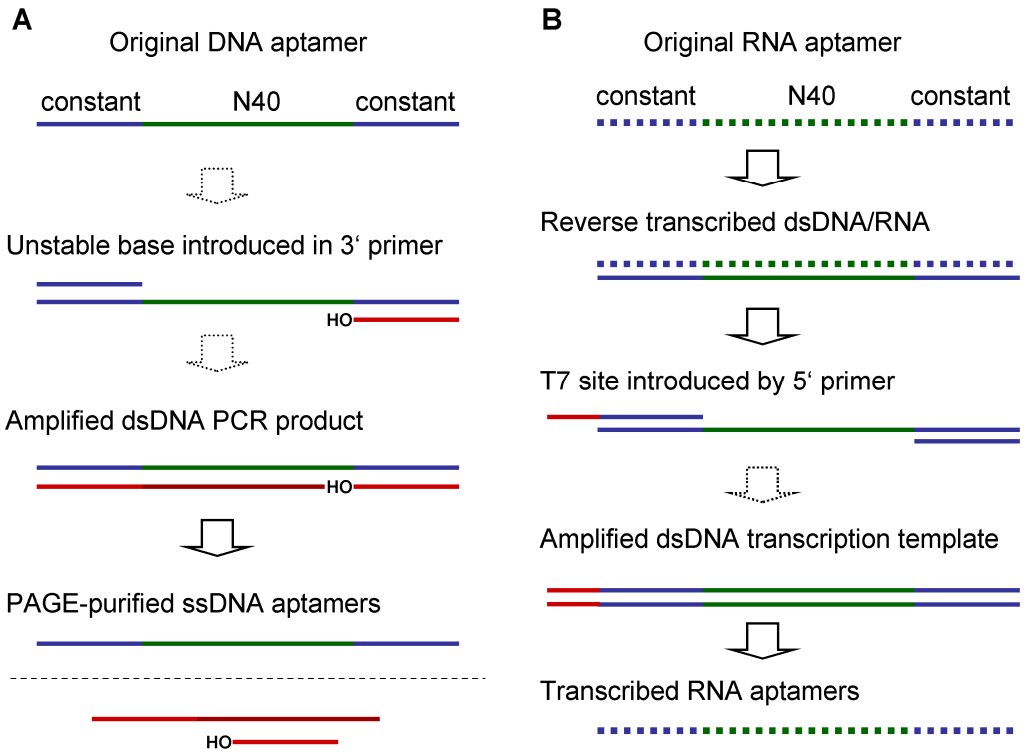

Figure 4: Scheme of both, DNA or modified RNA, aptamer production.

A, DNA aptamers can be amplified by PCR, introducing a pH-labile RNA base in the 3' primer. Strand separation can be accomplished under alkaline conditions followed by PAGE purification. B, RNA aptamers (dashed lines) need to be reversely transcribed to DNA templates that are subsequently applied in a PCR introducing a T7 binding site within the 5' primer. This dsDNA template enables RNA aptamer transcription finalised by purification via PAGE. Modified from Keefe and Cload (2008).

The progress of the enrichment of high-affinity binders can be determined by monitoring the cycle numbers needed to re-amplify applied aptamer pools to a fixed threshold, or by carrying out binding analysis in a dot blot assay (chapter 4.3.9). Once affinity saturation or constant high amounts of eluted binders are achieved, the enriched library is cloned and sufficient clones are sequenced to obtain information on diversity and enrichment of the aptamer pool. Individual sequences are further characterised on the basis of their ability to bind to the target with high affinity and specificity.

2.4.3 Candidate screening

Usually, between 5 and 20 clones per enriched pool are expected to be characterised. Each clone can be synthesised or transcribed and then assayed for target binding using a nitrocellulose dot blot assay (chapter 4.3.9)(Yarus and Berg, 1970). Target protein and radio-labelled aptamers are incubated to allow binding and subsequently partitioned on nitrocellulose and PVDF membranes. Complexes of target protein and bound aptamer are immobilised on nitrocellulose whereas unbound aptamers are captured by the PVDF membrane. The affinity can be calculated using the ratio of bound to unbound aptamer for each target protein dilution. Target specific aptamers that meet the affinity criterion (*e.g.*, K_D of 1 nM – 100 nM determined by dot blots) are then analysed in further cellular and functional assays.

2.5 Hepatocyte growth factor receptor (c-Met)

Receptor tyrosine kinases (RTKs) are key regulators of critical cellular processes such as cell growth, differentiation, neovascularisation, and tissue repair. In addition to their importance in normal physiology, aberrant expression of RTKs can contribute to the development and progression of many types of cancer (Eder *et al.*, 2009).

Hepatocyte growth factor receptor (HGF-R) or mesenchymal epithelial transition factor (c-Met) is a membrane RTK that is essential for embryonic development (Bladt *et al.*, 1995; Andermarcher *et al.*, 1996; Takayama *et al.*, 1996) and wound healing. It is normally expressed by cells of epithelial origin (Tsarfaty *et al.*, 1994; Gentile *et al.*, 2008). The primary single chain precursor protein is post-translationally cleaved to produce the alpha and beta subunits, which are disulfide linked to form the mature receptor (Figure 5). c-Met is a multi-domain protein comprised of an extracellular SEMA-domain (of 450 amino acids, a variant of semaphorin axon guidance proteins) that consists of two subunits α and β that are present after proteolytic cleavage, a cysteine-rich domain and at least four immunglobuline like domains (each of 90 amino acids consisting of two β-sheets). A transmembrane domain is followed by its intracellular kinase domain that includes several tyrosines and a serine capable of cross-phosphorylation upon dimerisation (Birchmeier *et al.*, 2003; Eder *et al.*, 2009). Binding of the natural ligand hepatocyte growth factor (HGF, or scatter-factor, SF) induces receptor dimerisation leading to phosphorylation of the cytoplasmic tyrosine kinase domain at two positions (Y1234 and Y1235) and activation of c-Met-mediated signalling (Longati *et al.*, 1994). In addition to c-Met homodimers, other receptors and cell surface proteins can interact

with c-Met that contribute to signal cross talk and oncogenesis (Lai *et al.*, 2009). Aberrant c-Met signalling due to dysregulation of the receptor or overexpression of HGF induces several biological responses that collectively give rise to „invasive growth“ (Eder *et al.*, 2009; Stellrecht and Gandhi, 2009).

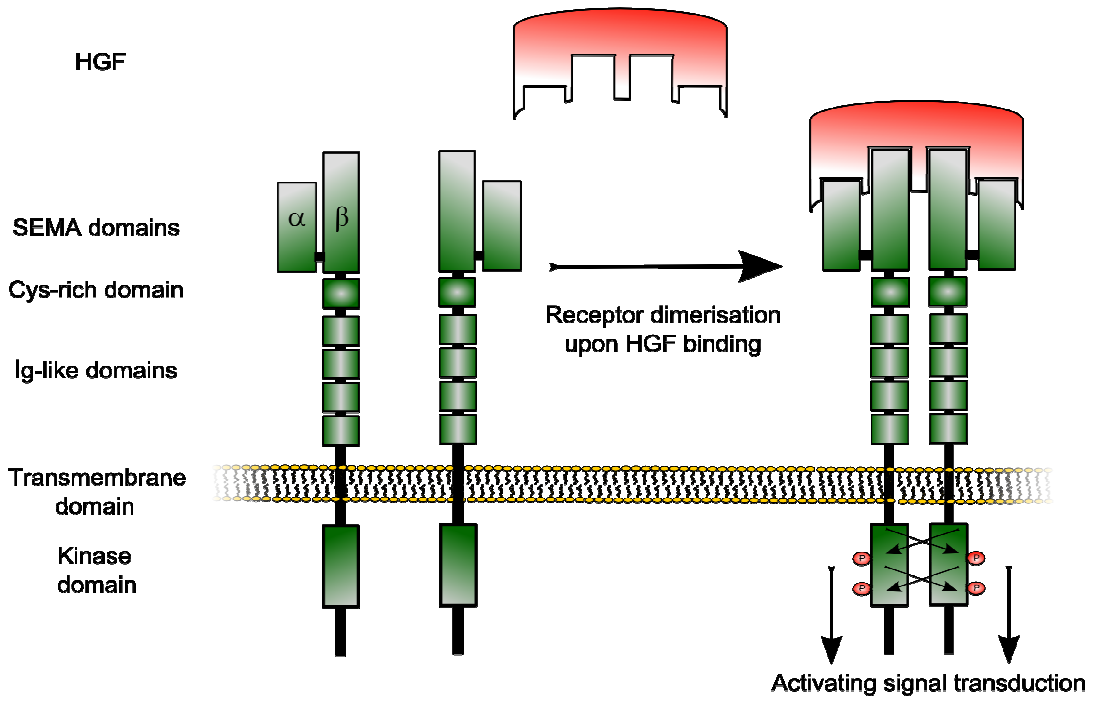

Figure 5: Domain structure and cellular function of c-Met.

c-Met (green) consists of two peptide chains, α and β refer to the subunits of the receptor that are present after proteolytic cleavage. Two SEMA domains build the receptor surface for binding of the ligand HGF (red), followed by one Cys-rich and four Ig-like domains, concluded by an intracellular kinase domain with five phosphorylation sites. HGF binding leads to dimerisation that induces kinase auto cross-phosphorylation of intracellular domains resulting in docking of activating signal transduction proteins and a variety of growth stimulatory responses.

Aberrant c-Met activation or over-expression in cancer correlates with poor prognosis, because of c-Met induction of tumour growth, formation of new blood vessels (angiogenesis) that supply the tumour with nutrients, and metastasis. c-Met is deregulated in many types of human malignancies, including cancers of lung, ovary, kidney, liver, stomach, breast, and brain (Birchmeier *et al.*, 2003;Comoglio *et al.*, 2008 ; Cipriani *et al.*, 2009; Eder *et al.*, 2009). In many of these tumour types, both receptor and ligand are overexpressed relative to surrounding tissue and overexpression of HGF induces tumourigenesis in mice (Takayama *et al.*, 1997). Gene amplification (Christensen *et al.*, 2005) or activation of HGF/c-Met signalling *in vivo* promotes cell invasiveness and triggers metastases (Zhang *et al.*, 2003),

whereas inhibition of receptor or ligand functions reverses cancer phenotypes such as motility, invasion, proliferation and in vivo tumor growth (Toschi and Janne, 2008).

This extensive evidence of a pathological role for c-Met in cancer and understanding of its contribution in several diseases generated considerable interest in c-Met and HGF as targets in cancer drug development. The three main approaches of c-Met-selective anticancer drug development included antagonism of ligand-receptor interaction, inhibition of the intracellular kinase activity, as well as blocking the cytoplasmic interaction between the receptor and its specific effector molecules. Recently, susceptibility of c-Met overexpressing cell lines to antibody-dependent cellular cytotoxicity (ADCC) was shown *in vitro* by applying two antibodies in parallel (van der Horst *et al.*, 2009). Preliminary clinical results of several c-Met antagonists such as monoclonal antibodies and small-molecule tyrosine kinase inhibitors have been encouraging (Toschi *et al.*, 2008; Eder *et al.*, 2009).

2.6 FcγRIII (CD16)

Although cellular receptors for immunoglobulins (FcRs) were identified nearly 40 years ago, their central role in the immune response was discovered only in the last decade. FcRs are key immune regulatory receptors, connecting humoral immune responses to cellular effector mechanisms. FcR functions include setting thresholds for B cell activation, regulating the maturation of dendritic cells, and coupling the exquisite specificity of the antibody response to innate effector pathways, such as phagocytosis, antibody-dependent cellular cytotoxicity (ADCC), and the recruitment and activation of inflammatory cells (Nakamura *et al.*, 2008). Receptors for all classes of immunoglobulins have been identified, including FcγR (IgG), FCεRI (IgE), FcαRI (IgA), FcμR (IgM) and FcδR (IgD) (Powell and Hogarth, 2008). The three existing FcγR subclasses, their polymorphisms and respective affinities to all IgGs have been studied in detail by Bruhns and colleagues (van Sorge *et al.*, 2003; Bruhns *et al.*, 2008). While FcγRI (CD64) is the only high affinity receptor, FcγRIII (CD16, P08637) is the only FcR expressed on natural killer cells (NK cells).

CD16α is an intermediate affinity receptor for polyvalent immune-complexed IgG1 and IgG3, but not for IgG2 and IgG4 (Vance *et al.*, 1993; Edberg and Kimberly, 1997; Bruhns *et al.*, 2008). CD16α is involved in phagocytosis, secretion of enzymes and inflammatory mediators, antibody-dependent cytotoxicity and clearance of immune complexes (Ravetch and Perussia, 1989; Nimmerjahn and Ravetch, 2006). Human CD16α is a 50 - 70 kDa type I

transmembrane activating receptor expressed by NK cells, δγ-T cells, monocytes, and macrophages. NK cell-derived CD16α runs at 50-55 kDa on non-reducing SDS-PAGE, un-glycosylated at 25 kDa (De *et al.*, 1994), whereas monocyte-derived CD16α runs at 68 kDa. The CD16 cDNA encodes 254 amino acids including a 16 amino acid signal sequence, a 191 amino acid ECD with two C2-type Ig-like domains and five potential N-glycosylation sites, a 22 amino acid transmembrane (TM) sequence and a 25 amino acid cytoplasmic domain. The isoelectric point (pI) of CD16α is 6.6 (Edberg *et al.*, 1990). CD16 binds the lower hinge region of IgG (Figure 6).

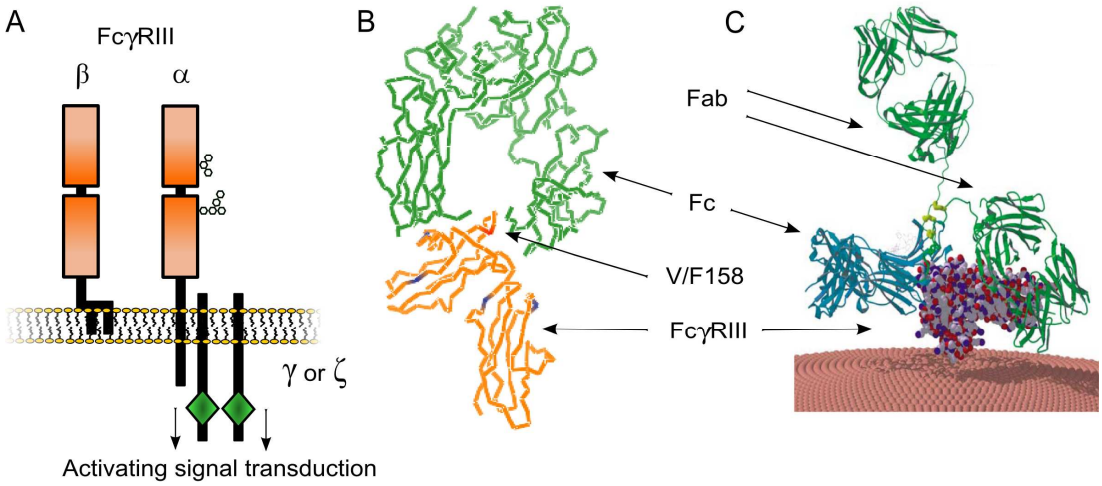

Figure 6: Scheme, crystal structure and antibody binding of CD16.

A, the two isoforms of CD16 comprise two extracellular Ig-like domains. CD16β is a glycosylphosphatidyl inositol-anchored protein, whereas CD16α as type I integral protein includes transmembrane and cytoplasmic domains. Since these domains are not capable of cell signalling, Fcγ or CD3ζ chains in complex with CD16 as hetero- or homo-dimers transduce activating signals via an immunoreceptor tyrosine based activating motif (ITAM, indicated as green rhombus). CD16 is a glycoprotein that exhibits cell type specific glycosylation patterns. B, crystal structure of CD16 (orange) bound to the Fc portion of an IgG1 (green, modified from PDB entry 1T83). The two Ig-like domains of CD16 can be distinguished. Amino acids differing between isoforms α and β are indicated in blue (with F187S out of structure). CD16α alloforms varying directly at the surface of the Fc binding site in position 158 (red) exhibit different affinity to IgG. C, a whole antibody (green and blue) is bound by CD16 near the hinge region between Fc and Fab portions (Radaev and Sun, 2001, modified).

Two allotypes exist in human CD16α, V158 and F158, which lead to higher and lower affinity, respectively. This can influence susceptibility to autoimmune diseases or response to therapeutic IgG antibodies (Wu *et al.*, 1997; chapter 2.8). In addition, glycosylation patterns, electrophoretic mobility and binding affinity differ between NK cell and monocyte CD16α (Edberg *et al.*, 1997). CD16α surface expression, but not correct folding, requires interaction of an accessory chain, either the common Fcγ-chain or CD3ζ (Lanier *et al.*, 1989; Kim *et al.*, 2003). A fine balance between inhibitory and activating receptors tightly regulates NK cell activation (Zompi and Colucci, 2005; Bryceson *et al.*, 2006a). Activation of receptors occurs

also through γ or ζ chains that contain immunoreceptor tyrosine-based activation motifs (ITAMs). Adapter proteins propagate strong activation signals through recruitment of tyrosine kinases Syk and z-associated protein of 70 kDa (ZAP-70), the same signal pathway as in CTL activation (Vivier *et al.*, 2004; Bryceson *et al.*, 2006a).

The isoform FcγRIIIβ (CD16β) is highly related to CD16α, sharing 97% amino acid sequence identity within the extracellular domain (ECD), but CD16β is a glycosyl-phosphatidyl-inositol-(GPI)-linked receptor expressed on human neutrophils and eosinophils. The differing 5 amino acids are found throughout the extracellular domain and result in a low affinity of CD16β to Fc (Anderson *et al.*, 1990; Vance *et al.*, 1993). Divergent residues do not occur in one specific paratope on CD16, but are located over the whole structure (Figure 6 B).

The ECD of both CD16α and CD16β can be proteolytically cleaved and retain binding activity in their soluble forms (Harrison *et al.*, 1991; Li *et al.*, 2007). Soluble FcγRIII (sCD16) can be detected in normal plasma and is increased in inflammatory diseases such as rheumatoid arthritis and in coronary artery diseases. The prevalent soluble isoform is neutrophils-derived sCD16β (Huizinga *et al.*, 1994), and the amount of sCD16α is negligible in healthy persons. Upon an immune reaction, sCD16α concentrations increase proportional to CRP, although it remains unclear whether this is due to increased cleavage or overall NK cell population (De *et al.*, 1994).

The monoclonal mouse antibody 3G8 (targeting both CD16α and CD16β) binds near or in the Fc-binding domain (Edberg *et al.*, 1997). Affinities to soluble CD16α were measured for IgGs with 560 and 710 nM for IgG3 or IgG1, respectively (Li *et al.*, 2007), 86 nM for 3G8 in a bi-specific scFv and 5.7 nM for monovalent binding of 3G8 (Bruenke *et al.*, 2004).

2.7 Natural Killer Cells

Natural Killer cells (NK cells) are unique in their ability to detect changes in tumour cells in the absence of stimuli and as such can reject tumours directly. Additionally, they can stimulate components of the adaptive immune system to eliminate tumours. 5-20 % of peripheral blood mononuclear lymphocytes (PBMCs) are bone marrow derived NK cells (Wallace and Smyth, 2005). NK cells are usually defined as $CD3^{-}CD56^{+}$ cells and can be further subdivided based on CD56 expression. Usually, 90 % of peripheral blood NK cells are $CD56^{dim}$, whereas $CD56^{bright}$ NK cells are more abundant in secondary lymphoid tissues

(Fauriat *et al.*, 2009). $CD56^{dim}$ NK cells express high levels of CD16 and perforin indicating their cytotoxic potential (Lanier *et al.*, 1986; Fauriat *et al.*, 2009). In contrast, $CD56^{bright}$ NK cells express low levels of or no CD16, have ten-fold lower perforin expression than $CD56^{dim}$ NK cells, and are mainly involved in cytokine-mediated immunoregulation (Fehniger *et al.*, 1999; Shibuya, 2003; Fauriat *et al.*, 2009). $CD16^{+}$ NK cells and γδ-cytotoxic T lymphocytes (CTLs) are less frequent in plasma than αβ-$CD8^{+}$ CTLs, but NK cells possess a variety of effector mechanisms enabling them to mount a potent anti-tumour response.

NK cell function is regulated by a complex balance of inhibitory and activating signals that allow them to selectively target and kill cells that display an abnormal pattern of cell surface molecules while leaving normal healthy cells unharmed (Wallace *et al.*, 2005; Terunuma *et al.*, 2008). Besides certain ligands for natural cytotoxicity and cell-bound IgG1+3 eliciting ADCC as described, NK cells can be activated by TNFα, IFNα, IFNβ, IL-12 secreted by activated macrophages (Murphy *et al.*, 2008) and especially IL-2 (Carson *et al.*, 2001). On the other hand it is not surprising that NK cells, with their unique role in bridging innate and adaptive immunity, are a potent sources of cytokines and chemokines that can among other functions can recruit T cells (Roda *et al.*, 2006). Since clinical data has been difficult to assess directly, most information is derived from cell-based methods which is then correlated to clinical studies. Activated NK cells release lymphotactin (LTN/ATAC; Hedrick *et al.*, 1997), regulated on activation normal T cell expressed and secreted (RANTES; Dorner *et al.*, 2004), macrophage-inflammatory protein 1 (MIP-1a/b; Taub *et al.*, 1995), interleukin 8 (IL-8; Somersalo *et al.*, 1994; Roda *et al.*, 2006), IFN induced protein 10 (IP-10, Murphy *et al.*, 2008) and macrophage-derived chemokine (MDC; Roda *et al.*, 2006) that can all induce T cell and most additional NK cell recruitment. Primarily, direct or monokine induced interferon γ (IFNγ or MIG) triggers $CD4^{+}$ TH_1 cell activation, monocyte and neutrophil ADCC (Reali *et al.*, 1994; Roda *et al.*, 2007), as well as increased tumour MHC I presentation leading to higher immunogenicity and modulation of FcγR towards activating receptors (Desjarlais *et al.*, 2007). With this plethora of secondary effects, NK cells could still have several, not yet fully understood effects on tumour growth as well as activation of further immune effector cells.

2.8 ADCC and NK cell recruitment in cancer therapy

Antibody-dependent cellular cytotoxicity (ADCC) originating from the interaction of Fc fragments of antibodies with Fcγ receptors (FcγR) plays a pivotal role in the therapy of various tumours (Sliwkowski *et al.*, 1999; Desjarlais *et al.*, 2007; Taylor *et al.*, 2008). Antibodies bound to the surface of tumour marker over-expressing cells are recognised by CD16 and other Fc receptors on NK cells. This induces a cross-linking of respective receptors leading to strong adhesion, granule polarisation, formation of a lytic synapse, and degranulation, all of which induce apoptosis of the tumour cell (Figure 7; Zompi *et al.*, 2005). NK cells share a common killing mechanism with $CD8^+$ cytotoxic T lymphocytes (Trapani and Smyth, 2002; Bossi and Griffiths, 2005) via a lytic synapse and use two major mechanisms to induce target cell apoptosis: the granule exocytosis pathway (Trapani *et al.*, 2002) and the death receptor pathway (Smyth *et al.*, 2003). While the perforin/granzyme granule exocytosis pathway has been extensively studied, less is known about NK cell death receptor function. The major proteins involved in the granule exocytosis pathway are perforin, a membrane-disruption protein, and a family of structurally related serine proteases known as granzymes (Smyth and Trapani, 1995). Cytolytic functions of granzyme B include at first activation of caspase 3 that cleaves the inhibitor of caspase-activated deoxyribonuclease (ICAD) off CAD which triggers this enzyme to induce DNA fragmentation. Secondly, the BH3-interacting domain death agonist protein (BID) is cleaved to truncated BID (tBID) inducing cytochrome c release from mitochondrial membranes leading to the formation of the apoptosom that activates several caspases that finally induce apoptosis (Murphy *et al.*, 2008).

The specific CD16α polymorphism F158 to V158 enhances its affinity for IgG1 and is associated with improved clinical outcome in tumour patients treated with therapeutical antibodies (Cartron *et al.*, 2002; Desjarlais *et al.*, 2007; Taylor *et al.*, 2008). In particular, RTK specific antibody-based therapeutics such as cetuximab (Erbitux) which targets EGF receptor or trastuzumab (Herceptin) which binds HER2/neu on cancer cells have been shown to elicit ADCC *in vivo* and *in vitro* (Roda *et al.*, 2007; Lopez-Albaitero *et al.*, 2009; Mani *et al.*, 2009). Several studies revealed ADCC as one major mode of action of antibody-based therapeutics and stimulated more interest in how to mobilise, expand and activate NK cells in humans (Wallace *et al.*, 2005). The importance of NK cells in anti-tumour immunity was also established in tumour models in mice. NK cells can reject a number of tumour cell lines, suppress metastasis and stop the outgrowth of tumours (Kim *et al.*, 2000). Tumour resistance in these mice was associated with an infiltration of innate leukocytes including NK cells,

neutrophils and macrophages into the peritoneum (Cui *et al.*, 2003). Work on insect cells by Bryceson and colleagues revealed that surface-bound antibodies induce lysis by both resting and IL-2-activated NK cells (Bryceson *et al.*, 2006b) and binding of CD16 can induce contact, degranulation and cytotoxicity, but not granule polarisation (Bryceson *et al.*, 2006a). Complementing CD16 functions, lymphocyte function-associated antigen 1 (LFA-1) seems to be the key player in mediating initially strong adhesion with the intercellular adhesion molecule 1 (ICAM-1) on target cells that facilitates polarisation followed by lysis. Taken together, engagement of CD16 may be the most applicable and affordable approach to harnessing NK cells for immunotherapy.

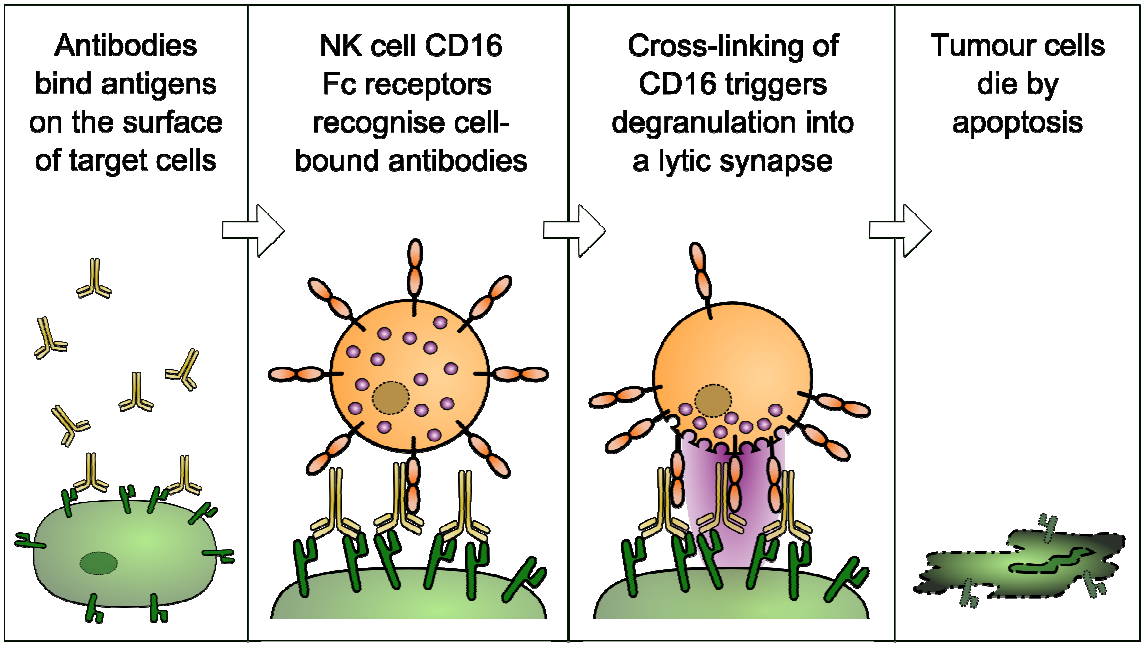

Figure 7: Scheme of antibody-dependent cellular cytotoxicity (ADCC) of NK cells.

The proof of concept for recruitment of NK cells to tumour targets via bi-specific binders was achieved in two laboratories in 1999 by McCall as well as Arndt and colleagues (Arndt *et al.*, 1999; McCall *et al.*, 1999). Scientists of the Fey lab optimised several stabilised bi-specific single-chain Fv (scFv) antibody NK cell recruiting constructs, also by introdution of an antibody-like third binding arm for increased affinity by avidity (Bruenke *et al.*, 2004; Bruenke *et al.*, 2005; Kugler *et al.*, 2010; Singer *et al.*, 2010). Since $CD16^+$ NK cell subsets are involved in cytotoxicity, whereas $CD16^-$ NK cell populations are responsible for cytokine-production (chapter 2.7), targeting CD16 should recruit cytotoxic NK cells without extensive cytokine-release, which is a major side effect of current antibody-based ADCC approaches (Tabrizi and Roskos, 2007).

Since NK cells share a common killing mechanism with $CD8^+$ cytotoxic T lymphocytes and serial killing of one effector cell to several tumour cells has been reported in CTL recruitment (Valitutti and Lanzavecchia, 1997; Bortoletto *et al.*, 2002; Hoffmann *et al.*, 2005). This therapeutic advantage could apply putatively also when recruiting NK cells, possibly due to high tumour specific antigen (TSA) affinity and lower effector specific antigen (ESA) affinity (Bortoletto *et al.*, 2002). On the other hand, as mentioned above, higher affinity could lead to enhanced ADCC. NK cells might also enhance adaptive immunity to tumours in a more indirect way. NK cell-mediated killing of tumour targets could provide increased access to tumour antigens for uptake by dendritic cells (DCs) thereby triggering their maturation. While the links between NK cells and adaptive immunity remain poorly defined at a molecular level, they are clearly important in the generation of effective anti-tumour responses (Wallace *et al.*, 2005).

Transgenic mouse models are available that reproduce the unique pattern of human gene expression for CD16α and β (as well as CD32α and β and CD64α), making *in vivo* studies for proof of concept possible (Li *et al.*, 1996; Nimmerjahn and Ravetch, 2008).

2.9 Further bi-specific therapeutic approaches

Besides efforts at NK cell recruitment, therapeutic approaches to engage the intact immune system via bi-specific molecules were broadened to include other effector cell populations. Constructs consisted mostly of an anti-tumour scFv linked to a second scFv-fragment specific for surface proteins expressed on effector cells such as Bispecific T-cell Engager molecules (BiTEs) (Loffler *et al.*, 2000; Wolf *et al.*, 2005; Baeuerle and Reinhardt, 2009) or triomabs like catumaxomab, a T cell retargeting agent that was approved in the European Union in April 2009 (Chames and Baty, 2009). Potent effector specific antigens (ESAs) besides CD16 are CD3ε on Cytotoxic T-Lymphocytes (CTLs), CD89 (FcαRI) on neutrophils, CD64 (FcγRI) on activated neutrophils, monocytes and macrophages as well as DEC-205 on dendritic cells (Kontermann, 2005; Kellner *et al.*, 2008). Surface proteins that have been chosen as tumour specific antigens (TSAs) so far are recapitulated among others by Das, Kontermann and Schrama (Kontermann, 2005; Schrama *et al.*, 2006; Das *et al.*, 2009).

2.10 Aptamer-dependent cellular cytotoxicity

Enabling ADCC in an aptamer-format could yield therapeutic effects similar to those of antibodies while at the same time sharing the advantages of aptamers such as potentially low or no immunogenicity, uniform and cost-effective production by chemical synthesis, as well as excellent shelf life stability. Since highly related soluble CD16β circulates in plasma and acts as decoy receptor without triggering activation (chapter 2.6), the high selectivity of aptamers to molecules with even very minor differences (Jenison *et al.*, 1994) could be of great advantage in this context: CD16α-specific aptamers would prevent interception of effector molecules by soluble CD16β-decoys. Additionally, therapeutical whole antibodies could support RTK activation by dimerisation upon simultaneous binding of both CDRs, thus acting as agonists (Stellrecht *et al.*, 2009). Bi-specific aptamers on the other hand can only bind in a mono-valent manner to tumour targets, exclusively acting as an antagonist in addition to potential ADCC activity. The adoption of the bi-specific format with aptamers might combine these advantages with the successful strategy of approved antibody-based therapeutics or the BiTE format in clinical trials.

So far, neither CD16α or c-Met specific aptamers nor bi-specific aptamers targeting different proteins for the introduction of additional tumour-effective functions have been published.

2.11 Aim of the work

The work presented herein aims to be a proof of concept for the specific re-localisation of NK cells to tumours by aptamers bi-specific for CD16α and c-Met to elicit "aptamer-dependent cellular cytotoxicity" (Figure 8).

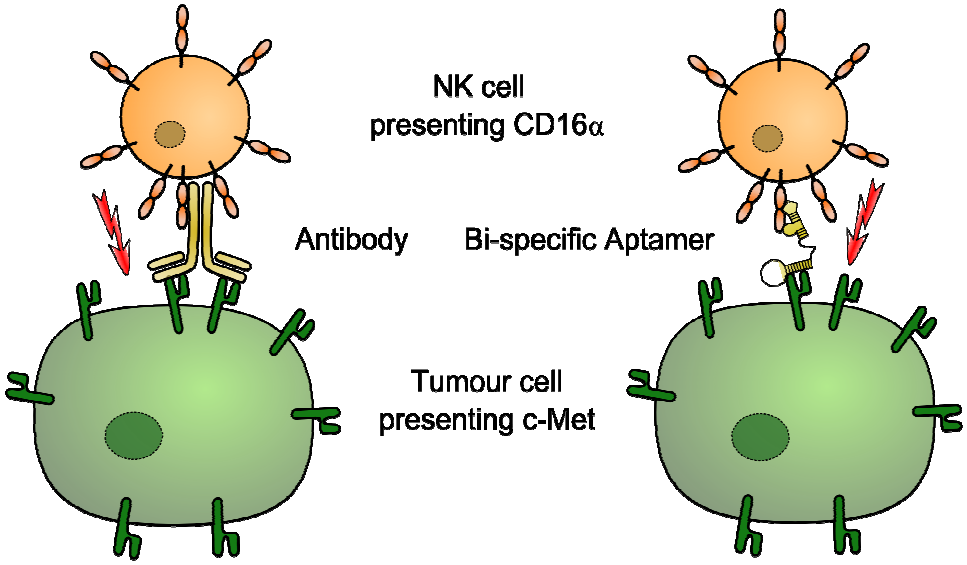

Figure 8: Concept of bi-specific aptamers mediating tumour cell lysis.

Bi-specific aptamers mimick ADCC by recruitment of NK cells via FcγRIIIα / CD16α to tumour cells with c-Met overexpression. A high density of effector molecules at the surface of tumour cells leads to cross-linking of CD16α on NK cells inducing polarisation, formation of a lytic synapse, degranulation and finally specific lysis of the target cells.

Hence, main objectives are the selection of aptamers with high affinity and specificity for cellular expressed CD16α and c-Met via SELEX as well as their characterisation and minimisation. Furthermore, suitable linkers need to be designed that bridge the required distance between both binding entities to elicit target cell lysis, but do not alter aptamer binding characteristics. Finally, functionality of the bi-specific aptamer approach has to be demonstrated in cellular ADCC assays.

3 MATERIAL

3.1 Bacterial strains and cell lines

Bacterial strains

E. coli One Shot TOP10 Competent Cells, C4040-10 Invitrogen, Karlsruhe, Germany

Genotype: F- *mcr*A Δ(*mrr-hsd*RMS-*mcr*BC) φ80*lac*ZΔM15 Δ*lac*X74 *rec*A1 *ara*D139 Δ(*araleu*) 7697 *gal*U *gal*K *rps*L (StrR) *end*A1 *nup*G

Cell lines

Jurkat E6.1	Human leukemic T cell lymphoblast Origin: ECACC 88042803 / ATCC No. TIB-152 Cultivation at 37°C, 5 % CO_2
Jurkat V158	Recombinant transformation of Jurkat E 6.1 with CD16α(V158) at Merck; origin and cultivation as above
Jurkat F158	Recombinant transformation of Jurkat E 6.1 with CD16α(F158) at Merck; origin and cultivation as above
GTL-16	Human gastric adenocarcinoma Origin: Paolo Porporato Novara, Merck KGaA Cultivation at 37°C, 10 % CO_2
MKN-45	Human gastric adenocarcinoma Origin: DMSZ No. ACC 409 Cultivation at 37°C, 5 % CO_2
EBC-1	Human lung squamous cell carcinoma Origin: Health Sc. Res. Resources Bank, JCRB0820 Cultivation at 37°C, 5 % CO_2
NIH-3T3	Mouse embryonic fibroblasts Origin: ATCC No. CRL-1658 Cultivation at 37°C, 10 % CO_2

3.2 Enzymes and proteins

3G8	BioLegend / Biozol, Eching, Germany
3G8-biotin	BioLegend / Biozol, Eching, Germany
3G8-FITC	Jürgen Schmidt, Merck, Darmstadt
3,3',5,5'-Tetramethylbenzidine (1step Ultra TMB)	Pierce/Thermo Scientific, Schwerte, Ger.
aCella-TOX ADCC assay kit	Cell Technol., Mountain View, CA, USA
Antarctic Phosphatase (AP)	New England Biolabs, Beverly, USA
Benzonase	Novagen, Nottingham, UK
Bovine serum albumin (BSA)	Merck, Darmstadt, Germany
Cetuximab (Erbitux)	Merck, Darmstadt, Germany
CD16α(V158)-6His (rhFcγR IIIα-6His)	R&D Systems, Minneapolis, MN, USA
CD16β-6His (rhFcγR IIIβ-6His)	R&D Systems, Minneapolis, MN, USA
c-Met-Fc (rhHGF-R-Fc)	R&D Systems, Minneapolis, MN, USA
cynoCD16α-8His	Merck, Darmstadt, Germany
DNA-dependent T7 RNA polymerase Y639L	PCS DA, Merck, Darmstadt
Fc-CD16α(V158)	PCS Boston, Merck, Rockland, USA
Fc-CD16α(F158)	PCS Boston, Merck, Rockland, USA
Goat anti mouse $F(ab')_2$ PE conjugate	Jackson ImmunoResearch, Suffolk, GB
Goat anti mouse peroxidase conjugate	Jackson ImmunoResearch, Suffolk, GB
Goat anti rabbit peroxidase conjugate	Jackson ImmunoResearch, Suffolk, GB
Goat anti hIgG $F(ab')_2$ FITC conjugate	Jackson ImmunoResearch, Suffolk, GB
Goat anti hIgG $F(ab')_2$ PE conjugate	Jackson ImmunoResearch, Suffolk, GB
MACS BSA stock solution	Miltenyi, Bergisch-Gladbach, Germany
MACS NK cell isolation kit, human	Miltenyi, Bergisch-Gladbach, Germany
muCD16α-Fc (huFc-muFcGRIV-ECD)	Merck, Darmstadt, Germany
Mouse anti penta His antibody	Qiagen, Hilden, Germany
Mouse anti rhHGF-R mAb (c-Met mAb)	R&D Systems, Minneapolis, MN, USA
Ni-NTA-peroxidase conjugate	Qiagen, Hilden, Germany
Rabbit anti human-Fc antibody	Epitomics, San Francisco, CA, USA
Reverse transcriptase (Thermoscript RT)	Invitrogen, Karlsruhe, Germany
Streptavidin-R-phycoerythrin conjugate (SA-PE)	Sigma-Aldrich, Steinheim, Germany
T4 polynucleotide kinase (T4 PNK)	New England Biolabs, Beverly, USA
T7 RNA polymerase Y639L mutant	Merck, Darmstadt, Germany,
Taq DNA polymerase (5 U/µl)	New England Biolabs, Beverly, USA

Trypsin-EDTA	Gibco (Invitrogen), Karlsruhe, Germany
TOPO-TA cloning kit	Invitrogen, Karlsruhe, Germany

Enzymes and proteins originating from Merck, Darmstadt, were produced inhouse at Merck.

3.3 Oligonucleotides

primer M13_for	CCCAGTCACGACGTTGTAAAACG
primer M13_rev	AGCGGATAACAATTTCACACAGG
oligo 5978	GGAGGGAAAAGTTATCAGGC (c.f. Tsang and Joyce, 1996)
oligo 5979	GGAGCGAGTACTCCAAAACTAAT/RiboC
oligo 5980	GACTGTAATACGACTCACTATAGGAGGGAAAAGTTATCAGGC
oligo 5981	GGAGCGAGTACTCCAAAACTAATC
oligo 5977	GGAGGGAAAAGTTATCAGGC$(N)_{40}$GATTAGTTTTGGAGTACTCGCTCC
oligo CLNX	5978-ATGCGCTAGCCGATCGAATCCCGTAGACATTCCGATCGAC-5981
oligo CLNC	AATGAAGGGGCAACTATCGTTAAACAGAACACTCGTCAGCTA CTCGAGGATATTAGCTCCGAACGAACTGCCACAATTCAGAAC GCCTGTCACATTATG

All oligonucleotides were purchased from Eurofins MWG Operon, Ebersberg, Germany, except for CLNC produced at IDT, Leuven, Belgium.

3.4 Chemicals

5x cDNA synthesis buffer	Invitrogen, Karlsruhe, Germany
6x DNA gel loading buffer	Novagen, Nottingham, UK
10x Taq polymerase buffer	NEB, Beverly, New England, USA
100 bp DNA ladder	NEB, Beverly, New England, USA
Ammonium persulfate (APS)	Merck, Darmstadt, Germany
Chloroform:isoamylalcohol 24:1 solution	Sigma-Aldrich, Steinheim, Germany
CleanGel IEF Ultra	Sigma-Aldrich, Steinheim, Germany
Coomassie plus protein assay reagent	Pierce/Thermo Scientific, Schwerte, Ger.
Coomassie R250 tablets	Serva, Heidelberg, Germany
Desoxy ribonucleotide triphosphates (dNTPs)	Novagen, Nottingham, UK
dH_2O	Merck, Darmstadt, Germany
Dithiotreitol (DTT)	Invitrogen, Karlsruhe, Germany
DMEM medium	Gibco (Invitrogen), Karlsruhe, Germany
Dulbecco's PBS (DPBS)	Gibco (Invitrogen), Karlsruhe, Germany
EDTA	Gibco (Invitrogen), Karlsruhe, Germany
Ethanol	Merck, Darmstadt, Germany
Ethanolamine	Sigma-Aldrich, Steinheim, Germany
Fetal calf serum (FCS)	Invitrogen, Karlsruhe, Germany
Fluoro- ribonucleotide triphosphates (fYTPs)	MP Biomedicals, Illkirch, France
Formamide	Merck, Darmstadt, Germany
$\gamma - {}^{32}P$ ATP	Perkin Elmer Life Sciences, MA, USA
Gel concentrate and diluent	National Diagnostic, Hessle Hull, England
Glacial acetic acid	Merck, Darmstadt, Germany
Glutamine	Invitrogen, Karlsruhe, Germany
Glycerine	Merck, Darmstadt, Germany
Glycogen	Roche, Mannheim, Germany
GMP	Sigma-Aldrich, Steinheim, Germany
Goat anti mouse IgG Dynabeads	Invitrogen/Dynal AS, Oslo, Norway
Isoelectric Focussing Calibration KIT	GE Healthcare, München, Germany
Inorganic pyrophosphate (400x ppi)	Sigma-Aldrich, Steinheim, Germany
Horse serum	Gibco (Invitrogen), Karlsruhe, Germany
Human serum albumin (HSA)	Sigma-Aldrich, Steinheim, Germany

Hydrochloric acid (HCl) mol. biology grade	Sigma-Aldrich, Steinheim, Germany
LDS sample buffer	Invitrogen, Karlsruhe, Germany
Magnesium chloride	Sigma-Aldrich, Steinheim, Germany
MEM Eagle medium	Sigma-Aldrich, Steinheim, Germany
MES hydrate	Sigma-Aldrich, Steinheim, Germany
Methanol	Merck, Darmstadt, Germany
Methotrexate (MTX)	Sigma-Aldrich, Steinheim, Germany
N-Hydroxysuccinimide (NHS)	Sigma-Aldrich, Steinheim, Germany
N-(3-dimethylaminopropyl)- N'-ethylcarbodiimide hydrochloride (EDC)	Sigma-Aldrich, Steinheim, Germany
Pharmalyte pH3-10	GE Healthcare, München, Germany
Phenol solution	Sigma-Aldrich, Steinheim, Germany
PKH2/6 fluorescent cell linker kits	Sigma-Aldrich, Steinheim, Germany
Potassium hydroxide pellets (KOH)	Sigma-Aldrich, Steinheim, Germany
Propidium iodide (PI)	Invitrogen, Karlsruhe, Germany
RPMI 1640	Invitrogen, Karlsruhe, Germany
Sample reducing agent	Invitrogen, Karlsruhe, Germany
SeeBlue Plus 2 prestained protein standard	Invitrogen, Karlsruhe, Germany
Sodium acetate (NaOAc, pH 5.2)	Merck, Darmstadt, Germany
Sodium azide	VWR International, Darmstadt, Germany
Sodium hydroxide (NaOH)	VWR International, Darmstadt, Germany
Sodium pyrovate	Invitrogen, Karlsruhe, Germany
Taq polymerase and 10x buffer	NEB, Beverly, New England, USA
TE buffer pH 8.0	Invitrogen, Karlsruhe, Germany
TEMED	VWR International, Darmstadt, Germany
tRNA from baker's yeast	Sigma (Fluka), Steinheim, Germany
Tween-20	Merck, Darmstadt, Germany
Ultra low IgG FCS	Gibco (Invitrogen), Karlsruhe, Germany
Urea	VWR (OmniPur), Darmstadt, Germany
Western blot diluent A	Invitrogen, Karlsruhe, Germany
Western blot diluent B	Invitrogen, Karlsruhe, Germany
Western blot wash solution	Invitrogen, Karlsruhe, Germany

3.5 Cell culture media

Jurkat E6.1	RPMI 1640 2 mM glutamine 1 mM sodium pyruvate 10 % (v/v) FCS
Recombinant Jurkat V158 and F158	RPMI 1640 2 mM glutamine 1 mM sodium pyruvate 10 % (v/v) FCS 100 nM MTX
GTL-16	DMEM 10 % (v/v) FCS
MKN-45	RPMI 1640 2 mM glutamine 1 mM sodium pyruvate 20 % (v/v) FCS
EBC-1	MEM Eagle 2mM glutamine 10 % (v/v) FCS
NIH-3T3	DMEM 10 % (v/v) FCS 2.5 % (v/v) horse serum
ADCC Assay medium	RPMI1640 10 % (v/v) ultra low IgG FCS (heat-inactivated 56°C 30 min)

3.6 Solutions and buffer

1x gel loading buffer	40 % formamide 2.5 mM EDTA
1x TC buffer	40 mM Tris-HCl (pH 7.5) 6 mM $MgCl_2$ 10 mM NaCl 2 mM spermidine
2x gel loading buffer	80 % (v/v) formamide 5 mM EDTA
5x RT buffer	1 M Tris-acetate pH 8.4 2 M potassium acetate 100 mM magnesium acetate
10x TBE buffer	890 mM Tris 890 mM boric acid 20 mM EDTA
ADCC assay medium	RPMI 1640 10 % (v/v) ultra low IgG FCS (heat-inactivated 56°C 30 min)
Cell SELEX binding buffer	0.05 % (w/v) BSA 0.03 % (w/v) sodium azide in DPBS
Coomassie staining solution	40 % (v/v) methanol 10 % (v/v) glacial acetic acid 16 tablets/l Coomassie R250
Coomassie destaining solution	35 % (v/v) ethanol 10 % (v/v) glacial acetic acid
DNA SELEX PCR mix	1x Taq buffer (for 200 µl final volume) 4 mM dNTPs (each) 1 µM primer 5978, 1 µM primer 5979

FACS binding buffer	1 % (w/v) BSA in DPBS
Filter elution buffer	7 M Urea 100 mM NaOAc pH 5 3 mM EDTA (pH 5.7 final)
IEF rehydration buffer	890 µl Pharmalyte pH3-10 1.22 g glycerine in 12 ml dH_2O
MACS buffer	4.9 ml MACS BSA stock solution 95.1 ml DPBS
Passive elution buffer	300 mM NaOAc 20 mM EDTA
Reverse transcription (RT) mix	1x cDNA synthesis buffer (50 µl final vol.) 4 mM dNTPs (each) 2 µM 3'primer 5981 5 mM DTT
TBE buffer	89 mM Tris 89 mM boric acid 2 mM EDTA
TC reaction composition	1x TC buffer 2 mM $MgCl_2$ 1.5 mM of each ATP, GTP, fCTP, fUTP 40 mM DTT 5x ppi 3.2 µg T7 RNA polymerase Y639L (1 µl)
Western blot antibody solution	2 ml western blot diluent A 1 ml western blot diluent B in 7 ml dH_2O
Western blot blocking solution	2 ml western blot diluent A 3 ml western blot diluent B in 5 ml dH_2O
Western blot wash solution	10 ml western blot wash in 150 ml dH_2O

3.7 Laboratory materials

4-20 % TBE gels	Biostep, Jahnsdorf, Germany
4-20 % Tris-glycine gels	Invitrogen, Karlsruhe, Germany
10 % TBE gels	Invitrogen, Karlsruhe, Germany
10 % TBE-Urea gels	Invitrogen, Karlsruhe, Germany
Abgene PCR plates	Thermo Scientific, Langenselbold, Ger.
Airpore tape sheets	Qiagen, Hilden, Germany
E gel 4 % agarose (HR)	Invitrogen, Karlsruhe, Germany
FortéBio tips	FortéBio, Menlo Park, California, USA
Gel blot paper	Whatman, Dassel, Germany
Glas pasteur pipettes	VWR, Darmstadt, Germany
Glas plates for electrophoresis	Whatman, Maidstone, UK
iBlot dry blotting components	Invitrogen, Karlsruhe, Germany
Lymphoprep tubes (Ficoll)	Axis-Shield, Heidelberg, Germany
Maxisorp microtiter plates	Nunc, Langenselbold, Germany
Micro Bio-Spin columns P-30 Tris, RNase-free	Bio-Rad, Munich, Germany
Nitrocellulose Centrex columns (0.45 µm)	Schleicher & Schuell, Dassel, Germany
Nitrocellulose membrane Protran BA85 (0.45 µm)	Schleicher & Schuell, Dassel, Germany
NuPAGE 4-12 % Bis-Tris gels	Invitrogen, Karlsruhe, Germany
Optiplate microtiter plates	Perkin Elmer Life Sciences, MA, USA
Plastic spacer for electrophoresis gels	Whatman, Maidstone, UK
Polypropylene round-bottom tubes for FACS	BS Biosciences, Massachusetts, USA
Polypropylene microtiter plates, black	Greiner Bio-one, Frickenhausen, Germany
PVDF filter membrane Hybond P	GE Healthcare, München, Germany
Thin layer chromatography plate	Merck, Darmstadt, Germany
Thermoscript RT-PCR system	Invitrogen, Karlsruhe, Germany
Tissue culture flasks “Cellstar”, 75 cm^2	Greiner Bio-one, Frickenhausen, Germany
Ultrafree-MC 0.22 µm pore size spin filters	Millipore, Schwalbach, Germany

3.8 Equipment

AlphaImager 12-bit dynamic range CCD camera	Alpha Innotech, Santa Clara, CA, USA
BioMek Synergy4 fluorescence reader	BioMek/BeckmanCoulter, Brea, CA, USA
CEDEX cell counter MS20C	Roche Innovatis, Mannheim, Germany
Centrifuge Megafuge 1.0 R	Kendro, Langenselbold, Germany
Dot blot S&S Minifold I Dot-Blot system	Schleicher & Schuell, Dassel, Germany
E gel PowerBase Ver.4	Invitrogen, Karlsruhe, Germany
Electrophoresis chambers	Invitrogen, Karlsruhe, Germany
FACScan cytometer	Beckton Dickinson, Heidelberg, Germany
FortéBio octet red	FortéBio, Menlo Park, California, USA
Geiger counter	Mini Instruments Ltd., Burnham, UK
iBlot dry blotting system	Invitrogen, Karlsruhe, Germany
Luminometer Varioskan Flash	Thermo Scientific, Schwerte, Germany
MACS autoMACS separator	Miltenyi, Bergisch-Gladbach, Germany
Magnet separators	Invitrogen/Dynal, Oslo, Norway
Nanodrop ND-1000 spectrophotometer	Peqlab, Erlangen, Germany
PCR machine/ Peltier Thermal cycler, Tetrad2	Bio-Rad, Munich, Germany
PhosphorImager Storm 860	GE healthcare, München, Germany
Power supply Power-Pak 300	Bio-Rad, Munich, Germany
Storage phosphor screen and cassette	GE healthcare, München, Germany
Table-top centrifuge Eppendorf 5415	Eppendorf, Hamburg, Germany
Tecan Washer HydroFlex	Tecan, Crailsheim, Germany
Thermomixer comfort	Eppendorf, Hamburg, Germany
UVS-26 EL Lamp, 115V, 254NM, 6W	VWR International, Darmstadt, Germany
Vacuum centrifuge Vacuum Concentrator 5301	Eppendorf, Hamburg, Germany
Vertical gel electrophoresis system	Whatman, Maidstone, UK

Further equipment comprised common laboratory instrumentation.

3.9 Software

BD CellQuest	Becton Dickinson, Heidelberg, Germany
BioEdit ver. 7.0.9.0	Ibis Therapeutics, Carlsbad, CA, USA
DNA Star ver. 7.2.1 SeqMan and EditSeq	DNA Star Inc., Wisconsin, USA
FortéBio octet data analysis ver. 6.2.1.1	FortéBio, Menlo Park, California, USA
Gen5 fluorenscence reader analysis ver. 1.04.5	BioMek/BeckmanCoulter, Brea, CA, USA
ImageQuant ver. 5.2	Mol. Dynamics/GE, München, Germany
Mfold ver. 3.2 by Zuker and Turner	http://mfold.bioinfo.rpi.edu/cgi-bin/dna-form1.cgi (Zuker, 2003)
Microsoft Office 2003	Microsoft Corp., Redmond, WA, USA
Origin ver. 8.1	OriginLabs, Northampton, MA, USA
Phoretix	Totallab, Newcastle upon Tyne, UK
Python	Python Software Foundation
SkanIt Software ver. 2.4.3	Thermo Scientific, Schwerte, Germany
XL fit ver. 2.1.1	IDBS, Surrey, UK

4 METHODS

4.1 Molecular biological methods

4.1.1 DNA aptamer production

4.1.1.1 Polymerase chain reaction

For specific amplification of DNA fragments or aptamer production, a polymerase chain reaction (PCR) was applied (Mullis *et al.*, 1986). Generally, a total volume of 200 µl for an initial small scale PCR (ssPCR) and 1 ml for a large scale PCR (lsPCR) was used to assemble 50 – 100 pmol, but also larger volumes could be applied to yield higher amounts of aptamers. The same PCR mix was applied in all DNA aptamer amplifications and contained up to 10 ng/ml template (pool or single aptamer); 1 µM forward and reverse primer 5978 and 5979, respectively (chapter 3.3); deoxyribonucleoside triphosphates at 0.2 mM of each nucleotide; appropriate amount of 10x NEB Taq buffer and 0.025 U/µl Taq DNA polymerase (native form, chapters 3.2 and 3.6).

10 rounds of amplification were performed for 30 sec each at 94°C for denaturing, at 50°C for annealing, at 72°C for extension and pausing at 4°C in a thermocycler (chapter 3.7). After 10 cycles, 5 µl of PCR reaction were added to 5 µl dH_2O on an 4 % agarose ethidium bromide E-Gel (chapter 3.7) and run for 7 min along with 0.5 µg NEB 100 bp marker (which includes 50 ng as 100 bp band, chapter 3.7). The PCR product was visually quantified compared to the reference marker band applying a trans-illuminator (AlphaImager, chapter 3.7). Additional PCR cycles were carried out to yield at least 10 ng/µl of the specific aptamer PCR product (sample is at the same intensity as the 100 bp band). Resulting PCR products were precipitated (chapter 4.1.5) and a strand separation was carried out (chapter 4.1.1.2). Aliquots of PCRs could be stored at -20°C for several months as a resource for additional aptamer productions.

4.1.1.2 Alkaline induced DNA strand break

PCR products were double stranded, but aptamers need to be single stranded DNA to adapt a correct conformation. The reverse primer 5979 used in DNA aptamer amplification contained a 3' terminal ribo-dCTP to enable an alkaline induced antisense strand break with subsequent PAGE (chapter 4.1.3.2) size exclusion strand separation to finally yield single stranded DNA

aptamers. To perform a strand separation on a pool or single aptamer in aqueous solution, 0.5 volumes 1M NaOH were added and incubated for 15 min at 90°C. Then, 0.5 volumes 1M HCl for neutralisation and 1 volume of 2X gel loading buffer (chapter 3.6) were added and boiled for further 5 min at 90°C. Samples were run on a TBE-polyacrylamide gel (chapter 4.1.3.2) and the desired 84 nt aptamer sense strand could be well separated from 24 nt and 60 nt antisense strand fragments. The aptamer band was extracted (chapter 4.1.4), precipitated (chapter 4.1.5), re-constituted in DPBS and the final concentration was determined (chapter 4.1.6). Figure 4 gives a short overview of DNA aptamer production.

4.1.1.3 DNA aptamer synthesis

DNA aptamers can be obtained in higher quantity (more than 100 pmol) simply by oligo synthesis. Single sequence aptamers were purchased in 200 nmol or 1 µmol synthesis scale from Eurofins MWG Operon (Ebersberg, Germany) or invitrogen (Karlsruhe, Germany). Aptamers with nucleotide lengths over 100 were synthesised as "ultramers" by IDT (Leuven, Belgium). A subsequent PAGE purification (chapter 4.1.3.2) ensured high quality. The appropriate aptamer band was extracted (chapter 4.1.4), precipitated (chapter 4.1.5), re-constituted in DPBS and the final concentration was determined (chapter 4.1.6).

4.1.1.4 Production of labelled aptamers

5' Fluorescein (FLO) labelling as well as both, 5' or 3' biotinylation of DNA aptamers were accomplished by coupling during synthesis and purchased PAGE-purified in a 200 nmol scale from Invitrogen (Karlsruhe, Germany).

4.1.2 Modified RNA aptamer production

Modified RNA aptamers can be synthesised at higher costs or transcribed from a double stranded DNA template applying a modification tolerating mutant DNA-dependent T7 RNA polymerase Y639L (chapter 3.2). The first steps of amplifying a reverse-transcribed pool or single aptamers are similar to DNA aptamer production and comprise ssPCR and lsPCR using a DNA template (chapter 4.1.1.1). The applied forward primer 5980 (chapter 3.3) elongates the original 20 nt 5' PCR flanking sequence by a T7 transcription start site. The resulting 106 nt dsDNA PCR product can serve as transcription template for an 84 nt RNA aptamer production.

The dsDNA fragments obtained by PCR were precipitated (chapter 4.1.5) and resuspended in nuclease-free H_2O to a concentration of 1.5 µM (0.1 volume of PCR, 100 ng/µl). Since high concentrations of dNTPs could inhibit the transcription reaction, the precipitated PCR reaction was additionally desalted using Biospin columns according to manufacturer's protocol. 20 µl of the desalted PCR template were applied in a total volume of 100 µl transcription reaction yielding a final concentration of 300 nM dsDNA template. The work presented herein was carried out with the rRfY pool comprising 2'-hydroxy-purines and 2'-fluoro-pyrimidines (chapter 2.4.1), the transcription composition is shown in chapter 3.6. The transcription reaction was incubated for 18 h at 32°C and yielded modified ssRNA aptamers. For transcription verification and purification, 1 volume of 2X gel loading buffer (chapter 3.6) was added and incubated for 5 min at 90°C. Samples were run on a TBE-polyacrylamide gel (chapter 4.1.3.2) and the desired 84 nt RNA aptamer could be separated from the longer dsDNA template. The aptamer band was extracted (chapter 4.1.4), precipitated (chapter 4.1.5), resuspended in usually 100 µl DPBS and the final concentration was determined (chapter 4.1.6). Figure 4 in the introduction shows a scheme of RNA aptamer production and purification.

4.1.3 DNA gel electrophoresis

4.1.3.1 Agarose gel electrophoresis

For analytical purpose, agarose gel electrophoresis was carried out applying the E-Gel system of invitrogen (Karlsruhe, Germany). For this, usually 5 µl of DNA sample solution were added to 5 µl dH_2O on a 4 % agarose ethidium bromide E-Gel and run for 7 min along with 0.5 µg NEB 100 bp marker (which includes 50 ng as 100 bp band, chapter 3.7). The PCR product was visually evaluated or quantified to the reference marker band for size and concentration applying a trans-illuminator (AlphaImager, chapter 3.7).

4.1.3.2 TBE polyacrylamide gel electrophoresis

For aptamer purification and analyses requiring precise resolution, polyacrylamide gel electrophoresis was applied. Analytical 4-20 % or 10 % TBE gels were run according to the manufacturer's suggestions (chapter 3.7). Preparative gels were made by adding 20 ml Gel Concentrate, 25 ml Gel Diluent, 5 ml 10x TBE, 200 µl 10 % APS and 100 µl TEMED (chapter 3.7, the two latter substances immediately before use) in a 50 ml falcon tube. The solution was inverted for complete mixing and poured between two glass plates blocked on

three sides by 1.5 mm plastic spacers. A comb was placed on top and the solution was allowed to polymerise at ambient temperature for at least 10 min before the gel was suspended into the running device.

Samples were loaded usually along with 10 µl of 6x DNA loading buffer (chapter 3.4) in a separate lane for visualization of the PAGE-progress. The gel was run at a constant voltage of 350 V for 1 h, or until the bromophenol blue dye marker was at the bottom of the gel. The glass plates were taken apart, the gel covered in plastic wrap and transferred onto a thin layer chromatography plate including a fluorescent dye. For visualisation, the DNA shadowing technique was applied: When excited with UV light (at 254 nm applying a hand lamp or the "epi short wave uv" function of the AlphaImager, chapter 3.7) the dye's fluorescence was quenched by oligonucleotide bands in the gel and could be imaged and marked.

4.1.4 Gel extraction

Desired bands were excised out of TBE polyacrylamide gels with a clean razor or scalpel and placed into a 1.5 ml tube. The gel piece was sheared using a pipette tip. Usually 400 µl passive elution buffer (chapter 3.6) were added, quickly homogenised by vortexing and incubated over night at 37°C to allow passive elution of aptamers into the solution. On the next day, the liquid containing the eluted sample was removed from the gel remnants and purified using a Millipore spin column (chapter 3.7), spinning for 1 minute at 13000 rpm. Finally, the aptamer solution had to be purified by ethanol precipitation (chapter 4.1.5).

4.1.5 DNA precipitation

Precipitation provided a basis to concentrate DNA and remove undesired proteins, salts and free nucleotides. The ladder ones are not removed completely, but sufficiently in many cases. If complete removal was critical, Biospin columns were applied in addition (chapter 3.7). Addition of mono-valent cations diminishing rejection of its negatively charged backbone with simultaneous solvent deprivation by ethanol addition leads to precipitation of DNA out of the solution. Glycogen applied as a carrier can further improve the recovery.

PAGE-eluted DNA and RNA aptamers were already in acidified solution containing 0.3 M sodium acetate and could be ethanol precipitated by the addition of 2 µl (40 µg) glycogen and 2.5 volumes ice cold 100 % ethanol p.a. to the aqueous solution into a 1.5 ml tube. This was followed by vigorous vortexing to ensure complete mixing and centrifugation for 30 – 60 min

at 13000 rpm and 4°C. The supernatant was decanted and discarded, and pellets were allowed to completely dry in open tubes for 1 h at ambient temperature or at 37°C for shorter time spans. The DNA usually was resuspended in 40 – 100 µl DPBS. Ethanol precipitation of PCR reactions was carried out essentially as described above, only differing in the addition of 0.1 volume of 3 M sodium acetate pH 5.0 (not yet included in the solution) instead of glycogen.

Isopropanol precipitation can reduce the amount of co-precipitated salts. It was carried out similar to the ethanol precipitation including glycogen as described above, but only 1 volume of isopropanol was applied. Complete drying of pellets was assured to avoid residual isopropanol that could interfere with subsequent reactions.

4.1.6 Determination of DNA concentration

The nucleic acid concentration of aqueous solutions can either be measured applying the law of Lambert-Beer via absorption of aromatic nucleobases at 260 nm or comparing the intensity of electrophoresis gel bands with quantitative marker bands run simultaneously.

In general, the concentration of purified DNA or RNA samples was determined with the UV spectrophotometer Nanodrop ND1000 (chapter 3.7) by adding 1.5 µl sample solution and measuring the 260/280-ratio as well as the absorption at 260 nm. 1 OD_{260} equates to a concentration of 50 µg/ml dsDNA, 35 µg/ml RNA or 33 µg/ml ssDNA. Evaluation of protein contents by measuring absorption at 280 nm allows for determination of purity of the sample: a protein-free nucleic acid solution should have a OD_{260}/OD_{280} ratio of about 2 : 1. Aptamers purified by gel electrophoresis were already examined for the correct size to exclude the possibility that absorption at 260 nm was caused by single nucleotides or degradation products that would decrease the concentration of the actual aptamer in solution. Sample that were measured but had not been analysed in this way were evaluated on a 4 % E-Gel (chapter 4.1.3.1) to ascertain their identity.

During PCR monitoring, PCR progress evaluation could not be carried out using the method described above due to free dNTPs and primers in the PCR solution. Here, a comparative agarose gel electrophoresis was carried out applying a quantitative marker along with the samples run on 4 % agarose E-Gels. This method is described in more detail in chapter 4.1.1.1.

4.1.7 Separation of pools into single aptamers

The analysis of single aptamers out of a library or selection required the separation of a pool into single entities representing one aptamer only. For this, double stranded PCR fragments containing a Taq polymerase derived adenine overlap were cloned into the TOPO-TA pCR4.0 cloning vector (chapter 3.7). This vector contained a death (CCD) gene and utilised a life/death screen: only in the presence of a vector with insert exchanged for the CCD gene a clone was able to grow. 1 µl of a 1 : 100 dilution of PCR product (generally at 10 ng/µl) was combined with 1 µl water, 0.5 µl salt solution and 0.5 µl TOPO TA pCR 4.0 vector (all provided in the cloning kit), mixed by gently flicking tube with a finger, centrifuged down for 10 sec in a microcentrifuge and incubated at ambient temperature for 30 min. Topo-cloning vectors were transformed into *E. coli* (chapter 4.4.1.). Single clones representing one single aptamer were analysed further by sequencing, since they were carrying one vector containing one single aptamer sequence as insert only.

4.1.8 Sequence analysis of single aptamer containing *E. coli* clones

Analysis of aptamers in a selected pool was carried out by sequence comparison of usually 96 aptamers to evaluate potential enrichment of single or similar aptamers. Single aptamers represented by *E. coli* clones transformed with a dsDNA-aptamer-Topo-vector were sequenced by MWG, Ebersberg, Germany. For this, a DNA preparation and sequencing with both M13_for and M13_rev primers (chapter 3.3) were carried out. Resulting sequences were obtained as ab1-files and processed in Python. Aptamers were brought in the correct orientation on the basis of known 5' and 3' flanking sequences, vector and invariant flanking sequences were clipped to leave only the 39 or 40 nt long variant fragment and these were stored in a multiple fasta file. The single sequences were grouped applying DNA Star SeqMan to sequence families of 90 % sequence identity, e.g. four bases in 40 were allowed to be altered. A unique identifier was assigned to the most prevalent aptamer in each sequence family. Sequence variants were listed for each aptamer and characterised later on as well, if the most prevalent sequence exhibited desired properties.

4.1.9 5' radioactive oligonucleotide labelling

Radioactive labelling represents an effective and sensitive method that does not alter initial aptamer characteristics. DNA aptamers and synthetic RNA can be labelled directly due to the lack of a 5' phosphorylation; RNA transcripts have to undergo a dephosphorylation step at

first. For this, 10 pmol of an aptamer clone or pool, 1 µl 10x AP buffer, 1 µl (5 U) antarctic phosphatase (chapter 3.2) and a respective volume of water were incubated in a total volume of 10 µl at 37°C for 15 – 45 min. Subsequently, the phosphatase was heat inactivated by incubation at 65°C for 10 minutes.

Either dephosphorylated RNA or DNA was then employed in a kinase reaction applying the T4 Poly Nucleotide Kinase (PNK, chapter 3.2). 10 pmol of aptamer, 2 µl 10x T4 PNK buffer, 0.5 µl (5 U) T4 PNK, 3 µl ^{32}P γ-ATP (30 µCi, chapter 3.4) and the respective volume of water in a total volume of 20 µl were incubated for 15 – 45 min at 37°C.

For removal of unincorporated ATP by non-interactive separation by size, Bio-Spin columns were used following the manufacturer's protocol (chapter 3.4). In brief, column bottom caps were removed and the columns placed in waste collection tubes, then top caps were removed and the initial flow-through liquid was removed by decanting. Tubes were centrifuged at 1,000 g (3,300 rpm) for 2 min. Columns were placed in new 1.5 ml tubes, 20 µl kinase reactions were added to the top of the resin and centrifuged at 1,000 g (3,300 rpm) for 4 min in the same centrifuge. The columns were discarded in ^{32}P radiation waste and the flow through was evaluated using a Geiger counter (chapter 3.8) to ensure a successful labelling reaction when samples registered high on the 100x setting.

To obtain an applicable working concentration, the obtained labelled aptamer solution was diluted 1 : 500 by adding 2 µl of labelled aptamer to 998 µl DPBS (chapter 3.4). The resulting solution was applicable for dot blots (chapter 4.3.9) with 1 nM for the respective aptamer, hence containing 5 fmol aptamer in 5 µl.

4.2 Systematic evolution of ligands by exponential enrichment

Systematic evolution of ligands by exponential enrichment (SELEX) is a method for selection of single aptamers that bind to a target of interest out of a pool of nucleic acid sequences. Aptamers are enriched by iterative steps of selection and amplification by PCR in 5 to 15 rounds. DNA SELEX consists of selection by aptamer binding, separation and washing followed directly by amplification via PCR, strand separation and PAGE purification of the new aptamer pool. RNA SELEX shares a similar selection route, but comprises amplification by reverse transcription, PCR, transcription of the respective composition and PAGE purification to yield a potentially enriched pool.

In order for SELEX to be successful, aptamer-target molecule complexes must be efficiently captured. The following paragraph describes three procedures for separation of binding from non-binding nucleic acids by immobilisation of nucleic acid : protein complexes on a nitrocellulose filter (filter SELEX, chapter 4.2.1), on the hydrophobic surface of a microtiter plate (hydrophobic plate SELEX, chapter 4.2.2) or whole cells (cell SELEX, chapter 4.2.3). For all selections, a DNA or rRfY oligonucleotide library containing a 40-base random sequence flanked by complementary priming regions on either end (chapter 3.3) was used as the starting point for an aptamer SELEX.

4.2.1 Filter SELEX

Filter SELEX was based on the immobilisation of the target protein to a nitrocellulose membrane after incubation of aptamer with target protein in solution, enabling separation of target-bound aptamers and washing off non-binding sequences.

4.2.1.1 Nitrocellulose filter capacity test

Since target molecules must be efficiently captured to not loose bound aptamers of interest, an initial nitrocellulose filter capacity test has to prove 100 % target protein binding to the applied filter. Nitrocellulose Centrex columns (chapter 3.7) were incubated at ambient temperature for 15 min with 1 ml of 0.5 M KOH solution to reduce non-specific binding of aptamers to the nitrocellulose. Filters were centrifuged at 2000 rpm for 1 min, flow-through material was removed from the bottom of the tubes, and columns were incubated with 1 ml dH_2O at ambient temperature for 3 min. Centrifugation and incubation were repeated two times with DPBS (chapter 3.4) to equilibrate the filter with the appropriate buffer. 200 µl target protein solution with the concentration maximally applied in SELEX rounds (usually 1 µM) were prepared and divided: 100 µl were applied to a pre-treated Centrex column collecting the flow-through, 100 µl were stored at ambient temperature. Equivalent volumes (20 µl) of both filter flow-through and original sample were directly compared by gel electrophoresis (chapter 4.3.2) and coomassie staining (chapter 4.3.4). Complete depletion of protein in the flow-through indicated sufficient filter capacity.

4.2.1.2 DNA SELEX

Carrying out DNA filter SELEX, desired target-bound aptamers were separated by immobilisation of target protein on a nitrocellulose filter and washing away unbound

aptamers that were discarded in the flow-through. Selection was carried out in a total volume of 100 µl in Dulbecco's PBS (DPBS) with increasing concentration of the non-specific competitor tRNA and washing volume as well as decreasing amounts of target protein to enhance stringency over the course of selection (all chapter 3.4). For round 1, 1×10^{14} molecules of the starting pool were used (with a final concentration of 1.66 µM) and in subsequent rounds, the output pool from the previous round were adjusted to 1 µM. The filters were pre-treated with KOH to reduce non-specific binding of the DNA pools to the filter as described in chapter 4.2.1.1, and filters were kept wet during the last washing step until selection.

For removal of filter-binding aptamers in a negative pre-selection (skipped in round 1), 50 µl pool/DPBS solution were added to pre-treated filters and centrifuged at 2000 rpm for 1 min. The flow-through was collected for use in subsequent positive / negative selection steps. A counterselection was applied if desired to remove aptamers against components not to be targeted (e.g. His-tags or Fc-fusion portions of applied recombinant target proteins; skipped in round 1) by adding protein and DPBS to the flow-through of negative selection to a final concentration of 1 µM protein in 90 µl total volume. After incubation for 1 h at 37°C, the pool/DPBS solution was added to pre-treated filters, centrifuged at 2000 rpm for 1 min and the flow-through was collected for use in a positive selection step.

Positive selection was carried out in case of a previous counterselection by adding target protein and competitor amount to 90 µl pool/DPBS flow-through to yield 1 µM protein in 100 µl total volume. In case of no counterselection, 50 µl target protein and competitor mixture were added to 50 µl flow-through solution from negative pre-selection. Positive selection mixtures were incubated 1 h at 37°C, then added to pre-treated Centrex columns and centrifuged at 2000 rpm for 1 min discarding the flow-through. Filters thereby caught desired protein:pool complexes. These were washed two times with pre-warmed 1000 µl DPBS (500 µl in round 1) and centrifugation discarding flow-through as before, and eluted with two times 200 µl 90°C pre-heated elution buffer (chapter 3.6) by incubation for 1 min and centrifugation as above combining both flow-through elution fractions (400 µl total). During this step, heat and urea denatured target proteins lost their correct folding releasing conformational epitope-binding aptamers that were collected in the flow-through. These aptamers were purified for subsequent PCR via isopropanol precipitation (chapter 4.1.5) and resuspended in 10 µl dH_2O.

Amplification of aptamer pools was achieved in a two-step PCR setup. Initial small scale PCRs (ssPCR) were carried out to adjust DNA concentrations to a standard concentration of 10 ng/µl, at the same time investigating indirectly the amount of selected aptamers by PCR cycle monitoring. The more aptamers were enriched, the less PCR cycles were needed to yield the desired concentration. In the next step, large scale PCRs (lsPCR) followed to yield sufficient aptamer material for subsequent selection rounds. PCRs were performed as described in chapter 4.1.1.1. A 50 µl aliquot of each ssPCR was stored at -20°C as stock sample for the respective selection round. lsPCR was carried out for 11 cycles under ssPCR conditions and confirmed by E-gel electrophoresis as described in chapter 4.1.1.1. Residual ssPCR- and lsPCR-volumes were combined in 15 ml tubes and precipitated (chapter 4.1.5). After removal of supernatant and drying as above, pellets were resuspended in 30 µl TE buffer pH 8.0 (chapter 3.4) and transferred to 1.5 ml tubes.

Single stranded aptamers had to be obtained via strand separation of the double stranded PCR products. The use of 3' ribo-modified reverse primers (oligo 5979, chapter 3.3) enabled alkaline induced strand breaks of the anti-sense strand (chapter 4.1.1.2) leading to one larger sense strand aptamer and two smaller anti-sense fragments that were separated by polyacrylamide gel electrophoresis (PAGE, chapter 4.1.3.2). Passive gel elution (chapter 4.1.4), DNA precipitation (chapter 4.1.5), and resuspension in 40 µl DPBS were completed by concentration determination (chapter 4.1.6) to yield an enriched aptamer pool ready for the next SELEX round.

4.2.1.3 rRfY SELEX

Filter SELEX of 2'-modified RNA aptamers comprised the same selection work-flow as DNA filter SELEX (chapter 4.2.1.2), but differed in two main aspects of amplification: Firstly, filter-eluted aptamers needed to be reversely transcribed to DNA to be amplified via PCR. For this, eluate precipitation was followed directly by resuspension in 50 µl of RT mix (chapter 3.6) and addition of 0.5 µl of Thermoscript Reverse Transcriptase (chapter 3.2). Reverse transcription was carried out at 65°C for 30 min. Subsequently, DNA aptamers in 50 µl RT samples were amplified in 400 µl total volume ssPCR as described in DNA filter SELEX (chapter 4.2.1.2). Application of oligos 5980 and 5981 (chapter 3.3) introduced a T7 transcription site 5' of the resulting DNA aptamer template for transcription back into rRfY composition in the next step. Since high concentrations of residual free dNTPs could inhibit the transcription, the PCR solution was ethanol precipitated (chapter 4.1.5) and desalted via

Biospin columns (as in chapter 4.1.9), yielding 40 µl of purified DNA aptamer templates. 20 µl were stored as aliquot at -20°C, 20 µl were combined with 80 µl transcription reaction mix (chapter 3.6) and rRfY aptamers were transcribed from DNA templates at 32°C for 18 h. Resulting modified RNA aptamers could be separated by PAGE from larger DNA templates carrying the T7 transcription site (as in chapter 4.2.1.2). In this manner purified rRfY aptamers were applicable for following SELEX rounds.

4.2.2 Hydrophobic plate SELEX

If target proteins could not be captured sufficiently to nitrocellulose filters, immobilisation onto the well of a hydrophobic plate and subsequent capture of binders to that surface displayed another opportunity for aptamer selection to recombinant proteins. A further advantage was the facile competition elution of pre-bound aptamers by addition of a potential competitor that bound to the immobilised target protein replacing aptamers bound to the same epitope. These desired aptamers found in the supernatant could be amplified by PCR.

Immobilisation was carried out with 100 nM protein target in 100 µl DPBS per Nunc Maxisorp plate well (chapter 3.7) for 30 min at ambient temperature, followed by 3 washes with 200 µl DPBS to remove unbound target. Target wells were further blocked with 200 µl 5 % HSA of DPBS and washed as above. For negative or counterselection steps (skipped in round 1), empty or counter protein wells, respectively, were blocked in the same way. Aptamer and competitor concentrations and volumes were applied analogue to DNA filter SELEX (chapter 4.2.1.2). For negative, counter and positive selection steps, 100 µl aptamer pools were incubated for 1 h at 37°C and transferred consecutively to all particular wells. The positive selection supernatant was discarded and wells washed 5 times with 100 µl 37°C pre-warmed DPBS. Elution was carried out analogue to filter SELEX with pre-heated urea elution buffer (chapters 3.6 and 4.2.1.2) yielding 400 µl eluted aptamer solution. For an alternative competition elution, the competitor (in this work antibodies 3G8 or cetuximab, chapter 3.2) was added to the fifth washing solution in high excess to target protein of 1 µM final concentration and incubated for 1 h at 37°C. The supernatant contained displaced aptamers and was removed as eluate. Aptamers in eluates were precitipated, amplified and purified as described for filter SELEX (chapter 4.2.1.2).

4.2.3 Cell SELEX

Since aptamers have been shown to be highly selective to the tertiary structure of their target proteins and folding could vary between cellular-bound and recombinant produced target proteins, SELEX directly on whole cells could yield better cell-targeting aptamers. To avoid enrichment of unspecific sequences, pre-selected but still diverse pools, e.g. from early filter SELEX rounds to the same target protein offer a promising base for cell SELEX. For the selection, high target expressing cell lines were preferred (~10^5 receptors/cell). Recombinant cell lines positive for the target protein („(+) cells“) were used that enable optimal negative selection when applying parental cells („(-) cells“). Adherent cells were detached from culture dishes, whereas suspension cells were used directly; cell density was determined via CEDEX (all as in chapter 4.4.2). Selection was initiated with 2 x 10^7 cells for positive selection with decreasing cell amount in later rounds, a negative selection was carried out from round 2-3 on. (+) as well as (-) cells were pelleted at 250 g (~1300 rpm) for 10 min at 21°C and the supernatant was removed applying a Pasteur pipette on vacuum (chapter 3.8). Cells were resuspended by screeding without medium followed by addition of 14 ml Cell SELEX binding buffer (chapter 3.6) and this washing step was repeated once. For negative selection, (-) cells were resuspended in an appropriate volume of binding buffer to yield 200 µl total volume after aptamer pool addition. Aptamers were incubated in 1 µM final concentration with parental (-) cells for 30 min at 37°C with gentle shaking of 300 rpm. For positive selection, (-) and (+) cells were pelleted at 1000 g for 2 min, (+) cell supernatant was discarded only and supernatant containing unbound aptamers was used to resuspend (+) cells. From round 2-3 on, 0.1 mg/ml tRNA competitor was added to the positive selection step, with increasing amounts up to 1 mg/ml in later rounds. Aptamers were allowed to bind during incubation for 30 min at 37°C with gentle shaking of 300 rpm. Cells were then washed three times with 1 ml (500 µl in round 1) of 37°C pre-warmed binding buffer and pelletisation as before. Subsequently, 500 µl DPBS (chapter 3.4) were added and cells were resuspended by trituration. To purify cell bound aptamers from cell debris and proteins, a phenol/chloroform extraction was carried out by adding 1 volume phenol (500 µl, chapter 3.4) and vigorous vortexing followed by centrifugation at top speed for 5 min. The top aqueous layer was transferred to a new microcentrifuge tube and 1 volume chloroform : isoamylalcohol (chapter 3.4) was added, followed by vortexing and centrifugation as before. The top aqueous layer was again transferred to a new microcentrifuge tube and purified aptamers were isopropanol precipitated (chapter 4.1.5). Purified Cell SELEX selected aptamers were resuspended in 30 µl DPBS and amplified via PCR as described in DNA filter SELEX (chapter 4.2.1.2).

4.3 Biochemical methods

4.3.1 Protein concentration determination

Protein concentration determination was carried out as described by Bradford (1976). BSA (chapter 3.4) served as standard reference protein in dilutions from 25 – 2000 µg/ml. 5 µl of each sample or standard dilution were combined with 150 µl of Coomasie Plus Protein Assay Reagent (chapter 3.4) in a microtiter plate well, incubated for 5 min in the dark and the extinction was measured at 595 nm. Comparison of samples with the calibration curve yielded the protein concentration.

4.3.2 SDS polyacrylamide gel electrophoresis

Separation of proteins due to their molecular mass was achieved by SDS polyacrylamide gel electrophoresis (PAGE) as described by Laemmli (1970). Protein samples were added to 0.1 volume of sample reducing agent and 0.25 volume of LDS sample buffer (both chapter 3.4), boiled at 90°C for 10 min and run along with 5 µl SeeBlue Plus 2 prestained protein standard marker (chapter 3.4) on 4-20 % Tris-glycine or NuPAGE 4-12 % Bis-Tris gels (chapter 3.7) at 200 V for 35 min. Subsequently, protein bands were visualised by coomassie staining (chapter 4.3.4).

4.3.3 Isoelectric focussing

Since an iso-electric point (pI) of lower than 5.5 can indicate improbable selection success, the pI of target proteins was evaluated before SELEX was started. Isoelectric focussing uses the fact that a protein in a gel with applied voltage and pH lower than its pI is positively charged and thus migrates through a gradient of increasing pH towards the cathode until the pH region that corresponds to its pI. At this point it has no net charge, hence migration stops and the protein becomes focussed into a sharp band at the pH corresponding to its pI.

For focussing, 20 µg target proteins were analysed on a CleanGel IEF Ultra rehydrated in IEF rehydration buffer for 60 min at ambient temperature in comparison to the Isoelectric Focussing Calibration KIT as reference. Samples were applied anodic and separated at 10°C in 4 steps: pre-focussing 30 min at 700 V, 6 mA and 4 W; sample entry 30 min at 500 V, 4 mA and 4 W; separation 90 min at 2000 V, 7 mA and 7 W and band sharpening 10 min at 2500 V, 7 mA and 9 W. The gel was coomassie-stained (chapter 4.3.4) and analysed using Phoretix by comparison to reference proteins.

4.3.4 Coomassie staining of proteins

PAGE-separated proteins could be visualised with coomassie staining solution (chapter 3.6) for at least 30 min followed by incubation with destaining solution (chapter 3.6) for 2 – 18 h and additionally in dH_2O if desired until background was totally discoloured.

4.3.5 Transfer of proteins to PVDF membranes

For subsequent immunological analyses, PAGE-separated proteins could be transferred to PVDF membranes (Towbin et al., 1989) using the iBlot dry blotting system following the manufacturer's instructions (chapter 3.8).

4.3.6 Immunodetection of proteins

Detection and quantification of particular protein species on PVDF membranes (4.3.5) were carried out by immunodetection applying specific antibodies. Unspecific binding of detection antibodies was prevented by blocking PVDF membranes with 10 ml western blot blocking solution (chapter 3.6) for at least 30 min with gentle shaking at ambient temperature. In between blocking and antibody incubations, membranes were washed 4 times with 15 ml western blot washing solution (chapter 3.6) for 1 min under gentle shaking. Penta His or other protein specific antibodies (chapter 3.2) were allowed to bind the target typically in a 1 : 1000 dilution in 10 ml western blot antibody solution (chapter 3.6) for 1 h at ambient temperature and gentle shaking. After washing, secondary goat anti mouse peroxidase-conjugated detection antibodies (chapter 3.2) were incubated usually in a 1 : 5000 dilution at same conditions. An aminobenzidine tablet was dissolved in the dark in 10 ml 1x TBE buffer and 12 µl 10 % hydrogen peroxide solution (added freshly). After repeated washing, antibody-decorated proteins of interest were visualised by enzymatic conversion of aminobenzidine to a colourful precipitation at the location of the respective protein. Detection was stopped by washing PVDF membranes with dH_2O.

4.3.7 Immunoprecipitation of proteins

Correct folding of proteins applied in SELEX could be confirmed by immunoprecipitation. Conformation sensitive mouse antibodies (e.g. 3G8 for CD16α, chapter 3.2) were allowed to bind to correctly folded protein of interest, subsequently self bound by magnetic bead coupled goat anti mouse antibodies and pulled out of solution by magnetic separators. Quantitative

capturing of target protein indicated thus eligible conformational folding. Initial antibody-protein binding was performed in each case applying 1 µg protein and/or antibody in a final volume of 100 µl DPBS + 2 % (w/v) BSA (chapter 3.4) for 20 min at ambient temperature. Simultaneously, magnetic goat anti mouse IgG Dynabeads (chapter 3.4) were prepared by 2 min vortexing, 50 µl aliquotation for each sample into a 1.5 ml tube, separation of beads for 20 sec on magnet separators (chapter 3.8) discarding the supernatant. Beads were washed for 1 min in first 250 µl DPBS + 0.01 % Tween-20 (chapter 3.4) and secondly DPBS as described above. For capturing of protein:antibody complexes, pre-incubated 100 µl samples were added to prepared beads and incubated for 20 min at ambient temperature rotating or shaking to avoid sedimentation of beads. After 1 sec centrifugation assuring the complete volume at bottom of tubes, the liquid was separated from beads as above and discarded. Samples were washed once with 250 µl DPBS + 0.01 % Tween-20 and two times with 250 µl DPBS as before, ensuring complete removal of supernatant in the last step. Captured proteins were resuspended in 19.5 µl DPBS and prepared by adding sample buffer to a total volume of 30 µl for PAGE and western blot, in which an equal amount of 15 µl was applied per each gel (as described in chapter 4.3.2). The original amounts of protein or antibody applied were loaded along the samples to enable quantitative comparison.

4.3.8 Enzyme-linked immunosorbent assay

Confirmation of specific interaction of two proteins was determined as well by an enzyme-linked immunosorbent assay (ELISA). All steps were conducted at ambient temperature in 100 µl total volume, except for blocking and washing with 300 µl. Usually, 1 µg 3G8 (chapter 3.2) or cetuximab (chapter 3.2) were immobilised in duplicate in DPBS (chapter 3.4) on a Maxisorp microtiter plate well (chapter 3.7) for 18 h at 4°C. The liquid was aspirated off with a Tecan washer (chapter 3.8) and wells were blocked for at least 1 h with freshly prepared 2 % BSA in DPBS (DPBS + BSA, chapter 3.2) to render free adsorbing surface inert to further protein binding. After washing with DPBS, target proteins were allowed to bind for 1 h; 2.5 µg or 1 µg CD16α-6His (chapter 3.2) were applied in DPBS + BSA for 3G8 or cetuximab samples, respectively. Unbound proteins were removed by washing once with DPBS + 0.05 % Tween-20 (chapter 3.4) and twice with DPBS. Specific labelling of bound target proteins was accomplished by addition of Ni-NTA-peroxidase conjugate (chapter 3.2, 1:500 in 100 µl) and incubation for 1 h. Washing as before was followed by addition of 100 µl TMB substrate (chapter 3.2), incubation for 1 – 10 min until sufficient colour development and termination of the enzymatic reaction by addition of 100 µl 0.5 M HCl

solution. Fluorescence was determined at 450 nm with a Synergy4 reader (chapter 3.8) and Gen5 software (chapter 3.9). Raw values were exported to Microsoft Excel (chapter 3.9), the mean background of the medium only reference was subtracted from each well; finally, mean and standard deviation were calculated.

4.3.9 Aptamer affinity determination by dot blot

Dot blots were applied to measure the binding affinity (i.e. the dissociation constant, K_D) of a nucleic acid pool or aptamer to a specific protein. Aptamer : protein complexes were captured by a nitrocellulose filter and unbound aptamers immobilised on a PVDF membrane; a sandwich assembly of both filters in combination with target protein dilutions allowed calculation of bound aptamer percentage and thus binding affinity determination.

Binding reactions were performed in 30 µl total volume, with 5 µl ^{32}P-labelled aptamers (chapter 4.1.9) in constant final concentrations of 200 pM lower than proteins at 1000 – 0.1 nM. Binding buffer was generally DPBS + 0.1 mg/ml BSA + 0.1 mg/ml tRNA (all chapter 3.4). Target proteins were typically 4-fold diluted serially from 1 µM in 8 point curves, sparing the last well with buffer only as negative reference. Aptamer and protein were combined in PCR plates, sealed by a plastic foil and incubated for 30 min at 37°C. In the meantime, adequately cut nitrocellulose filters were pre-treated with 0.5 M KOH solution for 15 min at ambient temperature to reduce non-specific aptamer sticking to the filter, and subsequently washed 5 min with dH_2O and DPBS. PVDF filters were pre-wet with methanol, washed with dH_2O and DPBS. Gel blot paper was soaked in DPBS for 1 min (all reagents chapter 3.4). Membranes were transferred to the lower dot blot manifold unit in the order from bottom to top: blot paper, PVDF membrane, and nitrocellulose filter. The top manifold unit was added and secured, and attached to vacuum.

Dot blot capture was performed by transferring solutions quantitatively from PCR plates to the dot blot manifold and allow the reactions to be pulled through the filters. After turning off the vacuum, each well was washed with 37°C pre-warmed 100 µl DPBS two times. Finally, vacuum was applied for further 2 – 5 min to dry filters, the manifold was disassembled, nitrocellulose and PVDF filters were covered with plastic wrap, placed in a phosphorimager cassette (chapter 3.8), and a screen was positioned on top of the filters. Filters were exposed to acquire an image usually 2 h (up to 18 h depending on label signal strength) and scanned on a storm phosphorimager (chapter 3.8).

Data analysis comprised quantitation of each dot on nitrocellulose and PVDF filters via ImageQuant 5.2 software (chapter 3.9), calculation of percentage of bound aptamer at each protein concentration using the equation:

$$\%\ aptamer\ bound = 100\ x\ \frac{cpm\ nitrocellulose}{cpm\ nitrocellulose + cpm\ PVDF}$$

Background was defined as % aptamer bound to buffer only sample in dot 8 of each dilution and % aptamer bound values were normalised according to the following equation:

$$adjusted\ \%\ aptamer\ bound = \%\ aptamer\ bound\ (sample) - \%\ aptamer\ bound\ (buffer\ only)$$

Values of adjusted % aptamer bound were plotted against protein concentration in MS Excel (chapter 3.9) and K_D values were calculated by non-linear fitting of a sigmoid binding curve with XL fit (chapter 3.9), using the equation:

$$y = Max \cdot \frac{(AptConc + x + Kd) - \sqrt{(AptConc + x + Kd)^2 - 4(AptConc \cdot x)}}{2 \cdot AptConc} + yInt$$

4.3.10 Epitope mapping by competition dot blot

Competition of antibodies or aptamers to selected aptamers of interest was evaluated applying the dot blot method: Displacement of radio-labelled aptamers by added non-radioactive competitors indicated a similar addressed epitope on the target protein. The experimental setup was equal to the dot blot procedure (chapter 4.3.9) including amounts (5 fmol in 30 µl) of radio-labelled aptamers. Target protein concentration was held constant near aptamer binding saturation, usually at 50 nM (1.5 pmol in 30 µl). Antibody or aptamer competitors were added in a dilution series with maximally 100-fold molar excess to target protein (150 pmol). All samples were referenced to wells containing target protein and analysed aptamer only. Negative controls included addition of non-binding control proteins or aptamers at the same highest amount as competitor molecules to exclude the possibility of unspecific displacement. Amounts of bound or displaced aptamers were calculated by:

$$\%\ aptamer\ bound = 100\ x\ \frac{cpm\ nitrocellulose}{cpm\ nitrocellulose + cpm\ PVDF}$$

Further, the amount of bound aptamer without competitor was set to 100 % and all associated measured values were normalised accordingly. A significant, titrated decrease of labelled, bound aptamers upon high molar excess addition of competitor indicated displacement, thus binding to the same or a similar epitope.

4.3.11 Bio-layer interferometry

Label-free determination of single or simultaneous binding of aptamers to proteins was carried out by bio-layer interferometry (BLI) on a forteBio octet red device (chapter 3.8). BLI applied the fact that any change in the number of molecules bound to a biosensor tip caused a shift in the interference pattern of reflected white light that was measured in real-time and could be translated back to the amount of applied binders. For determination of simultaneous target protein binding of bi-specific aptamers, c-Met-Fc fusion protein (chapter 3.2) was immobilised, aptamers were allowed to bind and subsequent binding of the second target protein CD16α was monitored. Target protein was immobilised on amino reactive sensor tips (AR tips, chapter 3.7) after activation of sensor tips with EDC/NHS. Fc-fusions were used for coupling since it was hypothesised that a sufficient amount would only be coupled via the Fc-portion leaving the target protein free of conformational changes. All measurements were conducted in 200 µl total volume in black polypropylene microtiter plates (chapter 3.7) with a „flow rate“ of 1000 rpm at 37°C.

AR tips were rehydrated for at least 1 h in DPBS (chapter 3.4) and put into the octet red device (chapter 3.8). Tips were further equilibrated for baseline measurements in DPBS for 60 sec, followed by activation for 600 sec with freshly prepared activation solution (0.1 M NHS / 0.4 M EDC in dH_2O, mixed 1:1, chapter 3.4) and coupling of 25 µg/ml C-Met-Fc fusion protein for 900 sec in 0.1 M MES buffer pH 6. Quenching was achieved with 0.4 M ethanolamine pH 8.5 (chapter 3.4) for 450 sec and tips were then equilibrated for 300 sec in DPBS pH 7.4. Bi-specific aptamers were bound to immobilised protein in 100 nM concentration for 600 sec, followed by a short washing step in DPBS of only 10 sec to avoid major dissociation. Binding of 2 µM Fc-CD16α(V158) (chapter 3.2) was monitored for 300 sec and dissociation in DPBS as well for 600 sec. A reference of the same setup but lacking bi-specific aptamer and a negative control of a single c-Met specific aptamer (usually CLN0003) were measured in parallel. The reference signal was subtracted from each sample and negative control to exclude false-positive signal of unspecific Fc-CD16α binding. A clear association and dissociation of Fc-CD16α higher than the negative control indicated simultaneous binding of the respective bi-specific aptamer to both target proteins.

4.3.12 Electrophoretic migration shift assay

An electrophoretic migration shift assay (EMSA) was applied based on a lower migrating distance of larger molecules in gel electrophoresis, e.g. if target proteins were bound by

aptamers. Both single- and bi-valent target binding could be monitored by an aptamer band shift when target protein was added. 5 pmol of bi-specific aptamer were incubated with 40 pmol (2 µg) CD16a-6His (chapter 3.2) and/or 15 pmol (2 µg) c-Met-Fc (chapter 3.2) in DPBS of 10 µl total volume for 30 min at 37°C. Subsequently, 2 µl 6x DNA gel loading buffer (chapter 3.4) were added, mixed and the total sample volume of 12 µl was run on a 4-20% TBE-gel for 120 min at 150 V (as in chapter 4.3.2, but additionally cooled with water of 17°C). Gels were incubated for 15 min in ethidium bromide solution (4.1.3.2) and bands were detected with a trans-illuminator (AlphaImager, chapter 3.7).

4.3.13 Determination of aptamer serum stability

DNA aptamer serum stability was tested for 2 days at 37°C with 10 pmol aptamer in 100 µl PBS-buffered fetal bovine serum (90 µl FBS + 10 µl 10x PBS, chapter 3.4). 2 pmol aptamer were radio-labelled (4.1.9) for detection purposes and combined with 8 pmol unmarked aptamer. For each measurement, 10 µl sample were transferred to a new 1.5 ml tube, combined with 90 µl 2x gel loading buffer (chapter 3.6) + 0.01 % SDS (chapter 3.4) and boiled for 10 min at 90°C to linearise serum proteins and detach them from aptamers to be analysed. Degraded aptamers were separated from intact molecules via PAGE (chapter 4.3.2) by loading 10 µl of each sample onto a 10 % TBE-Urea gel (chapter 3.7) skipping one lane at a time and running gels for 15 min at 200 V. Gels were disassembled, wrapped in plastic foil and aptamer bands were visualised by exposing the gels to phosphorimager screens in appropriate cassettes (chapter 3.8) for 2 h before scanning on a storm scanner (chapter 3.8). Intensities of lower degraded and upper intact aptamer bands were extracted applying ImageQuant 5.2 software (chapter 3.9) and the percentage of undegraded aptamer for a given time point was calculated by the following equation:

$$\%\ undegraded\ aptamer = 100\ x\ \frac{cpm\ upper\ band}{cpm\ upper\ band + cpm\ all\ lower\ bands}$$

Resulting values were used as a basis for curve fitting with Origin (chapter 3.9) applying least squares optimisation and the formula $y = y_0 + A \cdot e^{(-k \cdot x)}$ with A = 100 as starting point as well as fittable parameters k and $y_0 < 5$ as residual background signal of analysed gels . Finally, half lives were calculated as $T_{1/2} = \frac{\ln(2)}{k} = \frac{0.693}{k}$. Resulting data points and graphs were plotted using Microsoft Office Excel (chapter 3.9).

4.4 Cell-biological methods

4.4.1 Chemical transformation of *E. coli*

Plasmids were inserted into *E. coli* by heat shock transformation. One Shot Top 10 competent cells (chapter 3.1) were thawed on ice, 1 – 3 µl of plasmid solution was added to 50 ml cells, mixed gently by flicking tubes with a finger and incubated on ice for 20 min to allow adsorption of DNA to the bacterial surface. Cells were then immediately transferred to 42°C for 45 sec, placed on ice again for 2 min, 250 µl SOC medium (provided in cloning kit) was added to each tube and tranformants were allowed to recover for at 37°C for 30 min at 450 rpm in a shaking incubator. The transformation reaction was split to 30 and 270 µl and transferred to 2 pre-warmed LB agar plates including the respective selection antibiotics and plated out with a sterilised Drigalski spatula. For aptamer pool TOPO-cloning transformations, 75 µl cell solution were plated on each of 4 agar plates. Transformed clones were allowed to grow for 18 h in a 37°C incubator or 70 h at ambient temperature.

4.4.2 Culturing of cell lines

All human and mammalian cell lines were cultured under sterile conditions in Cellstar tissue culture flasks (chapter 3.7) using the appropriate media (chapter 3.5) at conditions described in chapter 3.1. Cell amount, viability and aggregation rates were determined with a CEDEX cell counter (chapter 3.8) by averaging countings from 20 images.

Adherent cell lines were detached for passaging or experiments applying trypsin-EDTA (chapter 3.2). Medium supernatants were transferred into 50 ml tubes and stored at ambient temperature whilst cells were washed two times with 10 ml 37°C pre-warmed DPBS without calcium and magnesium to deplete these trypsin-inhibiting bivalent cations. 5 ml trypsin-EDTA solution were added and cells fully detached at 37°C for 2 – 5 min. The enzymatic reaction was terminated by adding the original culture medium before transferring the complete suspension to a 50 ml tube for pelletisation at 250 g (1200 rpm) for 10 min at 21°C. The supernatant was discarded and cells resuspended in an appropriate amount of either fresh culture or respective assay medium.

4.4.3 Flow cytometry of antibodies and aptamers

Aptamer binding to cellular target antigen was evaluated by flow cytometry on human cell lines applying biotinylated aptamers detected via streptavidin-phycoerythrin (SA-PE).

Adherent cell lines were detached (chapter 4.4.2) or suspension cells used directly, the cell count was determined with a CEDEX cell counter (chapter 3.8) and 1 x 10^6 cells were used per sample. All washing and sample incubation steps were performed in FACS binding buffer (chapter 3.6). Cells were pelleted at 250 g and 4°C for 10 min, washed with 10 ml binding buffer, pelleted as before and resuspended in the appropriate volume to yield 1 x 10^6 cells in 90 µl binding buffer. Aptamer or antibody samples were prepared in 10 µl binding buffer in separate polypropylene round-bottom tubes (chapter 3.7). Initially 100 pmol aptamer or 10 µg (66 pmol) antibody were applied, in subsequent experiments this amount could be optimised by decreasing the concentration. 90 µl cell suspension were added to 10 µl sample solution, mixed well by flicking the tubes and incubated for 30 min at 21°C upon repeated mixing. Incubation was carried out at 21°C to find a balance between keeping cells in their original state (best at 4°C) and allowing sufficient aptamer binding (usually at 37°C). Each tube represented a separate binding reaction, including cells alone, SA-PE only, a biotinylated non-binding aptamer as negative controls as well as a respective aptamer or antibody positive control, usually 3G8 and cetuximab (chapter 3.2). The binding reaction was washed once with 1.5 ml binding buffer as described before, but only 5 min centrifugation to keep the duration of cells at ambient temperature as short as possible. Cells were resuspended in 90 µl binding buffer + 10 µl SA-PE solution (chapter 3.2) and streptavidin-phycoerythrin was allowed to anneal to cell-bound, biotinylated aptamers for 10 - 15 min at 21°C under repeated mixing. Two washing steps with 1.5 ml binding buffer as before were followed by resuspension in 995 µl binding buffer + 5 µl propidium iodide (chapter 3.4), allowing the exclusion of dead cells in later analyses. Samples were immediately measured via Fluorescence-activated cell sorting (FACS) using a FACScan device (chapter 3.8). For each binding reaction, 15.000 events were collected and analysed using CellQuest Pro software (chapter 3.9). Intact cells were identified by using a plot of FSC-H against SSC-H, fluorescein-labelled samples recorded using the FL1-H detector, PE-labelling with the FL2-H detector and propidium iodide-based dead cell exclusion in the FL3-H channel. A significant increase of respective histogram mean fluorenscence in comparison to all negative controls indicated evidence of cellular binding.

4.4.4 Preparation of peripheral blood mononuclear cells

Ficoll as the most common technique for separating peripheral blood mononuclear cells (PBMCs) was applied. Whole EDTA-stabilised blood from healthy donors (distributed by Merck's medical department) was mixed with a compound aggregating erythrocytes, thereby

increasing their sedimentation rate. The sedimentation of PBMCs was only slightly affected; they could be collected from a distinct layer between serum of the upper part and settled erythrocytes and granulocytes at the bottom of the tube.

For the separation of PBMCs, Lymphoprep tubes (chapter 3.7) were applied utilising one-step density gradient centrifugation with sodium metrizoate (Isopaque) and Ficoll (Boyum, 1968). 15 ml DPBS and 18 ml EDTA-blood were poured freely into Lymphoprep-tubes, mixed by inverting the tube and centrifuged for 25 min at 800 g and precisely 21°C. Serum was removed using a Pasteur pipette and the PBMC-layer was decanted into a fresh 50 ml tube. PBMCs were washed two times in respective medium by centrifugation for 10 min at 250 g and 21°C. Cells were rigorously resuspended in 1 ml of the same medium using a pipette to yield single cell suspensions and counted in a CEDEX cell counter in 1:100 dilution (10 µl cells + 990 µl medium).

4.4.5 Preparation of Natural Killer cells

Natural Killer cells (NK cells) were isolated from PBMC preparations of healthy donors (chapter 4.4.4) with a NK cell isolation kit (chapter 3.2) applying the MACS technique: Non-NK cells were depleted by indirect labelling with lineage-specific, biotinylated antibodies that were later coupled to streptavidin-coated magnetic beads enabling removal of these cells with a magnet. NK cells were not marked, hence enriched in the flow-through.

The procedure was carried out following the manufacturer's instructions. Briefly, all steps were carried out on ice, samples volumes are described for 1×10^7 PBMCs; cells were pelleted for 10 min at 250 g and 4°C, each 1×10^7 PBMCs were resuspended in 40 µl MACS buffer (chapter 3.6), 10 µl NK cell biotin-antibody cocktail were added, mixed well and antibodies were allowed to bind non-NK cells for 10 min. Then, 30 µl buffer and 20 µl NK cell microbead cocktail were added, mixed well and beads could bind to biotinylated antibodies during 15 min incubation. Cells were washed with 2 ml buffer, centrifuged as before, the supernatant was removed completely and cells were resuspended in 500 µl buffer. Separation was carried out using the autoMACS separator running program "depletes". The NK cell containing flow-through was collected in a fresh 50 ml tube and cells were counted in a CEDEX cell counter in 1 : 100 dilution (10 µl cells + 990 µl medium).

4.4.6 ADCC assay

The cytotoxic function of bi-specific aptamers or reference antibodies was determined by assaying Aptamer/Antibody Dependent Cellular Cytotoxcitiy (ADCC) *in vitro*. For this, tumour cell lines (GTL-16 or EBC-1, chapter 3.1) were exposed to isolated PBMCs (chapter 4.4.4) in absence or presence of effector molecules. The specific cell lysis was measured via release of Glyceraldehyd-3-Phosphate Dehydrogenase (GAPDH) in a coupled enzyme reaction with Luciferase (aCella-TOX kit, chapter 3.2). GAPDH was found to be abundantly present in all known living cells, catalysing the oxidative phosphorylation of D-glyceraldehyde-3-phosphate to 1,3-diphosphoglycerate. This served as substrate for 3-Phosphoglyceric Phosphokinase (PGK) to produce ATP which was further used by added Luciferase/luciferin yielding bioluminescence that was measured. More dead or dying cells lead to higher GAPDH release, increased ATP levels and thus a higher bioluminescence signal.

All ADCC measurements were conducted in Optiplate microtiter plates (later sealed with airpore tape sheets, chapter 3.7) at least in triplicates in 100 µl total volume ADCC medium (chapter 3.6) for 4 h at 37°C and 5 % CO_2. 10^4 tumour cells (of >90 % viability) were combined with PBMCs in a ratio of 80:1. This ratio was varied in later experiments from 80:1 to 5:1. Cetuximab (chapter 3.2) as positive antibody reference was applied in high concentrations of 50 nM (7.5 ng/µl) and bi-specific aptamers in serial dilutions from 500 nM to 1 pM. Aptamers and antibodies were pre-incubated for 15 min at 37°C before adding effector cells. Negative controls comprised mono-valent aptamers at comparable concentrations and samples lacking any additional molecules. Reference triplicate measurements were medium, target cells (spontaneous target cell lysis), effector cells (spontaneous effector cell lysis) and target cells for detergence-induced maximal lysis. The outer rows and columns of each microtiter plate were left out to avoid boundary effects in luminescence readings.

ADCC assay enzyme reactions were performed as suggested by the manufacturer. Briefly, 15 min prior to full incubation time 10 µl lytic agent were added to wells containing target cells for maximal lysis readout and microtiter plates further incubated at 37°C. For preparation of enzyme solutions, 4 ml green label enzyme assay reagent and 4 ml enzyme assay diluent A were combined as well as 700 µl magenta label detection assay diluent B with 3.15 ml dH_2O. Following steps were carried out uninterrupted: 28 µl green label G3P vial C solution were added to tube A, mixed and 100 µl dispensed in each microtiter plate well with

a multipette. Then, 77 µl magenta label vial B were added to tube B, mixed and exactly 50 µl were pipetted in each well. Microtiter plates were mixed by gentle shaking, transferred in the dark to a Varioskan luminometer (chapter 3.8) and bioluminescence was measured for 100 ms every minute for 10 min. Raw data was exported to Microsoft Office Excel (chapter 3.9), and the mean background luminescence of „medium only“ samples was calculated and subtracted from each individual well. Specific target cell lysis was calculated applying the formula

$$\%\ specific\ lysis = 100\ x\ \frac{sample\ lysis - spont.\ target\ cell\ lysis - spont.\ effector\ cell\ lysis}{maximal\ lysis - spont.\ target\ cell\ lysis}$$

Based on resulting values, specific target cell lysis mean and standard deviation were calculated and blotted for each aptamer concentration. Cetuximab-mediated tumour cell lysis of more than 30 % indicated the success of the respective ADCC assay measurement.

5 RESULTS

5.1 Determination of target protein quality

Since high target protein quality is crucial for the success of aptamer SELEX, several target protein quality controls were conducted before starting the selection of CD16α specific aptamers.

5.1.1 Assessment of purity and glycosylation

SDS-PAGE (chapter 4.3.2) with subsequent coomassie staining (chapter 4.3.4) demonstrated purity higher than 90 % of all His-tagged CD16 isoforms and the monoclonal antibody 3G8 (Figure 9, A, lanes 2-4). Electrophoretic migration at 50 kDa or 75 kDa indicated glycosylation similar to NK cell-presented CD16 for His-tagged or Fc-fusion proteins, respectively (Figure 9). Both CD16-HisTag fusion proteins could be pulled out of solution quantitatively by 3G8 (Figure 9, A, lanes 7 and 8), but not in its absence (Figure 9, A, lanes 5 and 6). CD16 allotype Fc-fusions exhibited high purity but partly aggregation (Figure 9, B, additional bands in lanes 2 and 3). Small fractions of applied Fc-fusion proteins could be pulled out of solution by 3G8 (Figure 9, B, lanes 7 and 8 in comparison to lanes 2). Unspecific binding of Fc-CD16α(V158) to beads (Figure 9, B, lane 5) was much weaker than specific signals via 3G8 (lane 7), leaving the validity of this sample unaffected.

5.1.2 Validation of correct target protein folding

Since aptamers could exhibit high selectivity for minor conformational changes in target proteins, validation of correct folding was crucial for success of SELEX and carried out by immunoprecipitation (IP) and enzyme-linked immunosorbent assay (ELISA) measurements. Immunoprecipitated samples (chapter 4.3.7) were analysed by SDS-PAGE (chapter 4.3.2) and coomassie stained (chapter 4.3.4) as well as detected by a western blot (chapters 4.3.5 and 4.3.6). For the specific detection of CD16α-6His and CD16β-10His fusion proteins, a mouse penta His antibody (1:2000) and a goat anti-mouse peroxidase conjugate (1:3000) were applied. For CD16 Fc-fucion proteins, a rabbit anti-human-Fc antibody (1:2000) and a goat anti-rabbit peroxidase conjugate (1:3000) were used (all described in chapter 3.2). The conformation-specific antibody 3G8 immunoprecipitated equivalent amounts of His-tagged CD16 proteins (Figure 9, A), thereby verifying correct folding of these recombinant soluble proteins. Fc-fusions of both CD16α allotypes were captured from solution by 3G8 more so

than in negative control samples, but in a clearly smaller portion than His-tagged proteins (Figure 9, B). This indicates a partly incorrect conformation or sterical hindrance by the Fc-fusion.

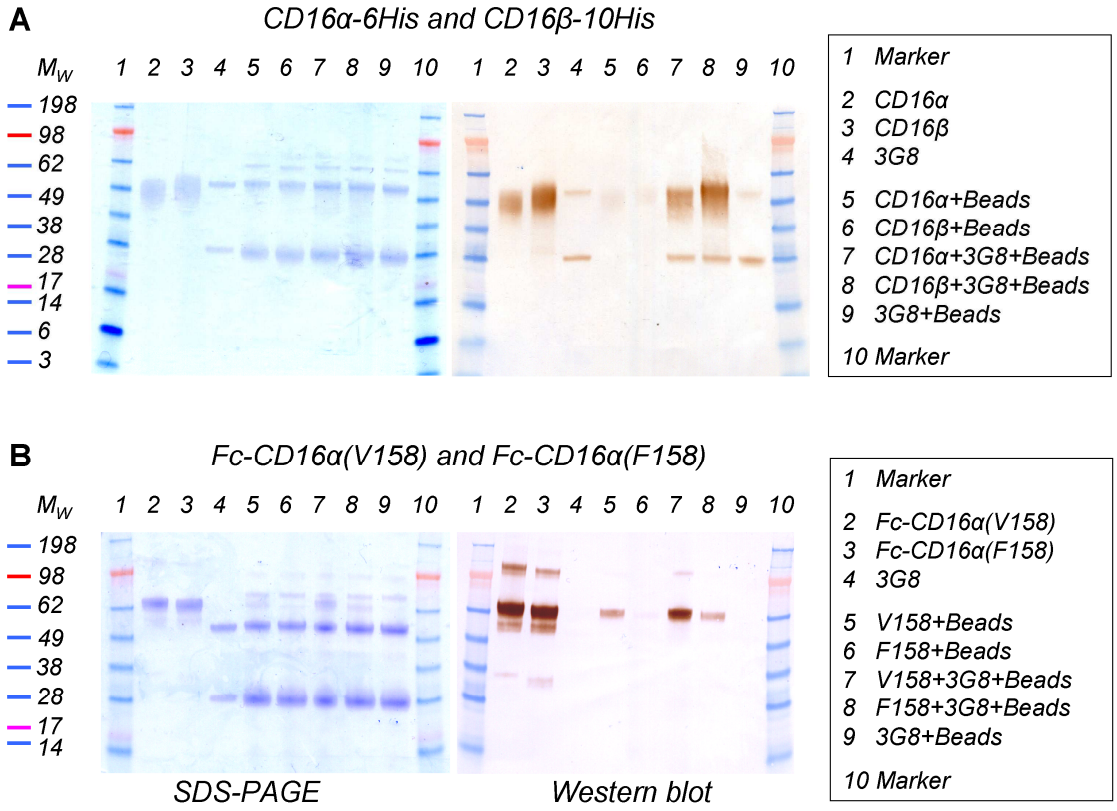

Figure 9: SDS-PAGE and immunoprecipitation of several recombinant CD16 proteins.

A, His-tagged CD16 isoforms and the monoclonal antibody 3G8 exhibited high purity (lanes 2-4). Both CD16 proteins were immunoprecipitated by 3G8 (lanes 7 and 8), but not in its absence (lanes 5 and 6). B, CD16 Fc-fusions were of similar purity but partly aggregated (lanes 2 and 3) and a small portion was immunoprecipitated by 3G8 (lanes 7 and 8). V158, Fc-CD16α(V158); F158, Fc-CD16α(F158); SDS-PAGE bands of IP samples in lanes 5 – 9 at 25 and 50 kDa represented the secondary goat-anti-mouse antibody detached from magnetic beads.

In ELISA measurements (chapter 4.3.8), binding of all recombinant CD16 proteins to 3G8 as well as cetuximab - CD16α-6His interaction confirmed functionality and hence correct folding of CD16 target proteins (Figure 10).

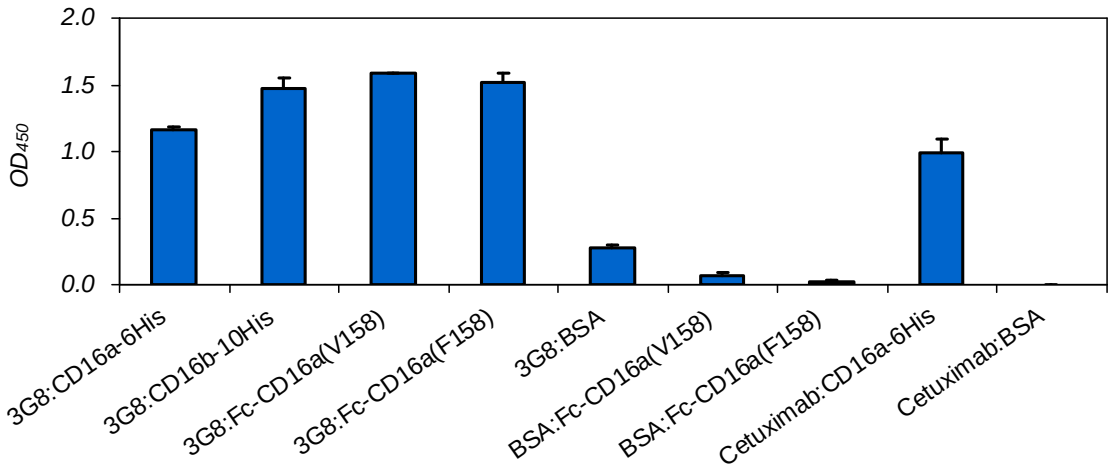

Figure 10: ELISA of all CD16 target proteins to conformation-sensitive antibodies 3G8 and cetuximab.

3G8, BSA or cetuximab were coated to microtiter plates and binding of CD16 His- and Fc-fusion proteins were analysed in triplicate. All recombinant CD16 fusion proteins were bound by 3G8 or cetuximab, while BSA negative controls exhibit only minor background binding. Bars represent mean values with standard deviation as error bars.

5.1.3 Determination of isoelectric properties

Since a low pI (<5.5) could impede aptamer selection due to repulsion between negatively charged groups of the nucleotide backbone and the target protein at physiological pH, the pI of CD16α-6His was determined via isoelectrical focussing (chapter 4.3.3). Differently charged His-tag residues lead to several bands for one CD16α molecule. However, the experimentally calculated mean pI of 6.6 ± 0.2 agreed with the *in silico* predicted value of 6.7 as determined by DNA Star Edit Seq software (chapter 3.9). This pI indicated that it is feasible to raise aptamers against CD16α.

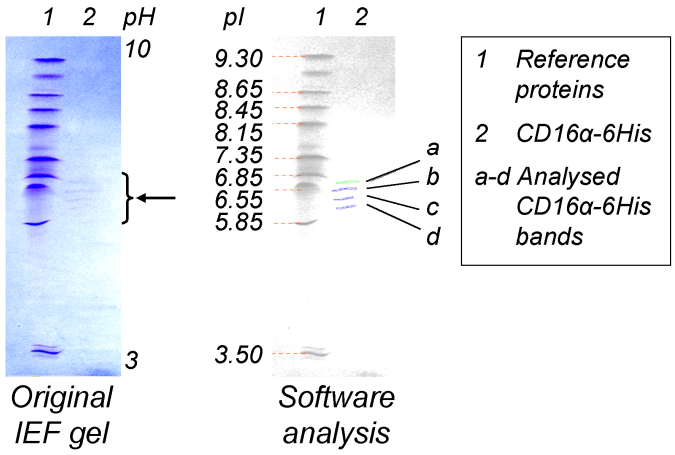

Figure 11: Isoelectric focussing of CD16α-6His.

Several protein bands were recognisable in the coomassie stained IEF gel (left) that resemble the same His-tagged CD16 protein in differently charged states. Comparison of CD16 bands to marker proteins lead to the calculation of a mean pI of 6.6 (right).

5.1.4 Nitrocellulose filter capacity test

To ascertain if there was a complete separation of all target protein bound from non-binding aptamers in SELEX, the CD16 binding capacity of nitrocellulose filter membranes was determined by a capacity test (chapter 4.2.1.1). The full amount of CD16α or CD16β used in initial SELEX rounds was captured quantitatively by nitrocellulose filters (Figure 12).

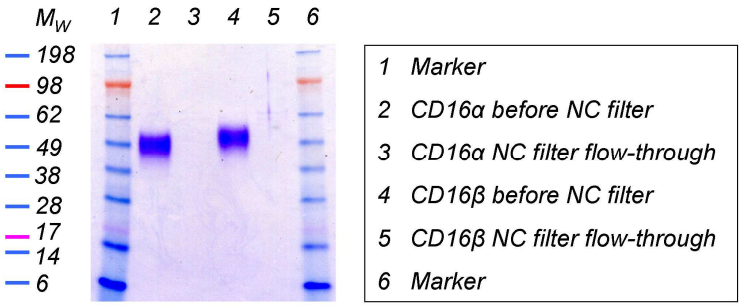

Figure 12: Nitrocellulose filter capacity test.

The full amount of CD16α (lane 2) or CD16β (lane 4) fusion proteins was absent in the flow-through (lanes 3 or 5, respectively), hence target proteins were captured completely by the filter.

5.2 Aptamer selection

With high quality target protein available, several SELEX approaches (Figure 13) were conducted applying both DNA and modified rRfY RNA aptamer pools for selection of specific and high affinity CD16α binders.

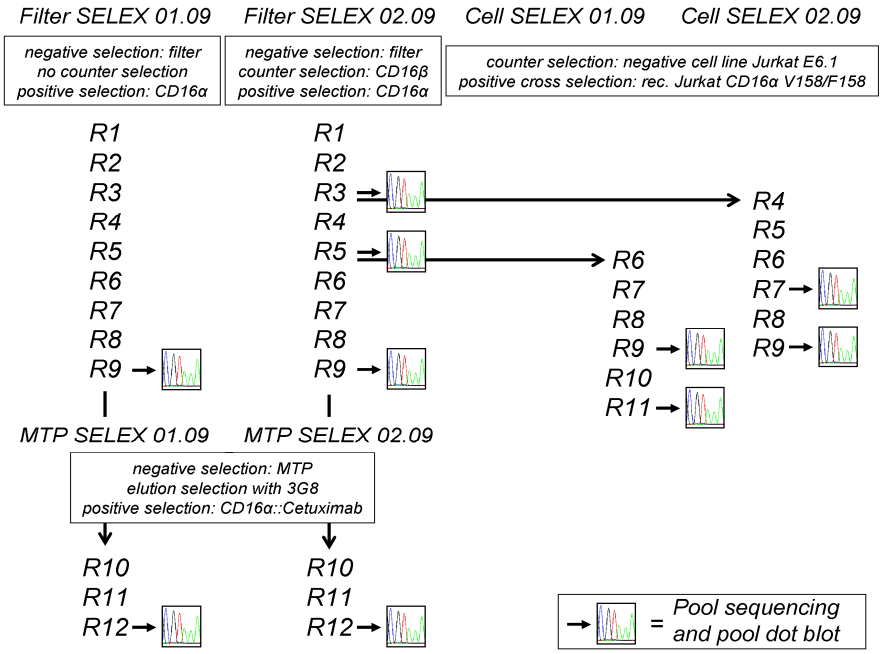

Figure 13: SELEX scheme of different CD16 DNA selection approaches.

Nine rounds of filter SELEX were conducted in parallel, only differing in the lack of counterselection in filter SELEX 01.09 (left). Additional rounds were performed using CD16 immobilised on microtiter plates and elution selection with monoclonal antibody 3G8 to enrich aptamers specific for the Fc binding domain of CD16. Filter SELEX R3 and R5 were used as pre-selected starting pools for two parallel selections targeting recombinant Jurkat cells in a cell SELEX (right). Filter, nitrocellulose filter; MTP, microtiter plate; CD16α, CD16α-6His; CD16β, CD16β-10His.

5.2.1 CD16 DNA filter SELEX

SELEX for DNA CD16 specific aptamers was initiated with nine rounds of filter SELEX (chapter 4.2.1.2) in parallel with both positive selection against CD16α-6His only (Figure 13, filter SELEX 01.09) and an additional counter-selection against CD16β-10His (filter SELEX 02.09). With each successive round, the target protein concentration was decreased while the amount of tRNA competitor was increased and PCR cycles were monitored (appendix, Table 4). Fewer numbers of PCR cycles from round 6 on indicated enrichment of aptamers, therefore radioactive labelling (chapter 4.1.9) of aliquots from both round 9 pools was used to determine the pool affinities towards CD16α and CD16β by dot blot measurements (chapter 4.3.9). Both round 9 pools bound with K_D values of 62 nM (filter SELEX 01.09) and 41 nM (filter SELEX 02.09) to CD16α, but not at all to CD16β. The naive R0 library exhibited minimal affinity to both target proteins that was repressed by addition of the unspecific competitor tRNA (Figure 14).

To specifically select for aptamers binding in the Fc binding domain of CD16 with a two-digit nanomolar affinity, two additional SELEX rounds were performed on microtiter plates (chapter 4.2.2) followed by one final filter SELEX round (chapter 4.2.1.2): Pre-selected R9 pools of both selections were allowed to bind MTP-immobilised CD16α, non-binders were washed off and then Fc-domain specific aptamers were eluted by addition of 3G8 in 100-fold molar excess. 3G8 was reported to bind in or near the Fc-binding domain of CD16 with at least 5.7 nM affinity and was used to potentially displace aptamers that bound this epitope. Finally, these aptamers were applied in a filter SELEX round 12 offering a CD16α - cetuximab complex with a reference affinity of 710 nM; only aptamers of higher affinities than that should bind to the target complex. Hence, aptamers enriched in such a way should bind near or in the Fc-binding domain of CD16α with low nanomolar affinity. PCR cycle monitoring revealed fewer cycles in round 12 were needed, which indicated an increased enrichment (Figure 14).

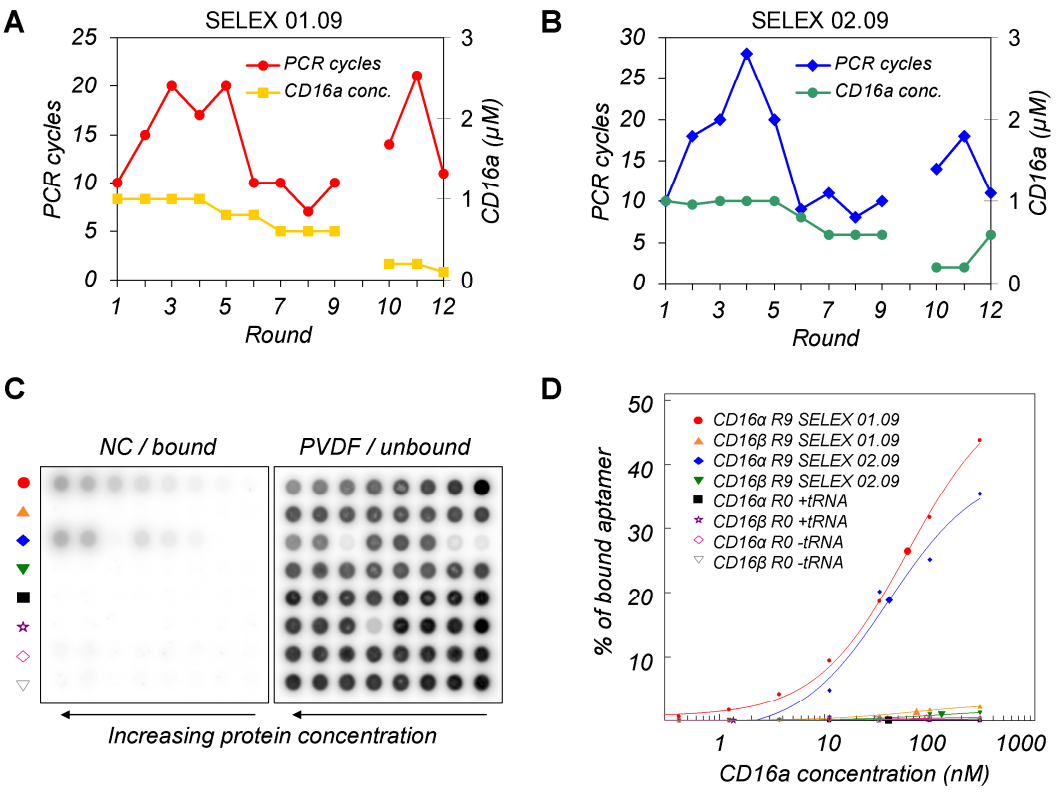

Figure 14: PCR cycle monitoring and determination of SELEX pool affinity via dot blot.

A and B, PCR cycle monitoring of aptamer SELEX 01.09 and 02.09, respectively. Filter SELEX was performed until round 9 and MTP SELEX in rounds 10 - 12. In later stages of both selections (rounds 6 – 9 and round 12), low numbers of PCR cycles needed for aptamer re-amplification indicated enrichment. C, Dot blot raw data readout of bound aptamers on the NC membrane or unbound molecules on PVDF. D, Processed dot blot data revealed that both round 9 pools exhibited two-digit nanomolar CD16α affinities (red and blue), but did not bind to CD16β (orange and green). Magnified circles indicate the calculated K_D values of 62 nM (filter SELEX 01.09) and 41 nM (filter SELEX 02.09).

Assessment of aptamer enrichment during filter and MTP SELEX steps was achieved by separation of pools into single aptamers by TOPO-cloning (chapter 4.1.7) and subsequent single sequence analysis (chapter 4.1.8) of rounds 9 and 12 for both selections. Both selections yielded similar sequences and were thus jointly analysed. 192 sequences of rounds 9 were sequenced, 185 of which were analysable (97 %). 86 % of all sequences were grouped in 13 main families of 90 % sequence identity (designated CLN0015 - CLN0027) and single aptamers were enriched up to 31 % of the whole pool (CLN0015, Figure 16). Sequencing of round 12 yielded five new aptamers (CLN0028 – CLN0032) with a prevalence of 1 - 11 % in the pool. Several motifs were found througout many aptamers, but also unique sequences were found. Figure 16 displays sequences of all selected DNA CD16 aptamers.

5.2.2 CD16 DNA cell SELEX

Since the aim of this work was the selection of aptamers binding to NK cell-expressed CD16α, SELEX was also performed directly on CD16α-overexpressing cell lines. To avoid massive enrichment of unspecific aptamers, two cell SELEX approaches were initiated with pre-selected but still variable libraries from filter SELEX 02.09 round 3 (cell SELEX 01.09) and round 5 (cell SELEX 02.09). Six additional rounds were performed (chapter 4.2.3) with alternating cross-selection using Jurkat cells that express recombinant CD16αV158 or CD16αF158 proteins to select for aptamers binding to both allotypes. PCR cycle monitoring exhibited a slight decrease in cycle numbers upon increased stringency (Figure 15, A and B). Direct affinity assessment of cell SELEX pools was achieved by 5' radioactive labelling of initial filter SELEX rounds 0, 3, and 5, cell SELEX 01.09 rounds 7 and 9 as well as cell SELEX 02.09 rounds 9 and 11 (chapter 4.1.9) followed by dot blot measurements of all these pools (chapter 4.3.9). In both selections, CD16α-6His pool affinity increased from no binding to 103 nM or 175 nM in round 9 (01.09) or round 11 (02.09), respectively. Binding to both allotypes was observed in both selections, while CD16β-10His was not bound at all (Figure 15, C - F).

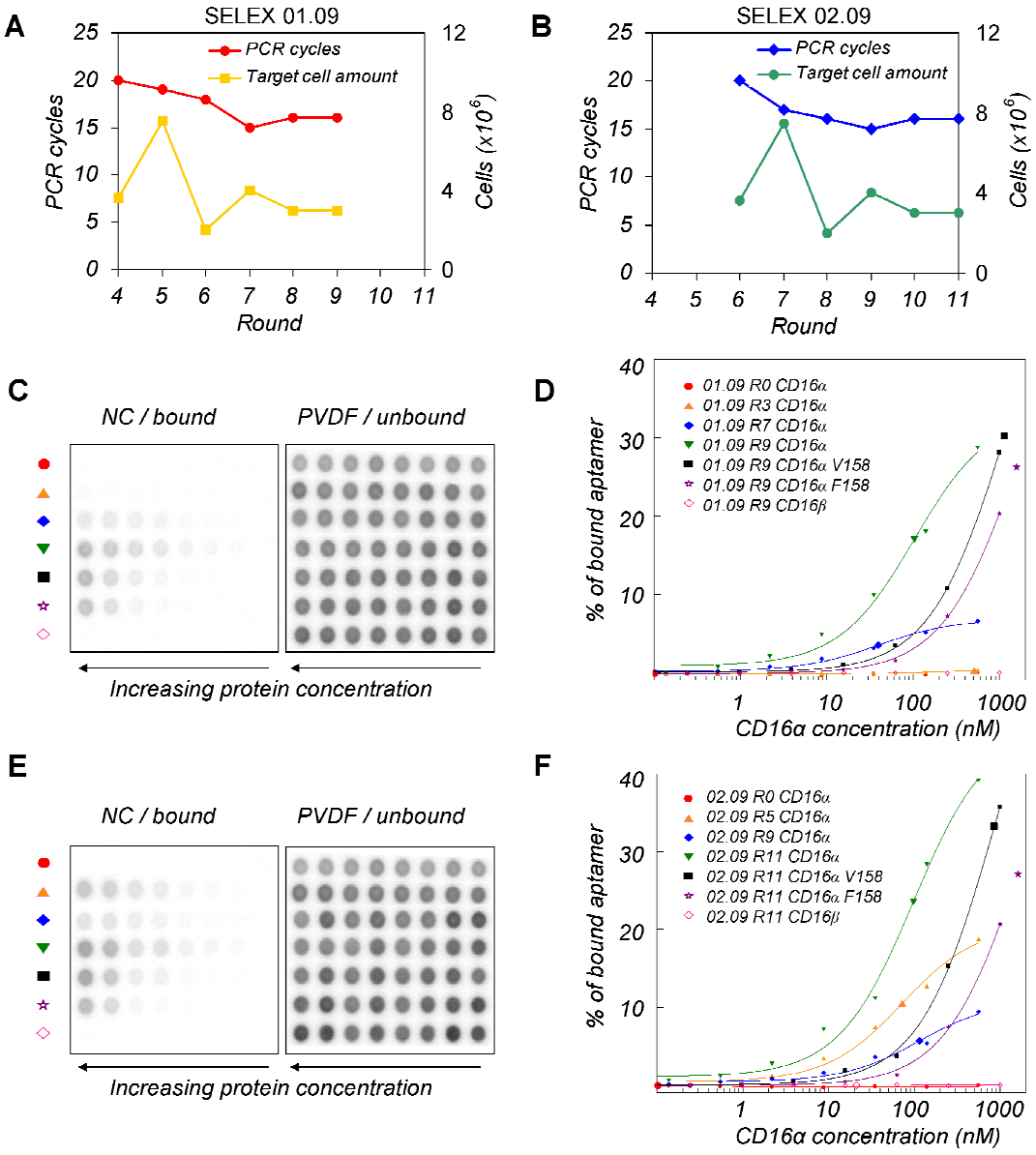

Figure 15: PCR cycle monitoring and pool dot blots for affinity determination.

A and B, PCR cycle monitoring of cell SELEX 01.09 and 02.09, respectively. Target protein concentration in form of applied cell amount was decreased over time, fewer cells were used in third rounds due to a lack of availability. PCR cycles decreased slightly indicating a putative enrichment. Cell SELEX 01.09 dot blot raw (C) and processed (D) data revealed an increasing pool affinity towards CD16α when comparing rounds 0, 3, 7 and 9 (red, orange, blue to green). Raw data (E) and calculated graphs (F) of cell SELEX 02.09 exhibited a similar pattern. CD16α, CD16α-6His; CD16β, CD16β-10His; CD16α V/F158, Fc-CD16α(V/F158).

Since pool affinity determination indicated enrichment of CD16α specific aptamers, cell SELEX pools 01.09 R7 and R9 as well as 02.09 R9 and R11 were applied to single aptamer separation by TOPO-cloning (chapter 4.1.7) and subsequent analyses of 96 single sequences (chapter 4.1.8). All pools were found to be highly enriched, containing only 3 – 19 % single sequences, but up to a 40 % occurrence of single aptamers (Figure 17). Eleven new aptamer sequence families (of 90 % sequence identity) were found in cell SELEX and designated CLN0118 – CLN0128 (Figure 16), but also 6 sequences already known from filter SELEX were enriched (CLN0015, 20, 21, 22, 28, 32). Unlike in filter selection, unique sequences to either SELEX approach indicated the essential impact of the composition of a starting pool for the outcome of a selection (Figure 17 and Table 6, appendix).

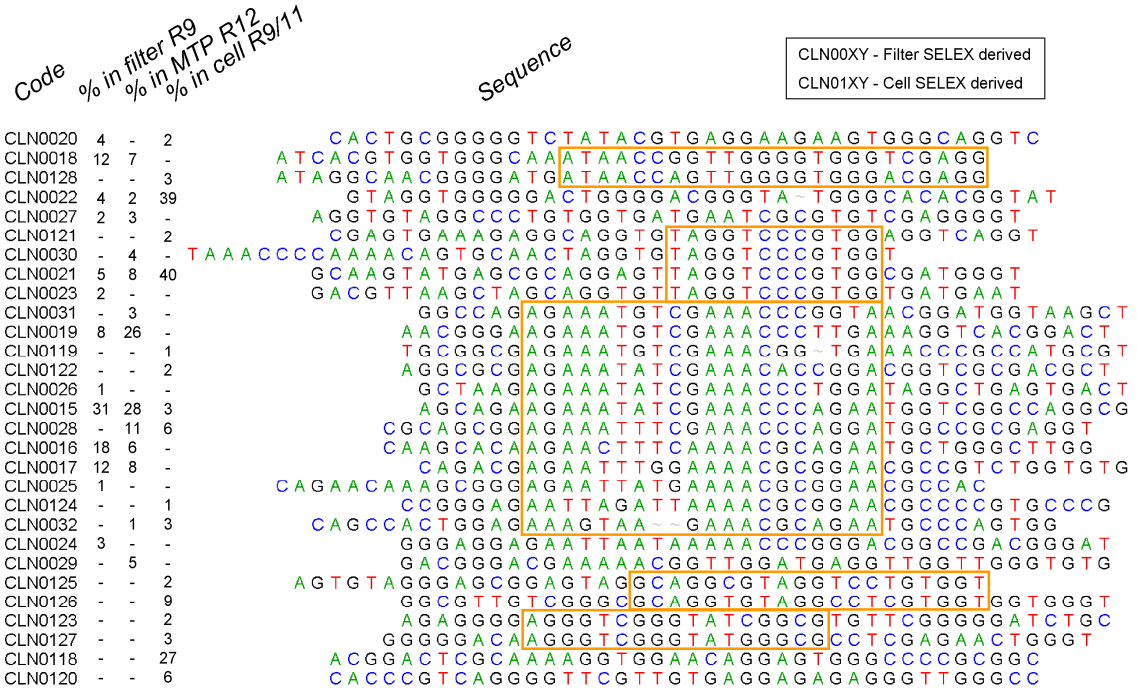

Figure 16: Alignment and frequencies of all selected DNA CD16 aptamers.

Sequence comparison of CD16 aptamers from different selections revealed several motif blocks (orange mark) that mostly contained both filter and cell SELEX derived sequences. CLN0015, 21 and 22 were found throughout all selections. Randomised regions are shown without invariant flanking sequences. Two-digit codes indicate filter SELEX derived aptamers, three-digit codes cell SELEX sequences.

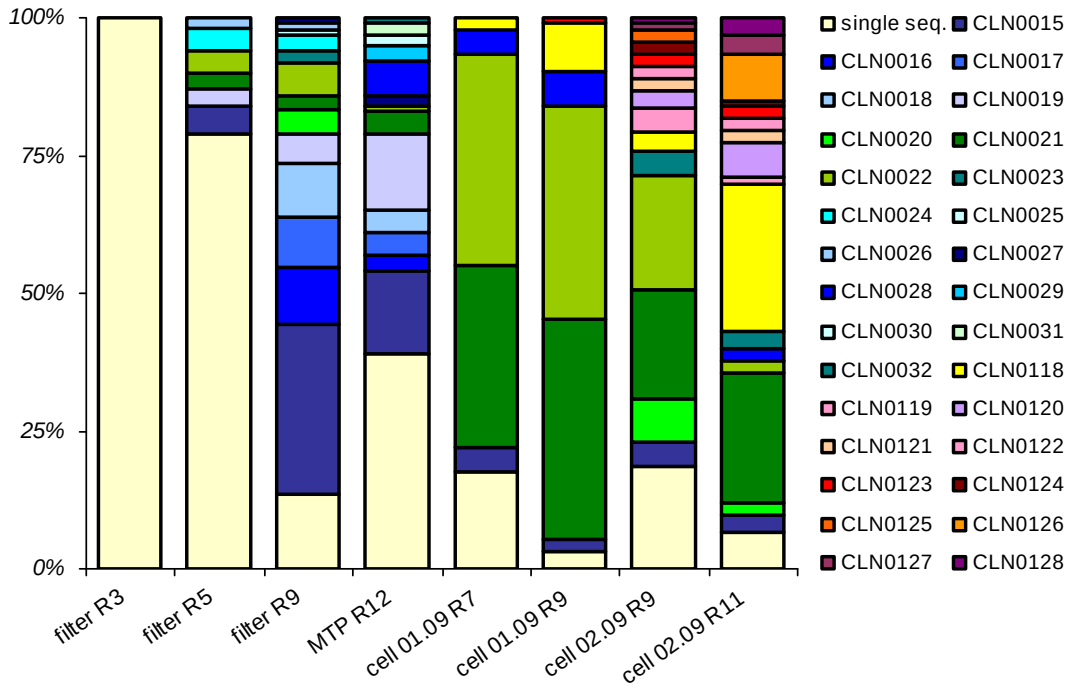

Figure 17: Variation of the aptamer pool composition during all DNA selections.

The initially totally variable pool of round 3 exhibited enrichment of several aptamers upon progression of each particular SELEX approach. Major filter SELEX sequences (blue and green colours) were found to some extent as well in cell SELEX pools, intermittent even highly enriched (green colours). Cell SELEX 02.09 yielded many aptamers not found in other selections (yellow and red colours). Filter and MTP SELEX approaches 01.09 and 02.09 were analysed jointly. R3, round 3 *et cetera*. Two-digit codes indicated filter SELEX, three-digit codes cell SELEX derived aptamers. Associated exact values can be found in Table 6, appendix.

5.2.3 CD16 rRfY filter SELEX

Since DNA aptamers are prone to low serum stability, putatively more stable aptamers of the rRfY composition were additionally applied for selection of specific and high affinity CD16α binders. rRfY SELEX (4.2.1.3) was performed for nine rounds with cross-selection of CD16α-6His(V158) and Fc-CD16α(F158) to select for aptamers binding to both allotypes while avoiding Fc- or His-tag-binders. Negative selection against filter was carried out from round 2 on and counterselection against CD16β-10His started in round 3 (Figure 18, panel A). PCR cycle monitoring showed a clear decrease in the required re-amplification cycles indicating enrichment of rRfY CD16 specific aptamers, even upon lowered target protein and increased tRNA competitor concentrations (Figure 18, B). R7 and R9 pools were 5' radioactive labelled (chapter 4.1.9) and the pool affinities were determined via dot blot (chapter 4.3.9). The naive R0 library exhibited desired low level CD16 affinity that could be repressed by tRNA competitor addition. Differences in labelling strength (e.g. last two lines) did not affect calculations since only relative values were used. Both selected pools showed strong binding (10 nM) to CD16α, but no binding to CD16β, as desired (Figure 18, D).

A

rRfY filter SELEX 01.09

Round	DNA conc. (µM)	Applied protein	Protein conc. (µM)	Neg. sel.	Counter sel. (µM)	tRNA (mg/ml)	PAGE	No. of PCR cycles
1	1.66	V158	1	none	0	0	yes	25
2	1	F158	0.8	filter	0	0	yes	24
3	1	V158	0.8	filter	0.8	0.1	no	20
4	1	F158	0.6	filter	0.6	0.1	yes	21
5	1	V158	0.5	filter	0.5	0.1	no	15
6	1	F158	0.4	filter	0.4	1	yes	13
7	1	V158	0.3	filter	0.3	1	yes	9
8	1	F158	0.2	filter	0.2	1	no	10
9	1	V158	0.1	filter	0.1	1	yes	9

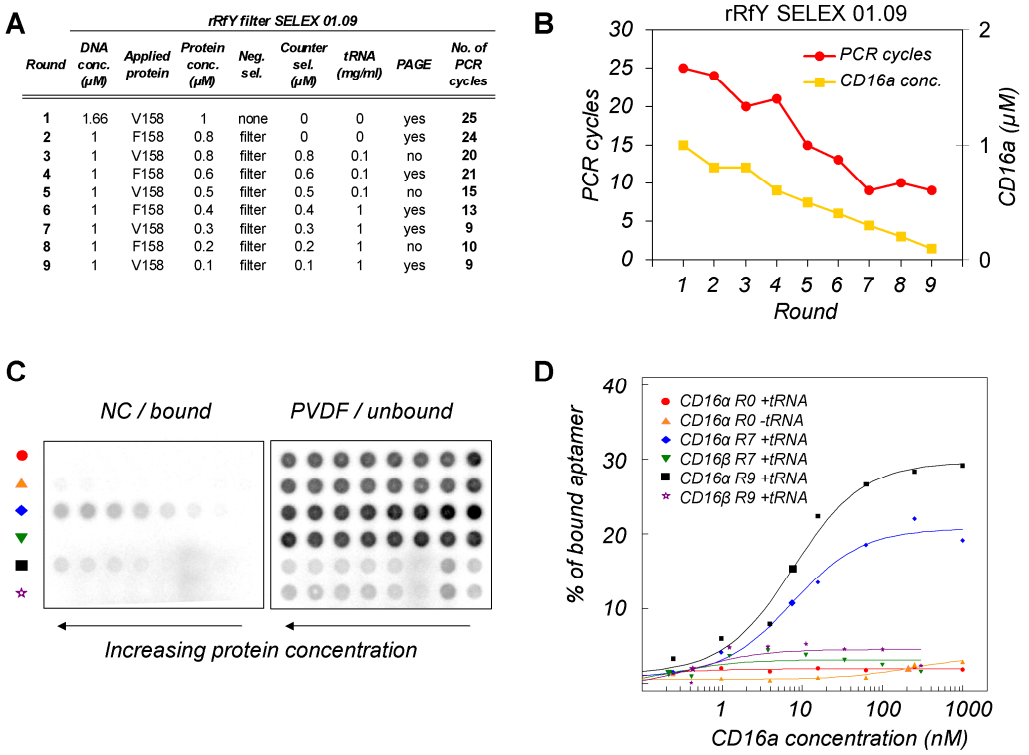

Figure 18: rRfY SELEX.

A, Specifications of rRfY SELEX approach. V158, CD16α-6His(V158); F158, Fc-CD16α(F158); counterselection target protein was CD16β-10His. B, PCR cycle monitoring indicated enrichement due to decreasing PCR cycles needed for re-amplification. C, Pool dot blot raw data showed strong binding of R7 and R9 pools (blue and black) as well as weak and reversible signals of R0 library (orange vs. red). D, Processed dot blot data revealed high affinity and specific binding of R7 and R9 rRfY pools to CD16α, but no binding to CD16β. Magnified symbols indicate calculated K_D values.

Since both PCR cycle monitoring and pool affinity measurements indicated enrichment of rRfY aptamers, 96 samples of round 7 and 9 pools were sequenced by separation of the respective ssPCR samples to single aptamers by TOPO-cloning (chapter 4.1.7) and subsequent single sequence analysis (chapter 4.1.8). 13 unique sequence families of 90 % sequence identity were found in round 7 and additional 4 aptamers in the round 9 pool (Figure 19). These rRfY CD16 aptamers were designated CLN0047 – CLN0063.

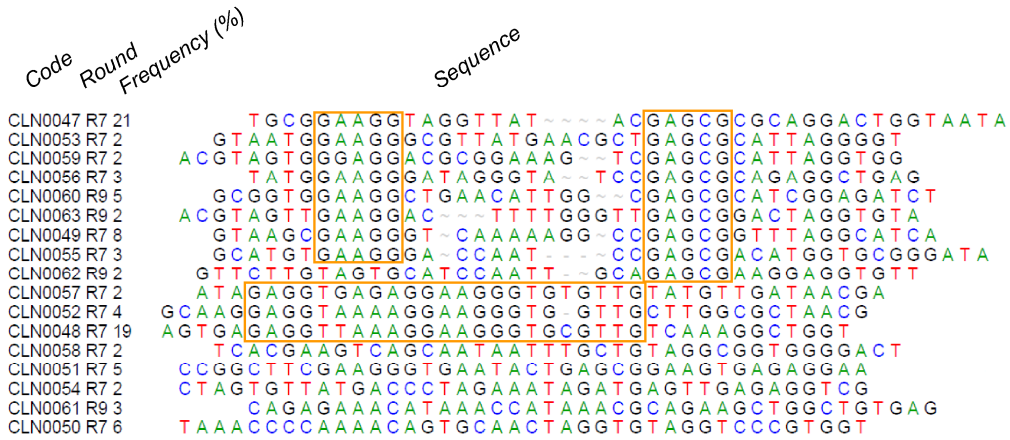

Figure 19: Overview of CD16 specific rRfY aptamer sequences.

rRfY aptamer families (of 90 % sequence identity) were enriched to 2 – 21 % in R7 and R9 pools. Several motif blocks (marked orange) as well as unique sequences were found. Randomised regions are shown without invariant flanking sequences.

5.3 Characterisation of aptamer hits

5.3.1 Affinity and specificity determination

Affinity determination for all filter and cell SELEX derived DNA CD16 specific aptamers towards all iso- and alloforms of CD16 was biochemically performed using dot blot assays. The three most abundant rRfY CD16 aptamer sequences were analysed in the same manner. Additionally, c-Met specific DNA aptamers CLN0003, CLN0004 and CLN0008 were kindly provided by Angelika-Nicole Helfrich (MerckSerono) and characterised towards c-Met specificity and affinity. CD16 and c-Met specific DNA aptamers selected by filter SELEX were synthesised (chapter 4.1.1.3) and PAGE-purified (chapters 4.1.3.2 - 4.1.5), whereas CD16 specific, cell SELEX derived aptamers were synthesised with a 3' biotin label and then purified by PAGE (chapter 4.1.1.4). rRfY aptamers were produced by PCR (chapter 4.1.1.1) using primers 5980 and 5981 (chapter 3.3), and 10 ng of sequence verified plasmid template, followed by transcription (chapter 4.1.2) and PAGE-purification (chapters 4.1.3.2 - 4.1.5). In all cases, the final concentration was determined (chapter 4.1.6). 10 pmol of each aptamer were then individually 5' radioactively labelled (chapter 4.1.9) and applied in a dot blot with their respective target proteins (chapter 4.3.9). Possible causes for wide variation in K_D values could be high sensitivity of the assay to deviation in protein batch, conformation and concentration as well as possible temperature variation (cf. chapter 5.3.2).

Most filter SELEX derived CD16 specific DNA aptamers exhibited low nanomolar affinities of 6 – 154 nM towards CD16α-6His, but no binding at all to CD16β-10His (Table 1). The four aptamers CLN0020, 21, 23 and 30 bound to both CD16α allotypes (example CLN0020 in Figure 20) and did not belong to the major motif block but comprised unique sequences (Figure 16). All other aptamers were allotype specific binders for the high affinity binding form CD16α(V158) (example CLN0015 in Figure 20 and Table 1). The negative control oligonucleotide CLNC (chapter 3.3) did not bind to any protein (data not shown, cf. Figure 30). As a representative aptamer, CLN0020 exhibited only minor binding to cynoCD16α with high three-digit nanomolar affinity as well as no binding at all to murine CD16α (data not shown). Nine aptamers were selected for further analyses and these included the five aptamers CLN0015, 18, 19, 28 and 30 with the highest affinities and the four sequences CLN0020, 21, 23 and 30 binding both CD16α allotypes.

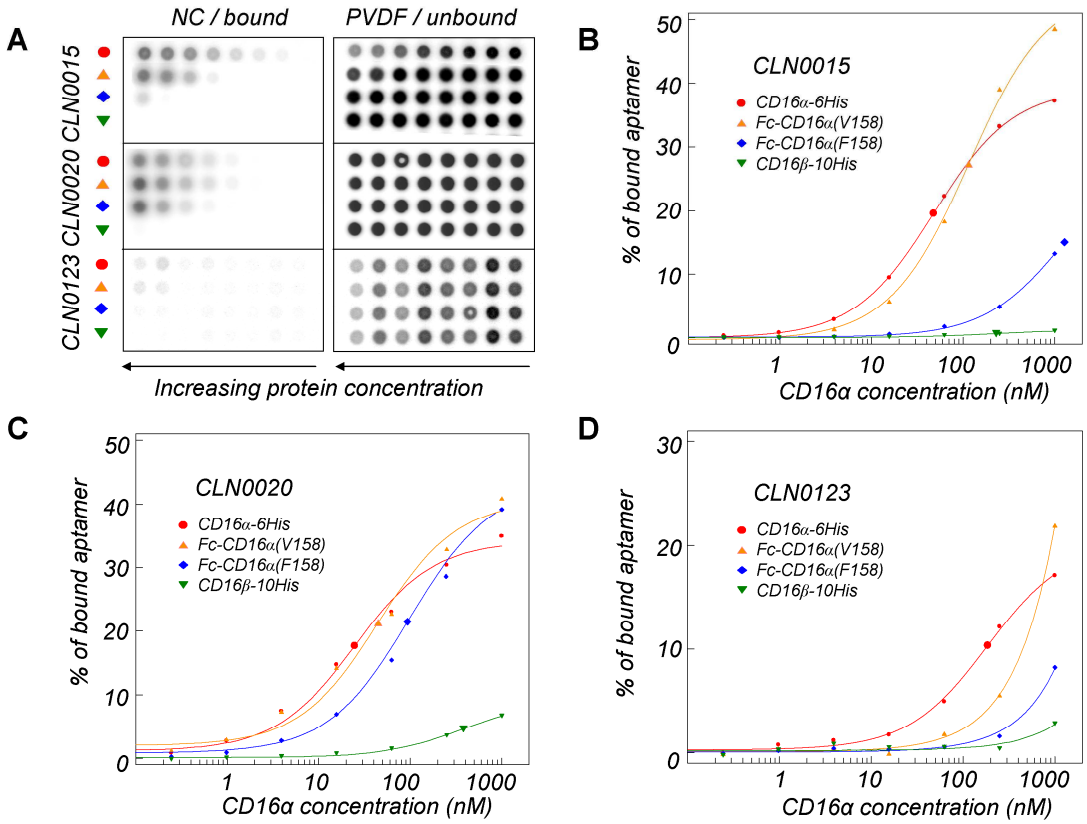

Figure 20: Examples of affinity determination by dot blot.

A, Dot blot raw data of three DNA aptamers from filter and cell SELEX. B, CLN0015, as representative of a large motif block, bound with two-digit nM affinity to CD16α V158 allotype (red and orange), much weaker to CD16α F158 (blue) and not at all to CD16β (green). C, CLN0020 exhibited high affinity to both CD16α allotypes whilst only very weakly binding CD16β. D, Cell SELEX derived CLN0123 bound with moderate affinity to CD16α-6His but less to the Fc-fusion of the same allotype. In comparion to Fc-CD16α(V158), binding to Fc-CD16α(F158) was weaker and CD16β was nearly not bound. Enlarged symbols represent calculated K_D values. NC, nitrocellulose membrane readout; PVDF, polyvinylidenfluoride membrane readout.

CD16 specific DNA aptamers isolated in cell SELEX were analysed in biotinylated form and exhibited intermittent no to low affinity of approximately 1000 nM to recombinant CD16α-6His (Table 1). The two abundant sequences CLN0118 and CLN0126 bound with 31 nM and 46 nM, respectively, to CD16α of both alloforms (dot blot data not shown). CLN0123 exhibited a K_D of 193 nM to CD16α-6His, preferentially binding the V158 allotype (Figure 20). Binding to CD16β-10His again was not observed as predicted when pre-selected pools were used. Already present in biotinylated form, all cell SELEX aptamers were further characterised for cellular binding.

Out of eleven selected CD16 specific rRfY aptamers, the three most prevalent sequences CLN0047, 48 and 49 were analysed and exhibited high affinity to CD16α-6His with 44 nM, 20 nM and 49 nM, respectively, whilst no binding to CD16β was detected (data not shown). In addition to these effector cell-specific aptamers, tumour-specific aptamers of rRfY composition were not selected or available. Additionally, for the design of bi-specific aptamers linkage by full synthesis was favoured over hybridisation (chapter 5.4.1) that would have enabled the use of diverse compositions. Thus, the rRfY aptamers were not characterised or applied any further.

Table 1: Dot blot determined affinities to CD16α-6His or C-Met-Fc fusion protein of all applied aptamers.

CLN code	*K_D (nM)*	*n*	*CLN code*	*K_D (nM)*	*n*	*CLN code*	*K_D (nM)*	*n*
CD16 DNA filter SELEX			***CD16 DNA cell SELEX***			***CD16 rRfY filter SELEX***		
15	24 ± 18	7	15	24 ± 18	7	47	44	1
16	48 ± 26	4	20	45 ± 28	10	48	20	1
17	42 ± 33	4	21	25 ± 19	5	49	49	1
18	38 ± 26	4	22	401 ± 79	2			
19	29 ± 11	4	28	76 ± 42	4			
20	45 ± 28	10	32	429 ± 8	2	***c-Met DNA filter SELEX***		
21	25 ± 19	5	118	31 ± 20	2			
22	401 ± 79	2	119	no binding	2	3	0.091 ± 0.040	3
23	18 ± 14	5	120	>1000	2	4	11 ± 5	6
24	61 ± 30	4	121	no binding	2	8	10 ± 9	2
25	105 ± 25	4	122	>1000	2			
26	154 ± 95	4	123	193 ± 29	4			
28	76 ± 42	4	124	1000	2			
30	6 ± 5	6	125	>1000	2			
31	81 ± 102	4	126	46 ± 11	2			
32	429 ± 8	2	127	no binding	2			
			128	1000	2			

Three c-Met specific DNA aptamers (designated CLN0003, CLN0004 and CLN0008) were kindly provided by Angelika-Nicole Helfrich. All sequences shared certain motifs (Figure 21) that in part included 3' flanking region of CLN0004 and CLN0008. The latter aptamer was excluded from further analyses due to a highly related sequence and affinity (Figure 21 and Table 1), only CLN0003 and CLN0004 were characterised further. Dot blots revealed high affinity binding to c-Met, but not to Fc, for CLN0003 and CLN0004 with averaged K_D values of 91 pM and 11 nM, respectively (Figure 21 and Table 1).

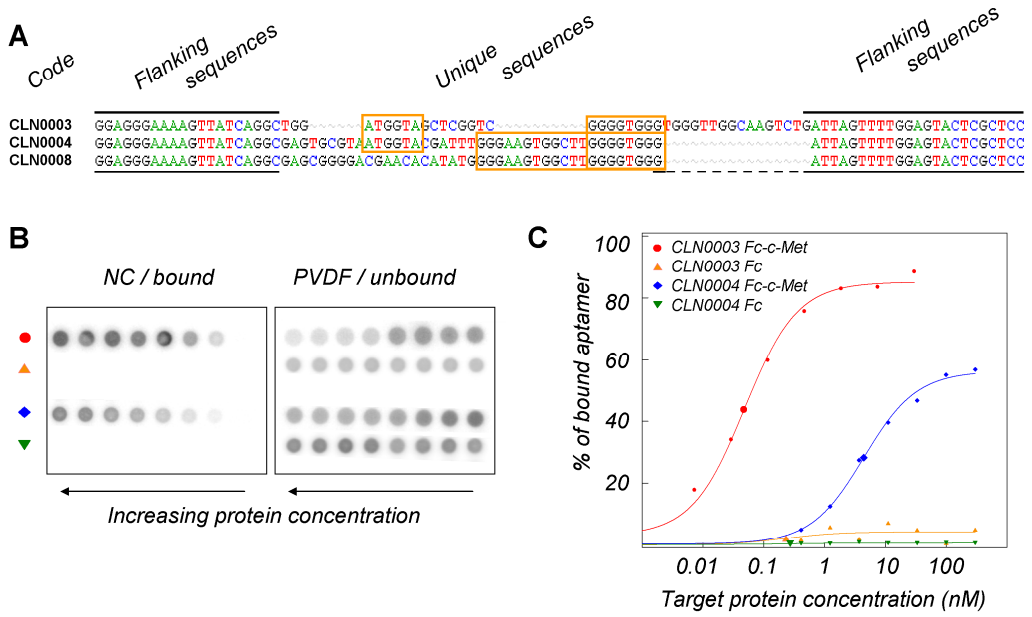

Figure 21: Sequence comparison and dot blot affinity determination of DNA c-Met aptamers.

A, Three analysed c-Met specific DNA aptamers shared certain sequence motifs (orange boxes) that included G61 in the 3' flanking region of CLN0004 and CLN0008. B, Representative dot blot raw data and C, fitted binding curves revealed high affinity binding to c-Met, but not to Fc, for CLN0003 and CLN0004. Enlarged symbols represent the respective K_D as aptamer concentration at half-maximal binding in fitted curves.

5.3.2 Temperature dependency of aptamer affinity

Since aptamer selection and dot blots had been performed at 37°C, but following characterisation could require binding evaluation at other temperatures, the affinity of six different 5' radioactive labelled (chapter 4.1.9) aptamers was determined via dot blot (chapter 4.3.9) at 4°C, 21°C and 37°C. The same aptamers, target protein dilutions and membranes were applied in parallel, altering only the temperature during incubation and of the used washing buffer. Affinity and binding properties were generally dependent on temperature, but varied from aptamer to aptamer (Figure 22, other data not shown). Less binding or lower affinity were observed in all cases at 4°C, while incubation at 21°C yielded similar or enhanced affinity in comparison to 37°C. Especially CLN0004 and CLN0020 showed

significantly less binding at 4°C. These aptamer-specific properties had to be taken into account when conducting subsequent binding assays, e.g. FACS measurements.

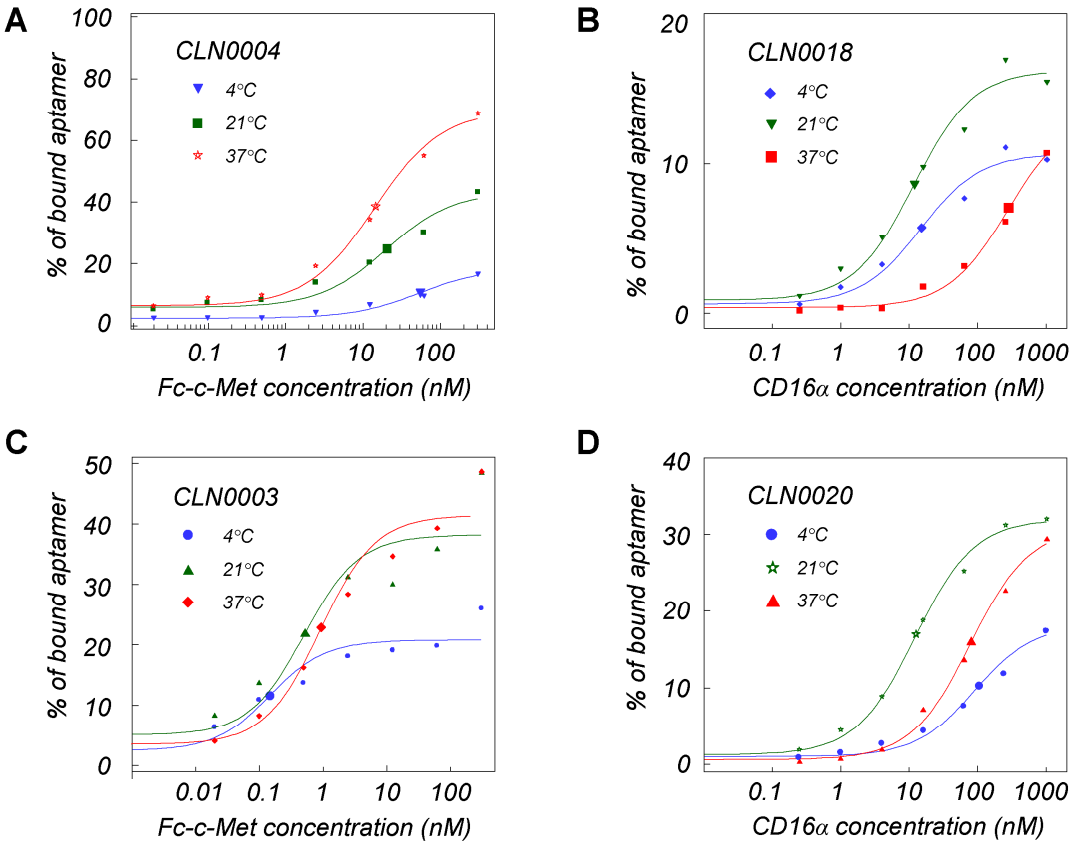

Figure 22: Temperature dependency of four selected DNA aptamers.

All aptamers exhibited high affinity at 21°C, clearly less binding at 4°C and varying behaviour at 37°C. A, CLN0004 clearly exhibited less binding and lower affinity upon temperature decrease. B, The optimal temperature for CLN0018 appeared to be in the range of 21°C, although it was selected at 37°C. C, CLN0003 showed less binding at 4°C while the overall affinity was only slightly altered. D, CLN0020 bound with clearly higher affinity at 21°C compared to 37°C, and less at 4°C. Small dots indicate dot blot-measured values, whereas lines and enlarged symbols represent a fitted binding curve including the derived K_D.

5.3.3 First minimisation

A first minimisation was performed to enable synthesis of shorter biotinylated aptamers in higher quantities. Cropped sequences for two c-Met and nine CD16α specific aptamers (chapter 5.3.1 and Figure 23) were synthesised in 25 nmol-scale at Invitrogen (chapter 4.1.1.3), followed by PAGE-purification (chapter 4.1.3.2), gel-extraction (chapter 4.1.4), precipitation (chapter 4.1.5) and determination of aptamer concentration (chapter 4.1.6). Minimisation constructs lacking five nucleotides or the full PCR flanking sequence on either the 5' or 3' end were then radioactively labelled (chapter 4.1.9) and the affinity was compared to the full length aptamer biochemically in a dot blot (chapter 4.3.9). Nine of eleven aptamers could be minimised to 40mers – 74mers, only CLN0003 and CLN0018 had to be applied at

full length (Figure 23). All cell SELEX derived aptamers were characterised further without minimisation. 5' or 3' truncations were denoted using a prefix or suffix, such as -20 nt.

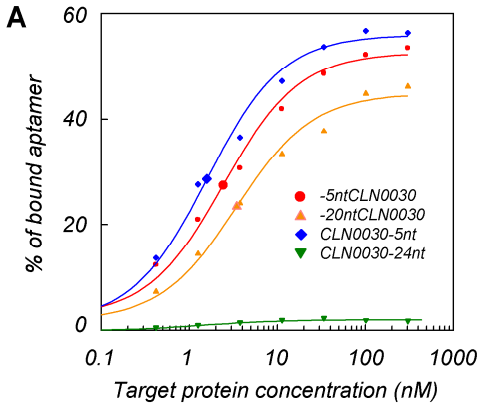

B

Aptamer code	Target protein	Minimisation construct	Length (nt)
CLN0003	c-Met	full length	84
CLN0004	c-Met	-20ntCLN04-5nt	69
CLN0015	CD16α	-5ntCLN15-24nt	44
CLN0018	CD16α	full length	84
CLN0019	CD16α	-5ntCLN19-5nt	74
CLN0020	CD16α	-5ntCLN20-24nt	55
CLN0021	CD16α	-5ntCLN21-5nt	74
CLN0013	CD16α	-5ntCLN23-5nt	74
CLN0024	CD16α	-20ntCLN24-24nt	40
CLN0028	CD16α	-20ntCLN28-24nt	40
CLN0030	CD16α	-20ntCLN30-5nt	55

Figure 23: First minimisation via dot blot affinity change assessment.

A, Dot blot binding curves of four differently cropped aptamer variants (here examplarily CLN0030) were compared in parallel in one measurement. Loss of binding properties (green) or significant affinity shifts (not shown) indicated undesired removal of essential sequence elements. B, Based on dot blot data, two c-Met and nine CD16α specific aptamers were minimised to lengths of 40 – 84 nt. A prefix "-20 nt" indicates a 5' fully flanking-cropped sequence, whereas a suffix "-5 nt" denotes removal of 5 bases on the aptamer 3' end.

5.3.4 Determination of cellular binding

Most aptamers exhibited affinities in the low nano-molar range in biochemical dot blot measurements, but since binding to cellular presented target protein was the essential property, cellular binding was analysed by flow cytometry. Two c-Met and nine filter SELEX derived CD16α specific aptamers were synthesised in minimised form (chapter 5.3.3), cell SELEX derived CD16α specific sequences as full length aptamers, all directly including 3' biotinylation (chapter 4.1.1.4). This approach enabled additional 5' radiolabelling (chapter 4.1.9) needed for dot blot analysis (chapter 4.3.9) to confirm unaltered binding properties of biotinylated aptamers. All analysed biotinylated aptamers had affinities similar to unlabelled original references (data not shown).

5.3.4.1 Binding analysis to cellular CD16α

In CD16 flow cytometry binding analyses (chapter 4.4.3), two antibody positive controls were applied to characterise all cell lines: the CD16-specific monoclonal mouse antibody 3G8 and the chimeric EGFR-antibody cetuximab that bound via its Fc-portion (Figure 24, chapter 3.2). Binding was assessed using freshly ficoll-isolated and MACS-enriched NK cells (chapters 4.4.4 and 4.4.5), recombinant Jurkat cells over-expressing either the V158 or F158 alloform of CD16α as well as maternal CD16α negative Jurkat E6.1 cells as negative control

(Figure 24, chapters 4.4.2 and 3.1). Cetuximab was detected with a goat anti hIgG F(ab')$_2$ specific, F(ab')$_2$ PE conjugated antibody that did not compete with Fc binding to CD16. 3G8 was applied as all aptamers in biotinylated form and detected via SA-PE (all in chapter 3.2).

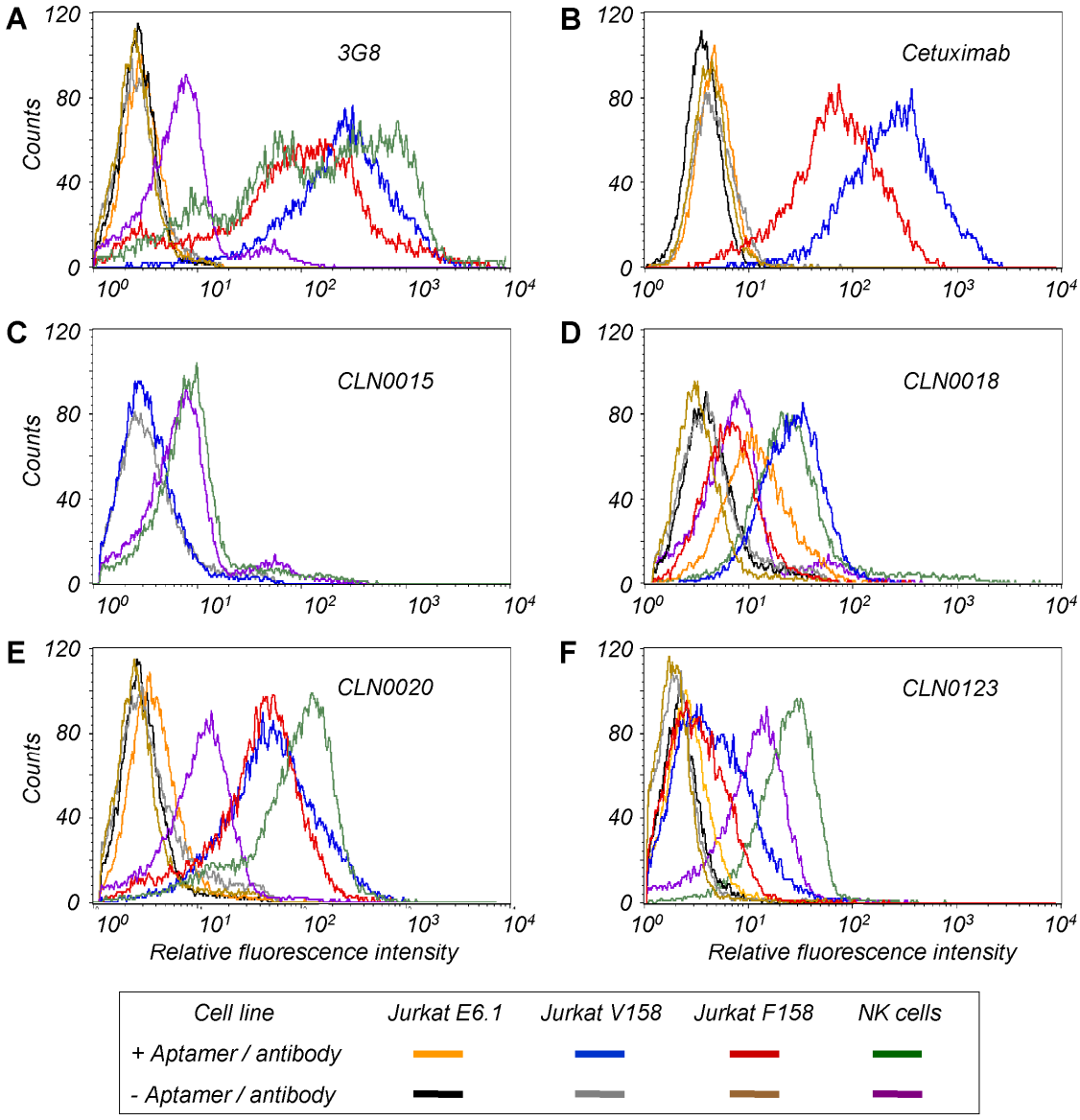

Figure 24: Binding of selected aptamers and reference antibodies to cellular CD16α by flow cytometry.

A, The CD16 specific antibody 3G8 bound to all CD16 positive cells, but not to negative reference Jurkat E6.1. Broadened histogram peaks might be due to internalisation during incubation at 21°C. B, Cetuximab bound to both over-expressing Jurkat cell lines, with stronger binding to CD16α(V158) cells reflecting the higher affinity of this Fc receptor alloform. NK cell binding was not evaluated. C, CLN0015 as representative did not bind to both NK or Jurkat CD16α(V158) cells. D, As expected, CLN0018 bound to NK and Jurkat CD16α(V158) cells and weaker to the CD16α(F158) allotype. Unspecific binding was also observed to CD16 negative Jurkat E6.1 cells (orange line). E, Unique sequence CLN0020 bound specifically to NK cells as well as to both alloforms of CD16α presented on Jurkat cells, as expected from dot blot characterisation. F, Cell SELEX derived CLN0123 exhibited weak but measurable binding to NK and CD16α(V158) positive Jurkat cells, weaker to CD16α(F158) positive Jurkat cells, but not to CD16 negative Jurkat E6.1 cells.

Both anti-CD16 antibody references exhibited expected specific binding to NK cells, recombinant Jurkat CD16α V158 and F158 cells and no binding to the maternal Jurkat E6.1 cell line. In contrast, binding to either of the cell lines could not be measured for most of both filter- and cell-SELEX derived aptamers. This included sequences with high affinity (for instance CLN0015, 19, 30) some of which were highly enriched in both selection screens (i.e. CLN0015, 21, 22, 118, 126). Additional 5' biotinylation or 5' fluorescein-labelling did not alter this result (data not shown). CLN0015 as a representative of a major sequence motif block is displayed in Figure 24 (cf. Figure 16). CLN0020 was the only filter SELEX derived aptamer found to bind cellular CD16α with high specificity and similar affinity for both allotypes on all tested CD16 positive cells (Figure 24, E). CLN0018 bound to NK and recombinant CD16 positive Jurkat cells as well, but also unspecifically to CD16 negative Jurkat E6.1 cells (Figure 24, D) and nearly all fractions of peripheral blood mononuclear cells (PBMCs, data not shown). Unexpectedly, most aptamers enriched in cell SELEX on Jurkat CD16α V158 and F158 cells did not exhibit binding to these cell lines in biotinylated form (data not shown). CLN0022 and CLN0128 exhibited very weak intensity shifts in FACS measurements (data not shown), but were not characterised further due to their low affinities in dot blot assays (see also chapter 5.3.1). CLN0123 was the only cell SELEX derived sequence to show specific and reasonable cellular binding that was in accordance with a relatively low affinity to CD16α-6His of 193 nM in dot blots. As expected, CLN0123 bound to NK and Jurkat CD16α(V158) positive cells better than to CD16α(F158) positive and did not bind to CD16α negative Jurkat E6.1 cells (Figure 24, F). Direct comparison of fluorescence intensities between antibody and aptamer measurements were not feasible due to on average four biotins per antibody to exactly only one per aptamer. All results were confirmed in two to eight independent measurements.

5.3.4.2 Binding analysis to cellular c-Met

The c-Met specific aptamers CLN003 and CLN0004 were analogously characterised by flow cytometry (chapter 4.4.3) along with a monoclonal anti c-Met mouse antibody as positive control (c-Met mAb, chapter 3.2) on different c-Met positive human cancer cell lines (GTL-16, MKN-45, EBC-1) and Jurkat E6.1 cells as a negative control. These cells were also characterised towards EGFR surface expression with cetuximab (chapter 3.2) to assess the use of this antibody as a positive control in ADCC assays. The c-Met mAb was detected with a goat anti mouse $F(ab')_2$ specific, $F(ab')_2$ PE conjugated antibody (chapter 3.2) and cetuximab as decribed above.

The three human cancer cell lines GTL-16, MKN-45 and EBC-1 were confirmed as both c-Met and EGFR positive, whereas Jurkat E6.1 provided an appropriate c-Met negative control cell line (Figure 25, A and B). Both c-Met specific aptamers bound to all three human cancer c-Met cell lines in a very distinct manner, but exhibited no unspecific binding to Jurkat E6.1 cells (Figure 25, C and D).

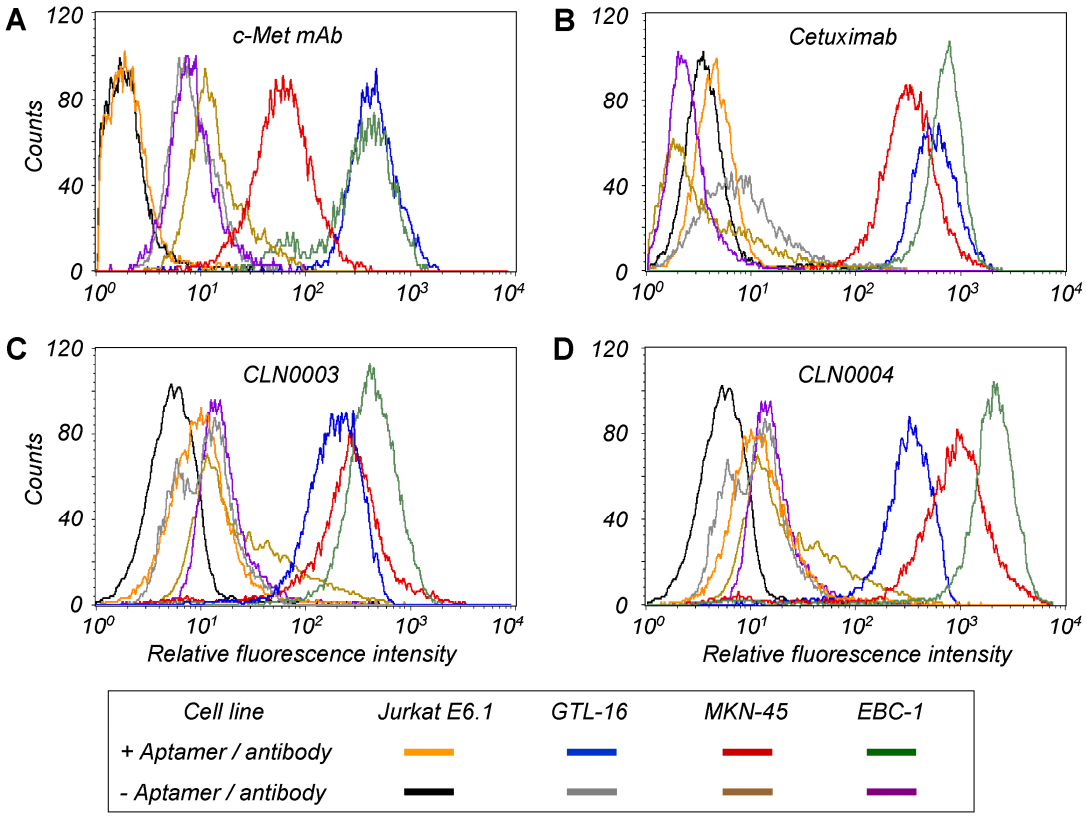

Figure 25: FACS determination of cellular binding of c-Met aptamers and antibody references.

A, The monoclonal mouse antibody c-Met mAb revealed that human cancer cell lines GTL-16, MKN-45 and EBC-1 were c-Met positive, while Jurkat E6.1 cells were c-Met negative, hence a suitable control. B, Cetuximab binding indicated additional strong EGFR surface expression on GTL-16, MKN-45 and EBC-1. C, CLN0003 bound clearly with high specificity to all c-Met positive cells, but not to the negative control Jurkat E6.1. D, CLN0004 exhibited specific cellular c-Met binding as well.

Taken together, two CD16α aptamers (CLN0020 and CLN0123) and two c-Met aptamers (CLN0003 and CLN0004) were found to bind with high specificity to the cellularly presented target proteins.

5.3.5 Structure prediction

Structure prediction for the remaining four DNA aptamers, calculated for physiological conditions of 150 mM Na^{+} concentration without Mg^{++}at 37°C using mfold (Zuker, 2003 and chapter 3.9), yielded only one proper structure suggestion for CLN0020 that predicted the last base of the 5' flanking sequence (C20) to be essential for structure formation (Figure 26). Other predictions included only minimal secondary structure interactions of less than 6 bases and were ignored. For both c-Met aptamers, a primary sequence comparison indicated two identical motifs instead (cf. Figure 21).

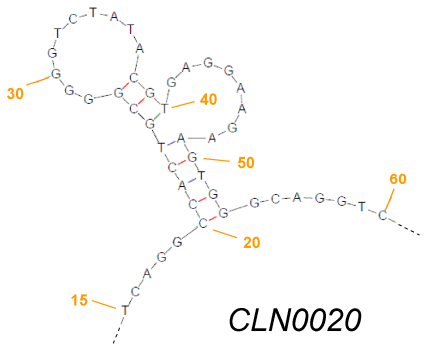

Figure 26: Structure predition for CLN0020.

Nucleotides from base 20 - 53 are predicted to be essential for structure formation. Orange numbering indicated base numbers of the full length aptamer.

5.3.6 Epitope mapping

Since binding multiple epitopes on CD16 could be valuable for bi-specific aptamer development, the binding sites of CLN0020 and CLN0123 were characterised in competition dot blots with antibodies 3G8 and cetuximab that bind near or in the Fc-binding domain. 5 fmol radiolabelled CLN0020 (chapter 4.1.9) was used in a competition dot blot (chapter 4.3.10) with 50 nM CD16α-6His and a dilution series of 3G8, cetuximab, or CLN0123. Additionally, CLN0020 itself was used as positive control as well as a non-binding antibody fragment BMP2-7 as negative control (Habicht and Siegemund, 2002). CLN0020 was clearly displaced by 3G8 and cetuximab, while similar amounts of BMP2-7 did not alter binding properties (Figure 27, A and B). Higher amounts of cetuximab were needed to replace CLN0020 as opposed to 3G8, which was in line with 3G8's higher affinity to CD16. Non-labelled CLN0020 replaced radiolabelled CLN0020 as expected, whereas CLN0123 and negative control CLNX did not compete with CLN0020 (Figure 27, C). Thus, CLN0020 was found to bind in or near the Fc binding domain.

Direct competition studies of CLN0123 with cetuximab could not be performed in a dot blot assay because low CD16α affinities of both CLN0123 and the IgG1 cetuximab enforced the use of too high protein amounts that could not be captured quantitatively on the nitrocellulose membrane. Competition studies by flow cytometry and bio-layer interferometry indicated

reduced binding of CLN0123 to CD16α in the presence of cetuximab (data not shown). Thus, CLN0123 bound to an epitope near or in the Fc binding domain different than the site recognised by CLN0020.

Similar sequence motifs of c-Met specific aptamers CLN0003 and CLN0004 (cf. Figure 21) suggested a putative specificity for the same epitope on c-Met. This assumption was confirmed by competition dot blots with 5 fmol radiolabelled aptamers (chapters 4.1.9 and 4.3.10) binding to 10 nM c-Met-Fc fusion protein (chapter 3.2). Radiolabelled CLN0003 was replaced by non-labelled CLN0004 and in the reverse assay labelled CLN0004 competed with unmarked CLN0003 (Figure 27, D). Higher amounts needed for CLN0003 competition by CLN0004 were in line with the lower c-Met affinity of CLN0004. This mutual replacement provided clear evidence that both aptamers recognise the same epitope on c-Met.

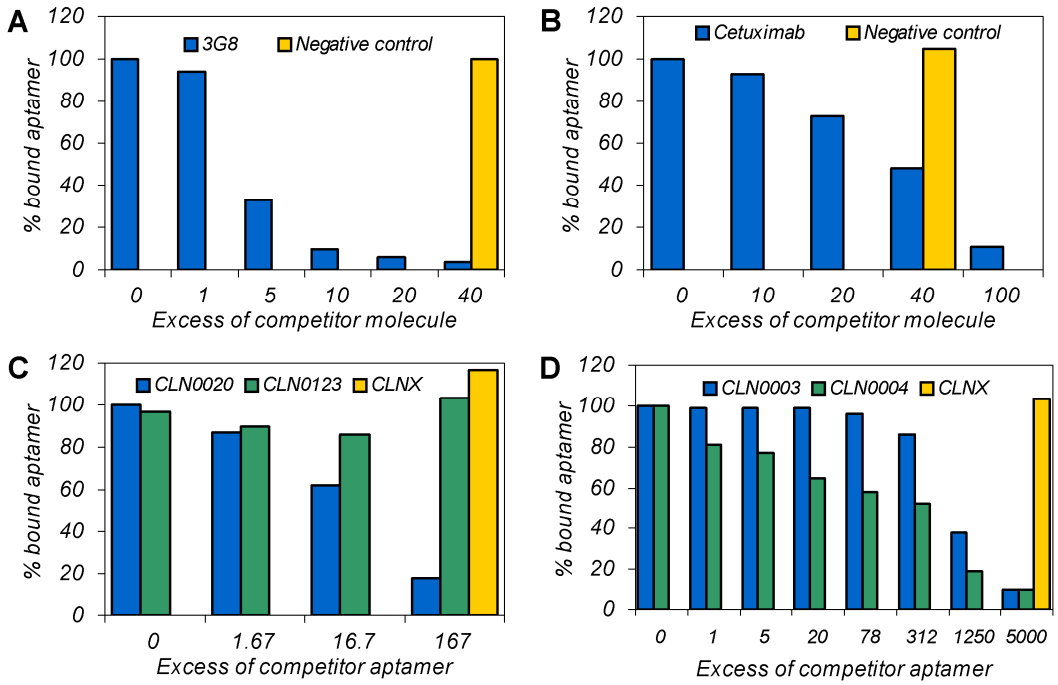

Figure 27: Competition dot blots of CD16α and c-Met aptamers.

A – C, Competition dot blots applying CD16α-6His and specific aptamers CLN0020 or CLN0123 in the presence or absence of putative competitors for epitope mapping. X-axes represent the molar excess of competitor over CD16α. A, Radiolabelled CLN0020 was rapidly replaced in a concentration dependent manner by the anti-CD16 monoclonal antibody 3G8, while the negative control antibody fragment BMP2-7 (orange) did not affect aptamer binding. B, Competition of the Fc-portion of cetuximab with CLN0020 binding on CD16α could be titrated as well, while addition of BMP2-7 did not alter aptamer binding. C, Radiolabelled and CD16α-bound CLN0020 was replaced by non-labelled CLN0020 as positive control (blue bars), but not by CLN0123 (green bars) or the negative control aptamer CLNX (orange, chapter 3.3). D, Mutual replacement of radiolabelled CLN0003 by non-labelled CLN0004 (blue bars) or radiolabelled CLN0004 by CLN0003 (green bars) indicated binding the same epitope. Addition of non-binding CLNX (orange) had no effect. X-axis, molar excess of unlabelled competitor aptamer over labelled aptamer bound to c-Met. For all experiments n = 1.

5.3.7 Second minimisation and sequence analyses

A prerequisite for the establishment of bi-specific aptamers was knowledge of the core sequences necessary for aptamer binding to assemble bi-specific constructs with well defined linker lengths. In addition to initial minimisations (chapter 5.3.3), further and more defined minimised aptamer constructs were screened based on mfold structure prediction of CLN0020 (chapter 5.3.5) and sequence analysis of CLN0003 and CLN0004 (Figure 21). Cropped sequences were synthesised in 200 nmol scale (chapter 4.1.1.3), PAGE-purified (chapter 4.1.3.2) and -eluted (chapter 4.1.4), precipitated (chapter 4.1.5) and the concentration was determined (chapter 4.1.6). Pure aptamers were then 5' radiolabelled (chapter 4.1.9) and the affinity was determined in a dot blot (chapter 4.3.9), directly comparing cropped sequences to the original 84 nt aptamer. Additionally, two sequence variants of CLN0004 found in the analysed SELEX pools were produced and their affinity determined in the same way. Generally, dot blot derived K_D values were prone to variation due to a high sensitivity towards changes in temperature and protein preparation; hence minimisation evaluation was based on direct comparison of parallel samples of one experiment.

While the c-Met specific aptamer CLN0003 generally exhibited a decrease in affinity upon truncation, CLN0004 could be minimised to a 41mer with a K_D of 83 nM or a 46mer with an affinity comparable to the full length aptamer (Figure 28, C and D). Interestingly, the base G61 of CLN0004 was suggested as an essential component by sequence comparison (to CLN0003, cf. Figure 21) and this was confirmed by dot blot minimisation (Figure 28, A). Removal of nearly all flanking bases of the CD16α specific aptamer CLN0020 led to a 41mer and further structure prediction based minimisation to a 34mer. Both minimised aptamers displayed unaltered affinity to CD16α-6His (Figure 28, B and E). The importance of the 5' flanking base C20, as suggested by structure prediction (Figure 26), was confirmed by testing two constructs differing only in this base (Figure 28, B, blue vs. red graphs). Flanking sequences of CLN0123 could be removed without major loss of binding properties, but CD16α affinity remained relatively low in all CLN0123 constructs, as expected (Figure 28, F).

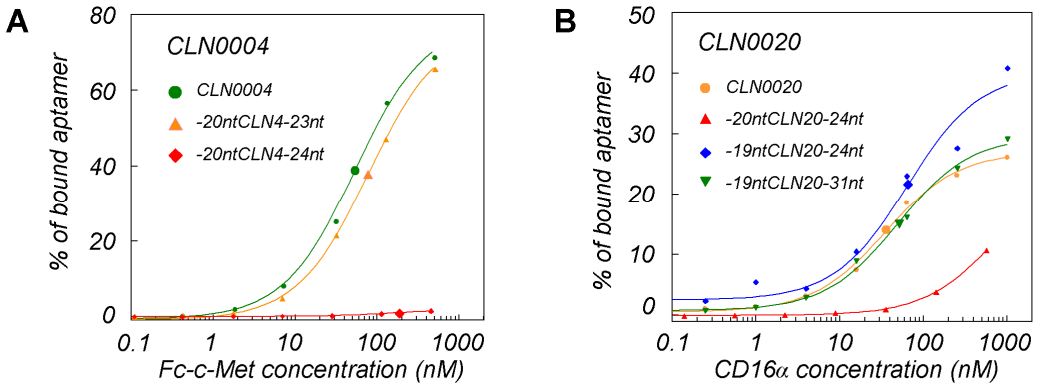

C — CLN0003

	K_D (nM)
GGAGGGAAAAGTTATCAGGCTGGATGGTAGCTCGGTCGGGGGTGGGTGGGTTGGCAAGTCTGATTAGTTTTGGAGTACTCGCTCC	0.091
GGAGGGAAAAGTTATCAGGCTGGATGGTAGCTCGGTCGGGGGTGGGTGGGTTGGCAAGTCTGATTAGTTTTGGAGTACTCGCTCC-Biotin	0.252
GAAAAGTTATCAGGCTGGATGGTAGCTCGGTCGGGGGTGGGTGGGTTGGCAAGTCTGATTAGTTTTGGAGTACTCGCTCC	0.750
AGTTATCAGGCTGGATGGTAGCTCGGTCGGGGGTGGGTGGGTTGGCAAGTCTGATTAGTTTTGGAGTACTCGCTCC	9
ATCAGGCTGGATGGTAGCTCGGTCGGGGGTGGGTGGGTTGGCAAGTCTGATTAGTTTTGGAGTACTCGCTCC	12
GGCTGGATGGTAGCTCGGTCGGGGGTGGGTGGGTTGGCAAGTCTGATTAGTTTTGGAGTACTCGCTCC	49
TGGATGGTAGCTCGGTCGGGGGTGGGTGGGTTGGCAAGTCTGATTAGTTTTGGAGTACTCGCTCC	54
GGAGGGAAAAGTTATCAGGCTGGATGGTAGCTCGGTCGGGGGTGGGTGGGTTGGCAAGTCTGATTAGTTTTGGAGTACTC	0.650
GGAGGGAAAAGTTATCAGGCTGGATGGTAGCTCGGTCGGGGGTGGGTGGGTTGGCAAGTCT	3
TGGATGGTAGCTCGGTCGGGGGTGGGTGGGTTGGCAAGTCT	52

D — CLN0004

GGAGGGAAAAGTTATCAGGCGAGTGCGTAATGGTACGATTTGGGAAGTGGCTTGGGGTGGGATTAGTTTTGGAGTACTCGCTCC	11
GGAGGGAAAAGTTATCAGGCGAGTGCGTAATGGTACGATTTGGGAAGTGGTTTGGGGTGGGATTAGTTTTGGAGTACTCGCTCC	154
GAGTGCGTAACGGTATGACTTGGGAAGTGGCTTGGGGTGGG	>500
GAAAAGTTATCAGGCGAGTGCGTAATGGTACGATTTGGGAAGTGGCTTGGGGTGGGATTAGTTTTGGAGTACTCGCTCC	19
GAGTGCGTAATGGTACGATTTGGGAAGTGGCTTGGGGTGGGATTAGTTTTGGAGTACTCGCTCC	3
GGAGGGAAAAGTTATCAGGCGAGTGCGTAATGGTACGATTTGGGAAGTGGCTTGGGGTGGGATTAGTTTTGGAGTACTC	~11
GAGTGCGTAATGGTACGATTTGGGAAGTGGCTTGGGGTGGGATTAGTTTTGGAGTACTC-Biotin	57
GAGTGCGTAATGGTACGATTTGGGAAGTGGCTTGGGGTGGGATTAGTTTTGG	67
GAGTGCGTAATGGTACGATTTGGGAAGTGGCTTGGGGTGGGATTAG	~65
GAGTGCGTAATGGTACGATTTGGGAAGTGGCTTGGGGTGGG	83
GAGTGCGTAATGGTACGATTTGGGAAGTGGCTTGGGGTGG	>1000
ATGGTACGATTTGGGAAGTGGCTTGGGGTGGG	230

E — CLN0020

GGAGGGAAAAGTTATCAGGCCACTGCGGGGGTCTATACGTGAGGAAGAAGTGGGCAGGTCGATTAGTTTTGGAGTACTCGCTCC	45
GAAAAGTTATCAGGCCACTGCGGGGGTCTATACGTGAGGAAGAAGTGGGCAGGTCGATTAGTTTTGGAGTACTCGCTCC	25
CACTGCGGGGGTCTATACGTGAGGAAGAAGTGGGCAGGTCGATTAGTTTTGGAGTACTCGCTCC	68
GGAGGGAAAAGTTATCAGGCCACTGCGGGGGTCTATACGTGAGGAAGAAGTGGGCAGGTCGATTAGTTTTGGAGTACTC	40
GGAGGGAAAAGTTATCAGGCCACTGCGGGGGTCTATACGTGAGGAAGAAGTGGGCAGGTC	22
GAAAAGTTATCAGGCCACTGCGGGGGTCTATACGTGAGGAAGAAGTGGGCAGGTC-Biotin	20
CAGGCCACTGCGGGGGTCTATACGTGAGGAAGAAGTGGGCAGGTC	68
CCACTGCGGGGGTCTATACGTGAGGAAGAAGTGGGCAGGTC	55
CACTGCGGGGGTCTATACGTGAGGAAGAAGTGGGCAGGTC	>1000
CCACTGCGGGGGTCTATACGTGAGGAAGAAGTGG	47

F — CLN0123

GGAGGGAAAAGTTATCAGGCAGAGGGGAGGGTCGGGTATCGGCGTGTTCGGGGGATCTGCGATTAGTTTTGGAGTACTCGCTCC-Biotin	195
AAAGTTATCAGGCAGAGGGGAGGGTCGGGTATCGGCGTGTTCGGGGGATCTGCGATTAGTTTTGGAGTACTCGCTCC	220
TCAGGCAGAGGGGAGGGTCGGGTATCGGCGTGTTCGGGGGATCTGCGATTAGTTTTGGAGTACTCGCTCC	169
AGAGGGGAGGGTCGGGTATCGGCGTGTTCGGGGGATCTGCGATTAGTTTTGGAGTACTCGCTCC	232
GGAGGGAAAAGTTATCAGGCAGAGGGGAGGGTCGGGTATCGGCGTGTTCGGGGGATCTGCGATTAGTTTTGGAGTA	83
GGAGGGAAAAGTTATCAGGCAGAGGGGAGGGTCGGGTATCGGCGTGTTCGGGGGATCTGCGATTAGTT	68
GGAGGGAAAAGTTATCAGGCAGAGGGGAGGGTCGGGTATCGGCGTGTTCGGGGGATCTGC	128

Figure 28: Dot blot based minimisation of c-Met and CD16α specific aptamers.

A, Removal of full flanking sequences of CLN0004 resulted in complete loss of binding in dot blot experiments (red), whereas addition of only G61 (orange) recovered nearly similar affinity as the original clone (green, cf. D and Figure 21, A). B, Removal of C20 in CLN0020 altered low nanomolar affinity (blue) to hardly any binding (red) as determined in a dot blot. C, Minimisation of CLN0003 generally led to decrease of affinity, however still remaining in a low nano-molar range. D, Sequence variants of CLN0004 (blue bases) and 3' truncations exhibited lower affinities, while the 5' flanking sequence was not essential for c-Met binding. E, CD16α aptamer CLN0020 was minimised to a 34mer core sequence while retaining a high affinity. F, Truncated CLN0123 constructs bound expectedly weak but with similar or improved affinities to CD16α. Intermittent, binding curves shifted due to temperature and protein batch variations; hence only direct, qualitative comparison to the original aptamer was feasible (indicated as ~11 nM in D). Binding was categorised as similar (green), altered but reasonable (orange) or severely shifted (red) in comparison to the original sequence (black).

Two sequence variants of CLN0004 found in the original SELEX pool exhibited weaker affinity to c-Met than the major sequence and were ignored (Figure 28, D, blue bases). Variants of CLN0003, CLN0020 and CLN0123 did not occur; several sequence variants of CLN0018 were not evaluated due to unspecific binding of the most prevalent aptamer.

Aptamers against c-Met and CD16α specifically binding to their respective cellular antigens were fully characterised and minimised and therefore suitable for linkage into bi-specific constructs.

5.4 Bi-specific aptamers

5.4.1 Design of bi-specific aptamers

With the goal of developing bi-specific aptamers featuring high affinities to c-Met and CD16α as well as an optimal linker length to mediate cytotoxicity, 24 different bi-specific aptamer constructs (bsA1 – bsA32) were designed (Table 2). CLN0020 was used as the effector specific portion in most constructs, and CLN0123 which bound with lower affinity to CD16α, was used in the construction of bsA15 and bsA16. As target specific aptamers, both CLN0003 and CLN0004 were applied. All aptamers were synthesised as one oligonucleotide chain. These constructs varied in orientation of the effector and target cell specific aptamer. Differently minimised aptamers were used to screen for a suitable linker length while retaining high affinities at the same time, and several kinds of linker were applied: A 15 dA linker (Muller *et al.*, 2007), up to 44 nucleotides as "original" linker derived from flanking regions of the full length sequence as well as shorter flanking region sequences known to not interact with the aptamer (c.f. Figure 28). Polyethylene glycol (PEG) linkers were applied as $PEG_{(3)}$ and $PEG_{(6)}$ bridging 9 or 18 C- and O-atoms, respectively. bsA14 incorporating a $PEG_{(24)}$ linker was planned but not produced due to positive progress with nucleotide linker constructs.

The core aptamer sequence was defined as those that retained similar binding properties in minimisations (green sequences in Figure 28). CLN0020 structure predition suggested a core sequence of C20 – G53 essential for structure formation (cf. Figure 26), yielding the exact borders that were essential for target binding. For example, all nucleotides downstream from G54 were defined as linker sequence.

Assuming an optimal bsA linker should bridge approximately the distance spanning from CDRs to the Fc binding domain in the hinge region of an antibody, this distance was estimated from measurement of PDB entry 1T83 (Radaev *et al.*, 2001) to be ~65 Å. The nucleotide to nucleotide distance in single stranded portions of DNA aptamers was determined by measuring 4 distances in PDB entries 1HUT and 1OOA, resulting in a mean distance of 7 Å. Hence, the putative linker lengths ranged from 20 Å of $PEG_{(3)}$ over 105 Å of a 15 dA linker to 357 Å of the 51 nt linker applied in bsA12. Although these values were a rough approximation, they could serve as a first estimation for the range of the desired linker length.

Table 2: Overview of bi-specific aptamer constructs.

CLN0004-5 denotes a 5 nt truncation 3' of CLN0004 and so forth. Bi-specific constructs bsA31 and bsA32 are direct derivatives of bsA3.

Construct	5' aptamer	Linker sequence	3' aptamer	Putative linker length (Å)	M_W
bsA1	-19CLN0020-24	GCAGGTC	-20CLN0004-23	49	25800
bsA2	-20CLN0004-23	none	-19CLN0020-24	0	25800
bsA3	-19CLN0020-24	GCAGGTCAAAAAAAAAAAAAAA	-20CLN0004-23	154	30500
bsA31	-19CLN0020-24	GCAGGTCAAAAAAAAAAAAAAA	-20CLN0004	154	37600
bsA32	-19CLN0020-31	AAAAAAAAAAAAAAA	-20CLN0004	105	35400
bsA4	-20CLN0004-23	GCAGGTCAAAAAAAAAAAAAAA	-19CLN0020-24	154	30500
bsA5	-19CLN0020-24	GCAGGTC + $PEG_{(3)}$ = C_9	-20CLN0004-23	69	26000
bsA6	-20CLN0004-23	$PEG_{(3)}$ = C_9	-19CLN0020-24	20	26000
bsA7	-19CLN0020-24	GCAGGTC + $PEG_{(6)}$ = C_{18}	-20CLN0004-23	82	26100
bsA8	-20CLN0004-23	$PEG_{(6)}$ = C_{18}	-19CLN0020-24	33	26100
bsA9	CLN0020	GCAGGTCGATTAGTTTTGGAGTACTCGCTCC	CLN0003	217	52700
bsA10	CLN0003	GGAGGGAAAAGTTATCAGG	CLN0020	133	52700
bsA11	-19CLN0020	GCAGGTCGATTAGTTTTGGAGTACTCGCTCC	CLN0003	217	46600
bsA12	-19CLN0020	GCAGGTCGATTAGTTTTGGAGTACTCGCTCCG GAGGGAAAAGTTATCAGGC	CLN0004-5	357	45100
bsA13	-20CLN0004	GCTCCGGAGGGAAAAGTTATCAGG	CLN0020-31	168	36700
bsA14	-10CLN0020-24	GCAGGTC + $PEG_{(24)}$ = C_{72}	CLN0003	144	42800
bsA15	CLN0123	GATTAGTTTTGGAGTACTC	CLN0003	140	52700
bsA16	-20CLN0004	ATTAGTTTTGGAGTACTCGCTCCGGAGGGAAA AGTTATCAGGC	CLN0123	308	46400
bsA17	-19CLN0020-24	GCAGGTC	CLN0003	49	39200
bsA18	-19CLN0020-31	ATCAGGC	-13CLN0004-5	49	33500
bsA19	-19CLN0020-24	GCAGGTCAAAAAAAAAAAAAAA	CLN0003-24	154	36400
bsA20	-19CLN0020-24	GCAGGTC	CLN0003-24	49	31700
bsA21	-19CLN0020-24	GCAGGTCAAAAAAAAAAAAAAA	CLN0003	154	43800
bsA22	-19CLN0020-31	AAAAAAAAAAAAAAA	CLN0003	105	41700

5.4.2 Affinity confirmation

High affinities to CD16α and especially to c-Met were expected to be crucial for the mediation of a cytolytic function of bi-specific aptamers and thus determined in dot blot measurements (Figure 29). All bi-specific aptamers were synthesised by IDT, Leuven, Belgium, and purified by PAGE (chapter 4.1.3.2), followed by gel extraction, precipitation and concentration determination (chapters 4.1.4 - 4.1.6). 10 pmol of each aptamer were then labelled with ^{32}P (chapter 4.1.9) and a dot blot (chapter 4.3.9) was performed 1 – 10 times to evaluate affinities to CD16α-6His and C-Met-Fc fusion protein (chapter 3.2). Resulting K_D values were compared to those of the corresponding parental minimised single aptamers (c.f. Figure 28).

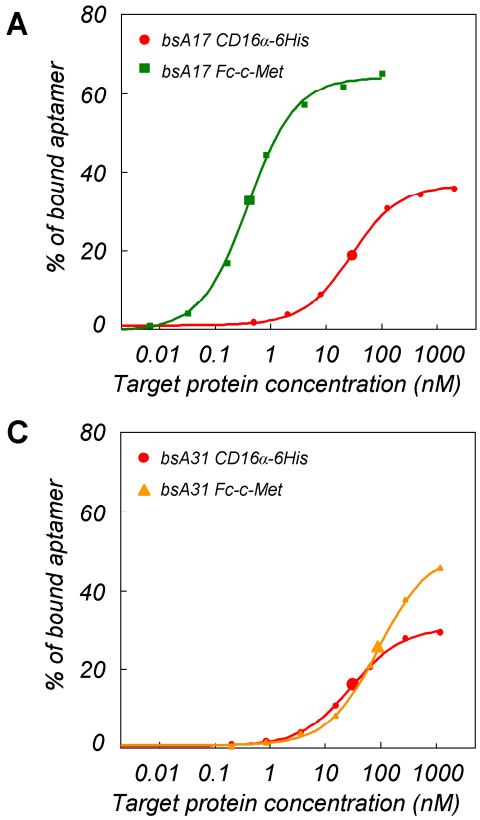

B

Construct	CD16α-6His Kd (nM)	n	Fc-c-Met Kd (nM)	n
bsA1	84	1	319	1
bsA2	51	1	220	1
bsA3	39 ± 10	3	141 ± 16	6
bsA31	24 ± 4	4	92 ± 41	3
bsA32	33 ± 1	2	119 ± 22	3
bsA4	78	1	105	1
bsA5	64	1	164	1
bsA6	51	1	370	1
bsA7	73	1	160	1
bsA8	102	1	271	1
bsA9	98 ± 6	2	0.160	1
bsA10	112 ± 5	2	0.157	1
bsA11	82 ± 9	2	0.162	1
bsA12	106 ± 17	2	18	1
bsA13	197 ± 3	2	18	1
bsA15	174	1	0.218	1
bsA16	178	1	102	1
bsA17	19 ± 2	3	0.352 ± 0.090	6
bsA18	15 ± 2	2	106 ± 7	2
bsA19	32 ± 0	2	38 ± 17	2
bsA20	23 ± 4	2	5.2 ± 1.8	2
bsA21	19 ± 2	2	0.276 ± 0.116	3
bsA22	27 ± 5	2	0.243 ± 0.103	3

Figure 29: Dot blot affinity determination of all bi-specific aptamers.

A and C, Dot blot binding curves of bi-specific aptamers bsA17 and bsA31, respectively. Affinities to CD16 were comparable (19 and 24 nM) and in accordance with the parental -19ntCLN0020-31nt (47 nM). In contrast, CLN0003-derived bsA17 exhibited picomolar c-Met affinity (A) whereas CLN0004-derived bsA31 bound with 92 nM Kd to c-Met (C), reflecting the different affinities of parental aptamers CLN0003 and CLN0004 (91 pM and 57 nM, respectively). B, Dot blot derived affinities to CD16α and c-Met for all bi-specific aptamers (except of bsA14 that was not produced). Generally, CLN0020 retained original affinity when used 5‘, whereas c-Met aptamers performed best fused to the 3‘ end (bsA3, 5, 7 17 – 22). Linked full length aptamers yielded affinities similar to parental single aptamers (CLN0003: picomolar Kd of bsA9-11, 17, 21, 22; CLN0004: 18 nM of bsA12, 13; CLN0123: 174 nM and 178 nM of bsA15 and 16, respectively). bsA1 and bsA2 without linker exhibited a c-Met affinity decrease. K_D values are shown as mean values and standard deviation of independent dot blot experiments.

Generally, most bi-specific aptamers exhibited high affinities to both target proteins similar to their respective parental single aptamers. Especially CLN0003-derived bsAs retained picomolar affinities to c-Met (bsA9, 10, 11, 15, 17, 21, 22) or low nanomolar K_D values when truncated (cf. 5 nM of bsA20 to 3 nM of CLN0003-24nt in Figure 28). CLN0004 was generally more suitable to linkage at the 3' end of bsAs (cf. Figure 28, D) and with a longer linker (bsA12 and bsA13) exhibited a similar affinity of 18 nM as the original aptamer. Further truncated derivatives and shorter linkers led to decreased but still reasonable c-Met affinities of 92 – 160 nM (bsA3, 31, 32, 4, 5, 7, 16, 18). CLN0020 performed best when fused 5' to a bi-specific aptamer, but not when applied 3' (as in bsA4, 6, 13). When CLN0020 constituted the 5' end of a bi-specific aptamer, mostly including the 7 nt linker sequence GCAGGTC that originated from the parental sequence, original affinities of low two-digit nanomolar K_D were generally retained (cf. Figure 28, E). CLN0123-derived bsA15 and bsA16 bound to CD16α-6His with 173 nM and 178 nM, respectively. These affinities were lower than those of CLN0020-containing bi-specific aptamers, but as high as the parental single aptamer CLN0123 (cf. Figure 20 and Table 1). Bi-specific constructs bsA1 and bsA2 lacking a linker, as well as bsA6 and bsA8 exhibited clear c-Met affinity decreases with K_D values of 220 – 370 nM. These bi-specific aptamers were not analysed further. All other bi-specific aptamers (bsA3 - 5, 7, 9- 22) were further evaluated for simultaneous binding to both target proteins.

5.4.3 Determination of simultaneous binding

Suitable affinities to CD16α or c-Met were confirmed for most bi-specific aptamers, but simultaneous binding to both target proteins had to be determined as prerequisite for a potential mediation of cytotoxicity as well. Electrophoretic motility shift assays (EMSAs) were primarily performed for all remaining bsAs, and positive results for major candidates were confirmed with bio-layer interferometry.

5.4.3.1 Electrophoretic motility shift assay

An EMSA was performed with 19 remaining bi-specific aptamers (bsA3-5, 7, 9-22; chapter 4.3.12). Sole binding to either CD16α-6His or c-Met-Fc fusion proteins was indicated by an additional slower migrating aptamer band. Simultaneous binding to both target proteins could be detected by a further shift in the migration distance upon addition of c-Met-Fc and

CD16α-6His in comparison to c-Met-Fc alone. A migration shift indicated a larger size of the bi-specific aptamer and hence simultaneous binding of both target proteins. Figure 30 shows representative results for CLN0003- and CLN0004- derived bi-specific aptamers. All constructs yielded similar results (data not shown).

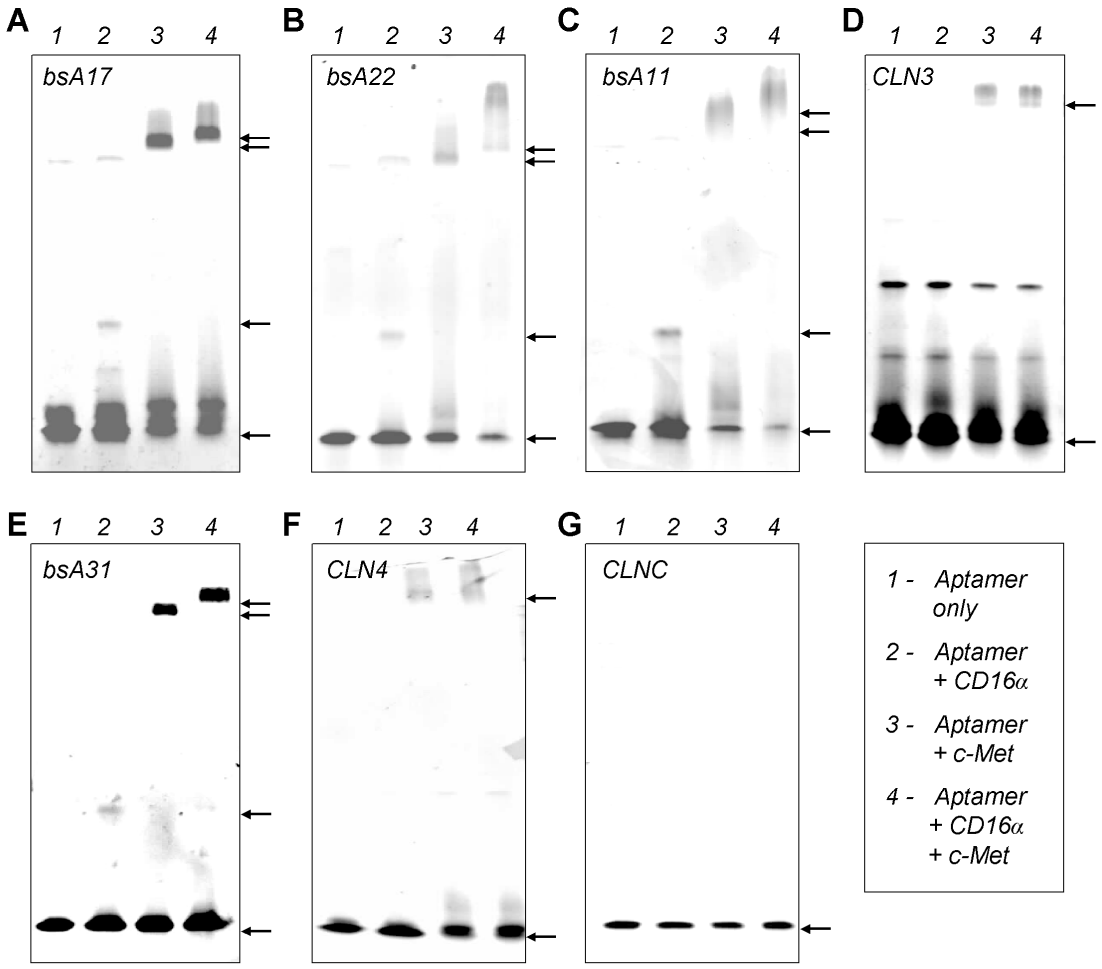

Figure 30: Electrophoretic migration shift assay proving simultaneous binding to CD16α and c-Met.

A – C, CLN0003-derived bsA17, bsA22 and bsA11 all exhibited binding to CD16α-6His (additional band in lane 2) or c-Met-Fc fusion proteins (additional band in lane 3). This c-Met-Fc bound aptamer band shifted again upon addition of CD16α-6His (lane 4). D, Negative control parental single aptamer CLN0003, in contrast, did not show this migration shift. E and F, bsA31 and original single c-Met specific aptamer CLN0004 exhibited the same pattern, while non-binding negative control aptamer CLNC did not bind to any protein, as expected. Application of a gradient gel and size differences between CD16α-6His and c-Met-Fc fusion protein led to differently extended migration (lanes 2 and 3) and an expectedly minor but clearly present migration shift upon addition of both target proteins (from lane 3 to 4). Arrows indicate the lowest migration frontier of specific aptamer bands. Weak additional bands in lanes 1 and 2 in A, B, C as well as all lanes in D could be due to unspecific aggregation.

5.4.3.2 Bio-layer interferometry

Four bi-specific aptamers with high affinities and different potentially suitable linkers were selected for additional confirmation of simultaneous binding via bio-layer interferometry using a fortéBio Octet Red device (chapter 4.3.11). Briefly, c-Met-Fc fusion protein was immobilised on amino reactive tips, bi-specific aptamers and suitable controls were allowed to bind and finally CD16α association and dissociation was monitored. In addition to c-Met-Fc binding, bsA17 clearly yielded simlutaneous Fc-CD16α binding, whereas c-Met specific single aptamer CLN0003 did not (Figure 31). Bi-specific aptamers bsA22 and bsA11 exhibited similarly strong bi-specific binding, whereas bsA31 bound weaker but measureable to both proteins (data not shown).

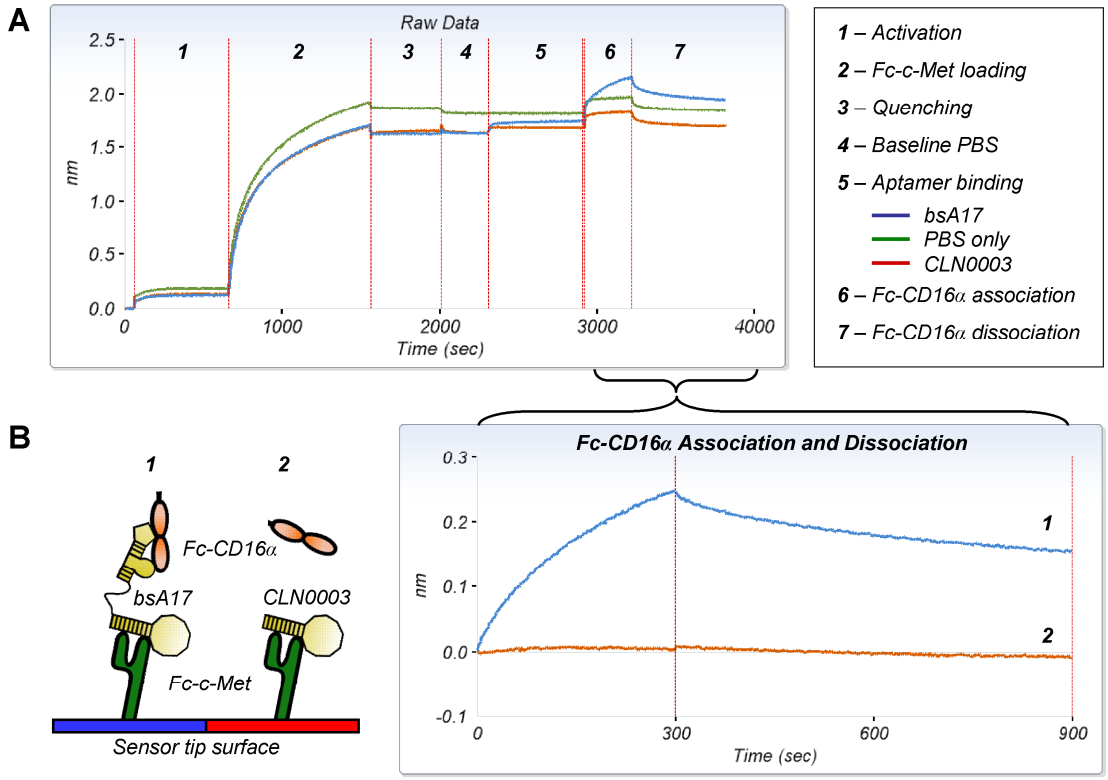

Figure 31: Proof of simultaneous binding of bsA17 to both target proteins via fortéBio Octet Red.

A, Raw data of applied AR sensor tips. c-Met-Fc fusion protein is immobilised on the tip surface (step 2), then bsA17 and CLN0003 bound to c-Met-Fc (blue and red curves in step 5), followed by Fc-CD16α association to bsA17 (blue curve in step 6). To exclude unspecific Fc-CD16α binding, the reference measurement lacking aptamer in step 5 (green) was subtracted from bsA17 and CLN0003 raw data, yielding the signal of specific simultaneous binding displayed by Fc-CD16α association and dissociation (B). c-Met-bound bsA17 exhibited additional Fc-CD16α binding (blue curve), while CLN0003 did not (red curve).

5.4.4 Serum stability

Since further functional assays demanded measurements in the presence of serum and stability was of interest for potential later applications of this therapeutic concept, serum stability was determined for CLN0004 and CLN0020 as well as for bi-specific aptamers bsA17 and bsA3 (chapter 4.3.13). DNA aptamers exhibited serum half lives of 9.8 h (CLN0004), 14.5 h (CLN0020), 6.4 h (bsA3) and 20.3 h (bsA17) in freshly thawed ultra low IgG FCS (also used for ADCC assay medium, chapter 3.2). bsA17 remained stable in DPBS for 48 h, indicating the long shelf-life of aptamers in general (Figure 32).

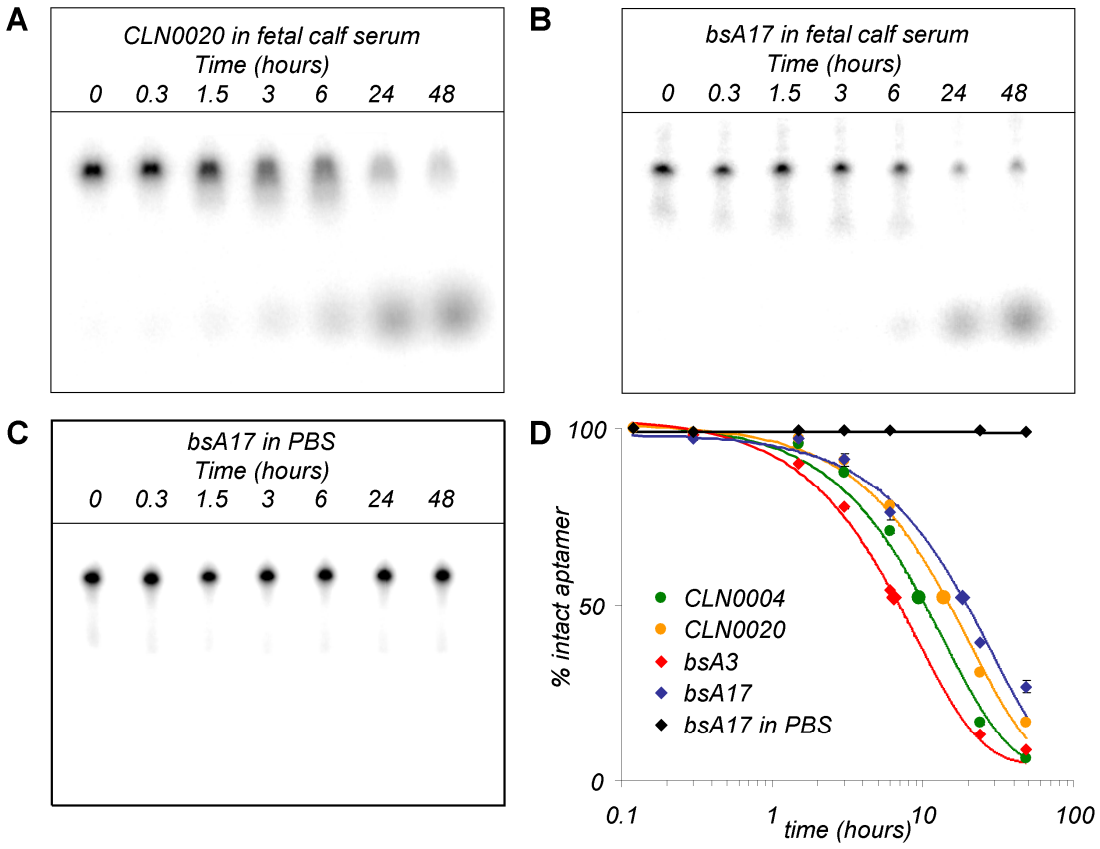

Figure 32: Serum stability of major DNA aptamers.

A and B, PAGE of CLN0020 or bsA17, respectively, after incubation in fetal calf serum at different time points. Bands at the migration level of the 0 h sample represented intact aptamer, while increasing signals at lower positions depicted breakdown products. C, bsA17 was stable in PBS over the whole time course, as debris could not be observed even after 48 h. D, Intensity values were extracted from gels as in A – C, the percentage of intact aptamer calculated and a curve fitted to the resulting time course. Half lives were determined as 6.4 h – 20.3 h. Enlarged symbols indicate the half life fit of each aptamer.

5.5 Functional screening of bi-specific aptamers

Bi-specific aptamers displaying high affinities and simultaneous binding to both target proteins as well as suitable serum stability were finally applied in a functional ADCC assay. ADCC in this case denoted antibody- or aptamer- dependent cellular cytotoxicity in the cases of antibody positive control or evaluated bi-specific aptamers, respectively.

ADCC assays were carried out using CLN0004-derived bsA3, 31, 4, 5, 7, 16, 18 (all with probably suitable linkers but relatively low c-Met affinities, Figure 34) and bsA12 and bsA13 (showing higher c-Met affinities due to long linker sequences). Further, CLN0003-based bi-specific aptamers bsA9, 10, 11, 15, 17, 20 and 22 were evaluated (sharing high c-Met affinities combined with varying linkers, Figures 33 and 34). bsA19, 21 and 32 were excluded due to lower affinity or less suitable linkers than related bsA20, 22 or 31, respectively. Initial evaluations were carried out with aptamer dilution series by applying peripheral blood mononuclear cells (PBMCs, chapter 4.4.4) to human gastric adenocarcinoma GTL-16 cells (chapter 3.1) in a ratio of 80:1 (chapter 4.4.6). Positive bi-specific aptamers were further analysed at 50 nM bsA with decreasing PBMC : target cell ratio. In addition, aptamer dilution series were carried out analogously to GLT-16 using human lung squamous cell carcinoma EBC-1 cells (chapter 3.1).

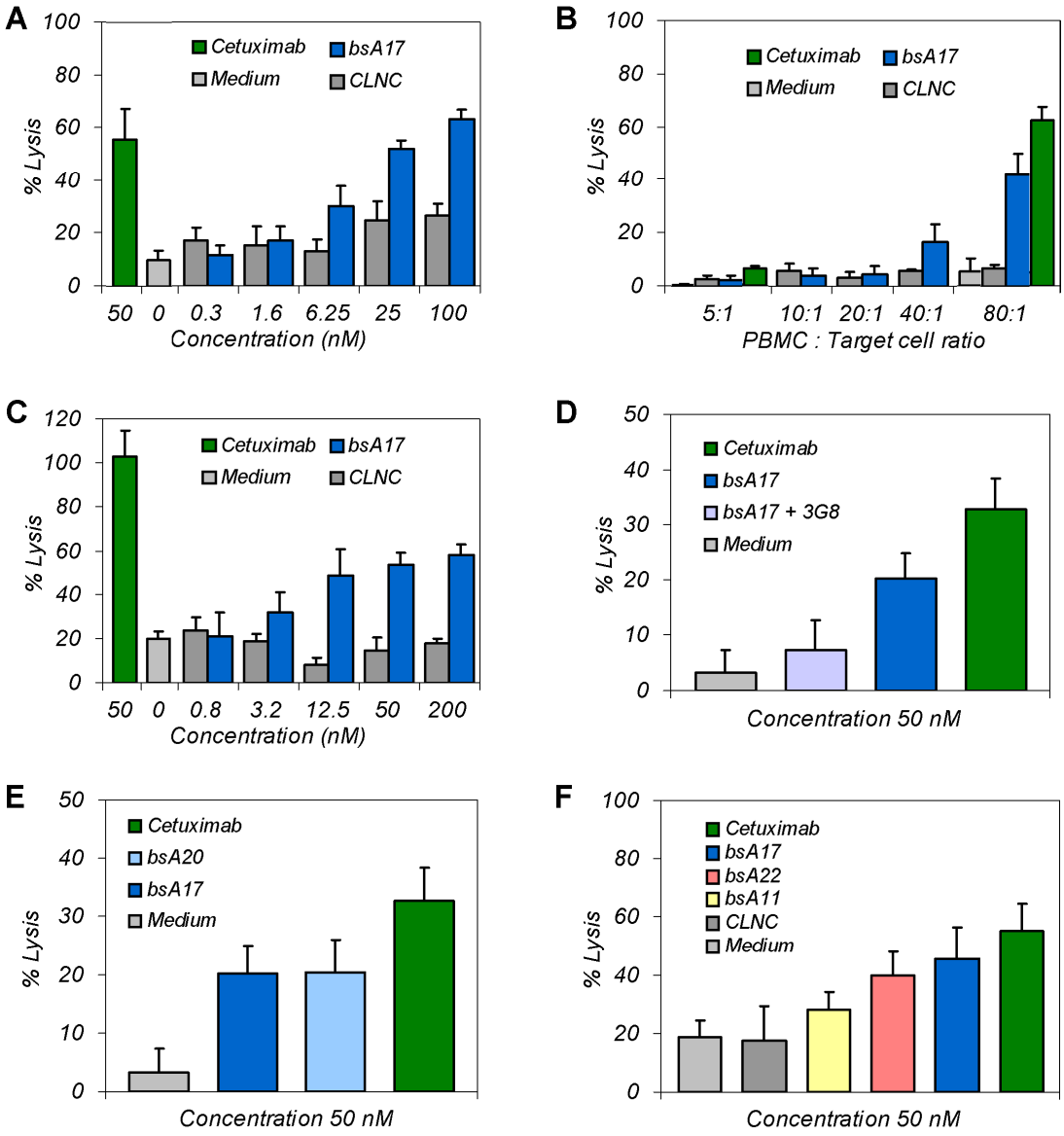

Figure 33: Functional ADCC assays of bi-specific aptamers on GTL-16 and EBC-1 cells.

A, Specific GTL-16 cell lysis mediated by bi-specific aptamer bsA17 at a similar magnitude as cetuximab as positive control. Aptamer titration led to decrease of & lysis to background levels of non-binding negative control aptamer CLNC and reference with medium only. B, PBMC : target cell ratio reduction diminished specific GTL-16 cell lysis of both bsA17 and cetuximab at 50 nM. Note that the actual effector : target cell ratio was approximately 8:1 when applying 80:1 PBMC : target cells. C, bsA17 mediated concentration-dependent specific EBC-1 cell lysis as well analogously to GTL-16 target cells (A). D, Addition of 20-fold molar excess of antibody 3G8 resulted in a significant decrease of bsA17-mediated GTL-16 lysis due to inhibition of bsA17-binding to CD16α. E, Affinity differences of 352 pM (bsA17) to 5 nM (bsA20) showed no influence on effectiveness of GTL-16 cell lysis, whereas longer linker sequences (approximately bsA17 with 49 Å, bsA22 with 105 Å and bsA11 with 217 Å) led to a decrease of bsA-mediated GTL-16 cell lysis (F). Maximal lysis varied between individual experiments due to donor and CD16α allotype dependency. ADCC assays were performed 5 times with n = 4 (A), 3 times with n = 3 (B), 4 times with n = 4 (C), 3 times with n = 9 (D), 1 time with n = 9 (E), 3 times with n = 9 (F) and representative measurements are shown as calculated mean values, error bars indicate standard deviation.

Bi-specific aptamer bsA17 mediated cellular cytotoxicity to GTL-16 and EBC-1 cells with a similar magnitude to antibody positive control cetuximab (Figure 33, A and C). This effect was reduced by both aptamer or effector cell dilution (Figure 33, B). In addition, blocking of aptamer binding to CD16α by addition of competing antibody 3G8 in 20-fold excess led to a significant decrease of specific cell lysis, further supporting the proposed mode of action (Figure 33, D). The bsA17-related bi-specific aptamer bsA22 similarly mediated specific GTL-16 cell lysis that could be diminished by reduction of aptamer concentration or effector cell amount (Figure 34, A and B). CLN0004-derived bsA31, showing lower c-Met affinity (92 nM), induced weaker, but significant cytotoxicitiy at higher concentrations above 100 nM (Figure 34, C). Bi-specific aptamer bsA15 (similar to bsA17, but composed of medium affinity CLN0123 instead of CLN0020 as CD16α binding entity) mediated specific GTL-16 lysis at comparable concentrations but to a lesser extent of 20 % (Figure 34, D).

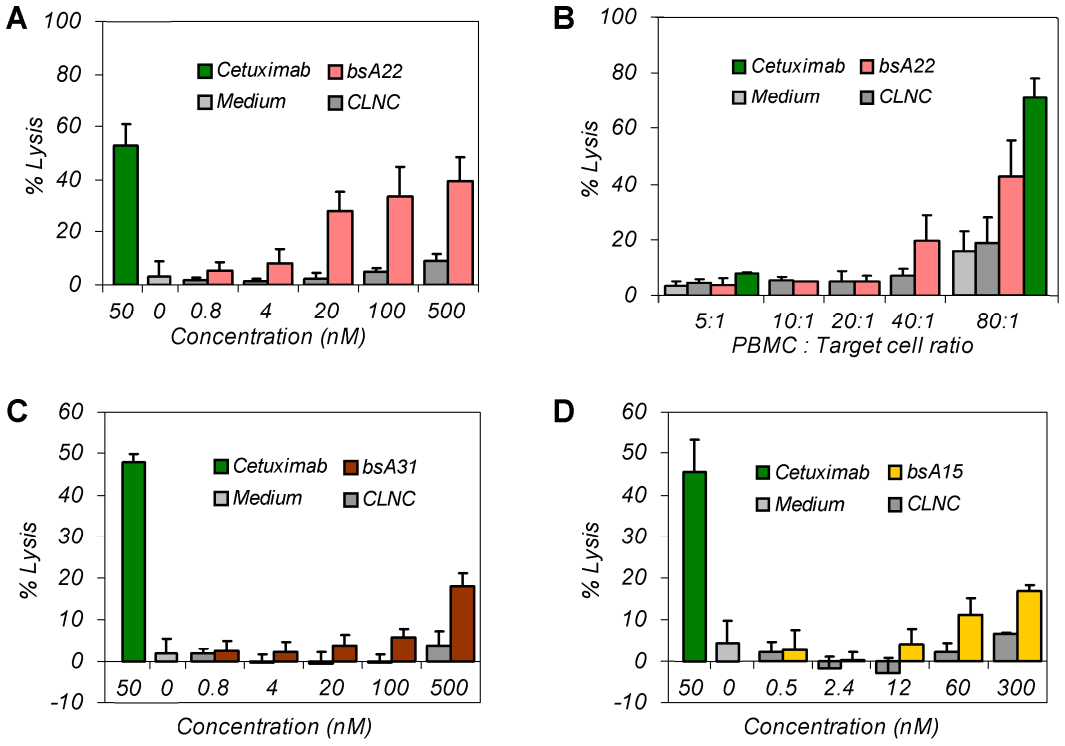

Figure 34: ADCC assays of bi-specific aptamers bsA22, bsA31 and bsA15.

A, Bi-specific aptamer bsA22 induced specific tumour cell lysis in a concentration-dependent manner. bsA22 was nearly as potent as cetuximab with significantly higher lysis than non-binding aptamer control CLNC or medium reference. B, At 50 nM fixed concentration, both bsA22- and cetuximab- mediated lysis was diminished by reduction of PBMC : target cell ratio. C, bsA31 with lower c-Met affinity induced weaker but significant lysis at higher concentrations. D, bsA15, composed of CLN0123 as lower affinity CD16α binding entity, mediated weak but significant cytotoxicity as well. Human gastric adenocarcinoma GTL-16 cells applied in all measurements. Mean values with standard deviation are shown. Assays were performed in triplicate (B) or n = 4 – 5 (A, C, D) 4 times (A), 1 time (B), 2 times (C) and 1 time (D) and representative measurements are shown.

Direct comparison of bsA17 and bsA20 that only differed in c-Met affinity of 352 pM to 5 nM, respectively, showed no difference of lysis effectiveness within this affinity range (Figure 33, E). However, the related construct bsA18, exhibiting 106 nM c-Met affinity, could not elicit cellular cytotoxicity (data not shown). Comparing similar constructs differing mostly in linker length only indicated putative linkers of approximately 50 – 100 Å (of bsA17 and bsA22) were more suitable than longer linkers (217 Å of bsA11, all Figure 33, F). It must be noted that putative linker lengths were calculated based on crystal structures of other DNA aptamers (chapter 5.4.1), so these were estimations only.

Although a precise EC_{50} determination was not feasible with mostly qualitative data obtained, the half effective dose of bsA17 and bsA22 was in the low two-digit nanomolar range of 1 – 50 nM (Figure 33, A and C as well as Figure 34, A).

Table 3 gives a concluding overview of reviewed bi-specific aptamers and all properties that have been characterised.

Table 3: Overview of all applied bi-specific aptamers with determined properties.

Green coloured values indicate suitable, yellow acceptable and red insufficient properties. Putative linker lengths estimated as decribed in chapter 5.4.1. MS1 denotes -19ntCLN0020-24nt; MS2, -20ntCLN0004-23nt; MS3, -19ntCLN0020-31nt; n.d., not determined. For further information, please refer to respective chapters.

bsA #	*1*	*2*	*3*	*31*	*32*	*4*	*5*	*6*	*7*	*8*	*9*	*10*	*11*
5' Aptamer	MS1	MS2	MS1	MS1	MS3	MS2	MS1	MS2	MS1	MS2	CLN20	CLN03	-19CLN20
Linker	7 nt	none	7 nt + 15dA	7 nt + 15dA	15dA	15dA	7 nt + PEG(3)	PEG(3)	7 nt + PEG(6)	PEG(6)	31 nt	19 nt	31 nt
3' Aptamer	MS2	MS1	MS2	-20CLN4	-20CLN4	MS1	MS2	MS1	MS2	MS1	CLN03	CLN20	CLN03
Size (kDa)	25.8	25.8	30.5	37.6	35.4	30.5	26.0	26.0	26.1	26.1	52.7	52.7	46.6
Length (nt)	82	82	97	120	113	97	82	82	82	82	168	168	149
Putative linker distance (Å)	49	0	154	154	105	105	69	20	82	33	217	133	217
Kd CD16a (nM)	84	51	33	24	33	78	64	51	73	102	92	107	73
Kd c-Met (nM)	319	220	141	92	119	105	164	370	160	271	0.160	0.157	0.162
Simultaneous binding in EMSA	n.d.	n.d.	yes	yes	yes	weak	yes	n.d.	weak	n.d.	weak	yes	yes
Simultaneous binding in fortéBio	n.d.	n.d.	n.d.	yes	n.d.	n.d.	n.d.	n.d.	n.d.	n.d.	n.d.	n.d.	yes
Aptamer mediated cytotoxicity	n.d.	n.d.	weak	weak	n.d.	no	no	n.d.	no	n.d.	no	no	no

bsA #	*12*	*13*	*14*	*15*	*16*	*17*	*18*	*19*	*20*	*21*	*22*
5' Aptamer	-19CLN20	-20CLN04	-10CLN20-24	CLN123	-20CLN04	MS1	MS3	MS1	MS1	MS1	MS3
Linker	51 nt	24 nt	7 nt + PEG(24)	20 nt	44 nt	7 nt	7 nt	7 nt + 15 dA	7 nt	7 nt + 15dA	15 dA
3' Aptamer	CLN04-5	CLN20-31	CLN03	CLN03	CLN123	CLN03	-13CLN4-5	CLN3-24	CLN3-24	CLN03	CLN03
Size (kDa)	45.1	36.7	42.8	52.7	46.4	39.2	33.5	36.4	31.7	43.8	41.7
Length (nt)	144	117	134	168	148	125	100	116	101	140	133
Putative linker distance (Å)	357	168	144	140	308	49	49	154	49	154	105
Kd CD16a (nM)	89	194	n.d.	173	178	19	15	32	23	19	27
Kd c-Met (nM)	18	18	n.d.	0.218	102	0.352	106	38	5.2	0.276	0.243
Simultaneous binding in EMSA	weak	weak	n.d.	weak	yes	yes	yes	yes	yes	yes	yes
Simultaneous binding in fortéBio	n.d.	n.d.	n.d.	n.d.	n.d.	yes	n.d.	n.d.	n.d.	n.d.	yes
Aptamer mediated cytotoxicity	no	no	n.d.	weak	no	yes	no	n.d.	yes	n.d.	yes

6 DISCUSSION

6.1 Selection and characterisation

CD16α specific DNA aptamers were selected in three different SELEX approaches (Figure 13) yielding abundant unique sequences (Appendix, Table 6). After nine rounds of filter SELEX, the aptamer pool was enriched containing 86 % binding aptamers (Figure 16). Successful CD16β counterselection led to CD16α specific aptamers that did not bind CD16β at all, although CD16β shares 97 % sequence identity and protein quality was confirmed in PAGE and immunoprecipitation (chapter 5.1). Of the few CD16 aptamers characterised by epitope mapping, all bound in or near the Fc-binding domain of CD16. Furthermore, both CD16α and CD16β were functionally folded, but differed in gel migration pattern (Figure 9 and Figure 12), possibly due to variation in glycosylation. CD16 isoform specificity of selected aptamers could be due to conformation-sensitive binding to epitopes that are influenced by the glycosylation pattern. This result supports the potential for aptamers as highly selective binding molecules. Although the specificity is surprising, it is in line with reported aptamers that show are highly specific (Jenison *et al.*, 1994) and can differentiate, for example, between closely related tumour cell types (Shangguan *et al.*, 2006). More importantly, the CD16α specificity could prevent decoy of therapeutically applied bi-specific aptamers by soluble CD16β vastly present in the blood (chapter 2.6), but ensure recruitment of suitable effector cells presenting mostly cell-bound CD16α. In comparison to therapeutic antibodies that are bound by both CD16α and CD16β isoforms, the CD16α specificity could increase the efficacy of therapeutic bi-specific aptamers.

In addition, the selected CD16α aptamer CLN0020 exhibited high affinity to both CD16α V158 and F158 allotypes (Figure 20 and Figure 24), whereas CD16α affinity of Fc-portions of antibodies and the resulting therapeutic effect is dependent on the CD16α V158 instead of F158 polymorphism. The V/V homologue is associated with higher ADCC and improved clinical outcome than F/F alleles (Cartron *et al.*, 2002; Taylor *et al.*, 2008). Application of CLN0020 in bi-specific aptamers would thus reduce this difference and potentially broaden the cytolytic effect to all patients.

Applying three additional rounds of CD16α hydrophobe plate selection (MTP SELEX) for competition elution with CD16 Fc-domain specific antibody 3G8 resulted in three unique sequences including CLN0030 with 6 nM affinity as well as two sequences that were also

found only in each of the cell SELEX approaches (Appendix, Table 6). In principle, MTP SELEX enriched binders should be specific for the Fc-binding domain of CD16α similar to antibodies, as the selection was driven with those aptamer initially bound to CD16α and replaced by 3G8. But since MTP SELEX derived aptamers did not bind to cellular CD16α, epitope specificity was not evaluated for these aptamers.

Unexpectedly, aptamers that were periodical highly enriched in cell SELEX and showed high affinity to recombinant CD16α in dot blot assays mostly did not exhibit cellular binding to the same cells used during their selection when applied in biotinylated form in flow cytometric measurements (CLN0021, 28, 118 and 126, cf. Table 1 and Table 6). Similarly, most filter SELEX derived CD16α specific aptamers bound to recombinant CD16α-6His with high affinity, but not to cellular CD16α presented on recombinant Jurkat or NK cells. This could be due to disruption of their tertiary structure by either biotinylation or more likely the subsequent binding of comparatively large streptavidin-phycoerythrine conjugates for staining purposes. Since such aptamers probably would not have been suitable to serve as one entity in bi-specific constructs, optimisation of the detection method (e.g. switching to direct dye labelling) was not performed. On the other hand, six rounds of cell SELEX could have been to few to evolve high affinity cellular binding aptamers and additional selection rounds would have increased the number of positive binders. Nevertheless, cell SELEX yielded additional unique CD16α aptamers with sufficient affinity (CLN0118, CLN0123, CLN0126, Table 1) and even utilisation of differently preselected starting pools (of filter SELEX rounds 3 or 5, respectively) resulted in selection of different new aptamers. This illustrates on the one hand the positive influence of initial SELEX rounds on recombinant target protein under characterised conditions to produce a diverse but already pre-enriched library that enables well-directed selection of cell-specific aptamers (Björn Hock, personal communication). On the other hand, the importance of a selection design to be as close as possible to the desired binder application conditions is emphasised.

Interestingly, the most prevalent aptamers did not always exhibit the highest affinity which was partly displayed by aptamers enriched very weakly and late during SELEX (e.g. CLN0030 with 6 nM CD16α affinity 2 % in MTP SELEX round 12, cf. Table 1 and Table 6, Appendix). Enrichment of aptamers during SELEX rounds using medium target protein concentrations could have also been due to intrinsic factors such as good compability for PCR amplification, while more stringent selection with decreased target protein but higher amounts of tRNA competitor could have yielded other binders with higher affinity. This implied a

mandatory characterisation of all aptamers that was carried out by testing the main representative of sequence families sharing 90 % sequence identity. In later stages, sequence variants of aptamer hits were analysed further for improved properties (CLN0004 in Figure 28). Furthermore, temperature-dependent affinity variation was observed with most, but not all characterised aptamers (Figure 22). This indicates the need to characterise every aptamer hit and adjust subsequent assays accordingly. Selection and characterisation of potentially therapeutic aptamers were performed at 37 °C, and some aptamers exhibited less binding or lower affinites at 4 °C (Figure 22). In contrast, flow cytometry binding reactions are generally carried out at 4 °C for reduction of the cell metabolism to preserve an original cell surface composition as well as to reduce undesired antibody dissociation (Chao *et al.*, 2006, step 15). Thus, flow cytometry was performed at ambient temperature, balancing both influences with the drawback of allowing undesired variations such as internalisation or autolysis of effector cells (e.g. 3G8 on NK cells in Figure 24, A).

An additional CD16α rRfY SELEX with counterselection to CD16β yielded a still variable but already highly enriched pool of CD16α binders (Figure 19), again exhibiting no binding to the highly related CD16β (Figure 18, D). Dot blot derived affinities of 20 – 49 nM were comparable to selected DNA aptamers, but since no vast stability increase was assumed by pyrimidine 2' fluoration only (Peng *et al.*, 2007) and no tumour specific aptamers of this composition were accessible, rRfY CD16α specific aptamers were not applied further in this study. Nevertheless, if future research generates high affinity rRfY tumour specific aptamers, the sequences presented herein could be further characterised by flow cytometry and minimisation and finally applied in bi-specific approaches.

Selected c-Met specific aptamers CLN0003 and CLN0004 exhibited desirable properties such as high affinity and clear cellular binding. In addition, both aptamers shared two sequence motifs (Figure 21) and recognised the same epitope on c-Met (Figure 27). Although binding to different epitopes on c-Met would have been interesting to examine (cf. Bluemel *et al.*, 2010), varying affinities and minimisation results enabled the construction of 24 different bi-specific aptamers that permitted an evaluation of binding strength and linker length for aptamer function. This work represents the first description of DNA aptamers that show high specificity and affinity to c-Met.

During aptamer characterisation, application of CD16α Fc-fusion proteins in dot blot assays generally yielded lower affinities in the direct comparison of V158 allotypes of Fc-CD16α to CD16α-6His (Figure 20). This effect could be due to sterical hindrance or slight

conformational changes induced by the Fc-fusion. Consequently, K_D values were measured in dot blots by applying CD16α-6His only. Since the F158 allotype of CD16α was only available as Fc-fusion, comparisons of aptamer binding affinity to the different allotypes could be carried out qualitatively only. Dot blot binding curves with Fc-CD16α(V158) and Fc-CD16α(F158) were compared directly and resulting K_D values were used not as absolute values but as indicators of allotype specificity. Furthermore, shifts in dot blot derived binding curves and resulting K_D values of independent measurements could be due to variation of ambient temperature affecting affinity (cf. Figure 22) or conformational changes of target proteins that would not affect the measurable applied protein concentration but reduce the actual bound protein portion and hence lead to a binding curve shift.

Structure determination through crystallisation was not available and application of *in silico* structure prediction via the mfold tool (Zuker, 2003) was only used to narrow minimisation efforts that had to be confirmed in the lab (chapter 5.3.5, cf. Sayer *et al.*, 2004). Predictions for CLN0020 structure were in accordance to minimisation results and defined a 34mer core structure essential for CD16α binding. Removal of only one base C20, predicted to participate in a stem structure, reduced binding properties drastically (cf. blue to red curve in Figure 28, B and Figure 26). However, similar predictions could not be retrieved for any other DNA aptamer, possibly due to energetically unstable sequences that become structured upon ligand binding only (Hermann *et al.*, 2000). Sequence comparison of c-Met aptamers CLN0003 and CLN0004 revealed a putatively important base G61 in CLN0004 (Figure 21). Truncation of only this base led to a total loss of binding in dot blot assays (orange to red curves in Figure 28, A). These results demonstrate that sequence analyses such as structure predictions via mfold and sequence comparisons may not be reliable in all cases but can be an important source of information that subsequently can be rapidly evaluated or confirmed in the laboratory (as clearly reported by, for example, Sayer *et al.*, 2004).

6.2 Bi-specific aptamers

The design of bi-specific aptamers included the development of linkers which approximately match the distance between CDRs and the Fc binding domain in whole antibodies. Micking antibody architecture may improve the chance of enabling a similar cytotoxic effect. The definition of aptamer linker and core sequences, with the exception of -19ntCLN0020-31nt (chapter 5.3.5), were only based on affinity reduction observed in truncation studies (Figure 28). Additionally, calculated linker lengths were based on measurements of nucleotide

distances in single stranded portions of DNA aptamer crystal structures and it was assumed that linker sequences did not interact with themselves or other parts of the binding entities. Hence, linker lengths represented an estimate and were utilised only for an approximate comparison of the distances bridged in antibodies to that in bi-specific aptamers.

Upon characterisation through minimisation, c-Met specific aptamer CLN0004 with an initial affinity of 11 nM as a 84mer (Table 1) was truncated to a 41mer with 83 nM or a 64mer showing 3 nM affinity (-20ntCLN0004-19nt or -20ntCLN0004, respectively in Figure 28, D). When a minimised CD16α specific CLN0020 was linked 5', resulting bi-specific aptamers exhibited lower CD16α affinities with 134 nM of bsA3 or bsA31 with 92 nM, respectively, while application of nearly full length CLN0004-5nt in bsA12 shared unaltered high affinity of 18 nM. This fact suggests steric hindrance of a second aptamer could have distorted CLN0004 and thus decreased c-Met affinity. A desired shorter linker was consequently only accessible at the cost of reduced affinity. In contrast, the c-Met specific aptamer CLN0003 exhibited unaltered picomolar affinity only as full length aptamer in which flanking regions were important but not essential for affinity (Figure 28, C). This indicated that a longer sequence needed to be synthesised including a shorter, less characterised linker. This aptamer was therefore chosen as main tumour-specific entity. CLN0003-based bi-specific aptamers showed c-Met affinities of 157 pM (bsA9 with long linker) to 38 nM (bsA19 containing truncated CLN0003-24nt), while CLN0004-derived bi-specific aptamers had expectedly lower affinities (92 nM of bsA31 to 370 nM of bsA6 constructed from minimised -20ntCLN0004-19nt at the 5' end of the bi-specific aptamer). Both approaches were tested in functional ADCC assays, since both affinity and defined linker length were potentially important features to be evaluated and optimised.

Regarding the CD16α specific portion of bi-specific aptamers, CLN0123 generally showed a lower CD16α affinity and was only used for the construction of the two bi-specific aptamers bsA15 and bsA16. CLN0020 was mainly used as a minimised 41mer (-19ntCLN0020-24nt, Figure 28, E). A core sequence was well characterised (Figure 26) and this aptamer contained a 7 nt linker from the original full length sequence that retained the aptamers suitable original affinity of about 20 – 50 nM. Mostly, linkers were designed based on the sequences from corresponding full length aptamers, since minimisation studies had shown that these sequences were not essential and also did not interfere with high affinity binding as determined in dot blot assays. As a further nucleotide-based sequence, 15 dA linkers were used as described by Müller and colleagues (Muller *et al*., 2004). In addition, PEG linkers

could also be introduced directly during synthesis and were used to bridge a more precisely defined distance between the two aptamer binding moieties.

Serum stabilities were analysed in ultra low IgG FCS (chapter 4.3.13) as this was a component of the ADCC medium applied in later functional assays. Although the serum was freshly thawed, stabilities measured in mouse or human serum may vary and remain to be determined as key characteristics for subsequent *in vivo* experiments. Measured stabilities of single and bi-specific aptamers of 6.4 – 20.3 h are in accordance with comparable studies of DNA aptamer degradation in human serum and plasma that reveal strongly differing stabilities varying from several minutes to 42 hours (Schmidt *et al.*, 2004; Di Giusto *et al.*, 2004; Peng *et al.*, 2007). Differences may reflect diverse applied methods, serum and plasma samples (Shaw *et al.*, 1995; Di Giusto *et al.*, 2004). But more important, nuclease degradation is also strongly dependent on the sequence (Choi *et al.*, 2010) and properties such as a rigid structure or exposed termini (Di Giusto *et al.*, 2006). It must be noted that analogous to the present work, most comparable studies evaluated residual intact aptamer bands of mono-radiolabelled sequences in gel electrophoreses, but the determination of the functional half-life by assessment of residual binding would be a more proper analysis method (similar to Di Giusto *et al.*, 2004). Nevertheless, in addition to the proof of simultaneous binding in two different experimental setups (chapters 5.4.3.1 and 5.4.3.2), resulting serum stabilities provided clear evidence of the suitability of bi-specific aptamers for functional evaluation.

6.3 Functional evaluation

Properties of 16 bi-specific aptamers had been determined to be potentially suitable for recruitment of NK cells to c-Met positive tumour cells; therefore, their ability to mediate specific target cell lysis was evaluated in functional ADCC assays. Certain bi-specific aptamers elicited cellular cytotoxicity of a magnitude comparable to the therapeutically applied monoclonal antibody cetuximab (chapter 5.5). Since the ADCC mediating antibodies R13 and R28 (van der Horst *et al.*, 2009) were reported only recently and were not available for comparative studies, cetuximab was used as positive antibody control in ADCC assays. Cetuximab targets the receptor tyrosine kinase EGFR and not c-Met, hence a quantitative comparison of antibody- and aptamer- dependent cellular cytotoxicity was not possible. Positive cetuximab-mediated target cell lysis was instead used as a qualitative indicator for a valid experimental setup including sufficient target cell viability and suitable NK cell reactivity. Literature-based, quantitative potency comparisons of bi-specific aptamers and

antibodies or further scFv-based bi-specific formats are discussed later in this section. Variation in total cell lyis at high aptamer or antibody concentrations was commonly observed in between single measurements. Specific lysis mediated by bi-specific aptamers varied from approximately 20 to 60 %. Cetuximab induced 30 – 100 % lysis (Figure 33 and Figure 34) which is comparable to reported maximal lysis of bi-specific scFv formats (Kellner *et al.*, 2008; Kugler *et al.*, 2010; Singer *et al.*, 2010) as well as therapeutical antibodies alemtuzumab (appr. 40 %), trastuzumab and rituximab (40 – 80 %) and optimised variants eliciting up to 100 % specific cell lysis (Figure 3 in Lazar *et al.*, 2006). Variation of maximal lysis in between different measurements can be due to biological variance of target cell preparations, blood donors with varying effector cell reactivities and CD16α V/F158 polymorphisms. PBMCs were applied in a ratio of 80:1 to target cells which translates to an effector to target cell ratio of approximately 8:1 assuming ~10 % of PBMCs are CD16α positive effector cells (Wallace and Smyth, 2005). Specific lysis may have been increased through the use of IL-2 or IL-21 activated and enriched NK cells (e.g. as reported by McCall *et al.*, 1999) in a higher E:T ratio. Additionally, longer incubation could have further increased maximal lysis (Mack *et al.*, 1995; Figure 2 in Brischwein *et al.*, 2006). On the other hand, results were significant when applying PBMCs and the design of these *ex vivo* assays was chosen to be as unartificial as possible.

The coupling of bi-specific aptamers was achieved by complete synthesis rather than hybridisation to obtain more uniform bi-specific aptamers. This advantage for potential therapeutic molecules outweighs the drawback that only aptamers of the same composition can be linked easily. Further use of polyethylene glycol linkers was not necessary due to positive results with pure oligonucleotide chains, but polyethylene glycol nevertheless shares the advantage of well characterised linker lengths, and is therefore a potentially applicable linker format. Linker lengths were chosen to vary from no linker in bsA2 to approximately 357 Å (51 nt) in bsA12 to cover a broad range of bridged distances (Table 2). As the goal of bi-specific aptamers was to mimic antibody effector function, linker lengths resembling the approximate distance between the CDRs and the Fc binding domain of antibodies were expected to produce a similar cytotoxic effect. As discussed above (chapter 6.2), putative linker lengths were estimated from truncation studies. The two binding entities in bsA17 were separated by approximately 49 Å, while bsA22 span 105 Å and 217 Å were supposedly bridged in bsA11. In a more precise examination, CLN0003 minimisation indicated that the 5' flanking region is important for binding but not essential: for example, the affinity of truncated -13ntCLN0003 was decreased in comparison to 91 pM but still high with 12 nM

(Figure 28, C). Therefore, bi-specific aptamers bsA15, bsA17 and bsA22 may comprise a lower affinity c-Met binding entity but potentially longer linker that more accurately resembles the distance in antibodies. In functional ADCC assays, these high affinity bi-specific aptamers with linkers of around 65 Å, similar to the distance in antibodies mediated cytotoxicity. In accordance to these findings, effective bi-specific scFv molecules contain Gly-Ser-linkers bridging similar distances (e.g. 110 Å in Singer *et al.*, 2010). In addition, decreased cytolytic efficacies were observed with increasing linker lengths (Figure 33, F) and linkers with putative separation distances over ~200 Å did not elicit significant cytotoxicity, regardless of high affinities to both target proteins (e.g. bsA9, bsA11 and bsA12, Table 3). This indicates the importance of the spatial distance for polarisation of NK cells and the formation of a lytic synapse (as evaluated in another way by Bluemel *et al.*, 2010). Bi-specific aptamers bsA17 and bsA22 combined picomolar c-Met aptamer CLN0003 linked to CD16α aptamer CLN0020 with affinities of ~20 nM and induced strong cytotoxicity. In addition, application of medium affinity aptamers CLN0004 (in bsA31 binding with 92 nM to c-Met) or CLN0123 (yielding 173 nM affinity to CD16α in bsA15) resulted in weaker, but still distinct and concentration-dependent cytotoxicity (Figure 34). This illustrates the importance of suitable affinities for both binding entities in bi-specific aptamers but also further validates the functionality of the bi-specific aptamer approach.

So far, ADCC to c-Met overexpressing tumour cells was only elicited by applying two antibodies synergistically (van der Horst *et al.*, 2009). Other published c-Met antibody therapeutics comprise only Fab-fragments (Pacchiana *et al.*, 2010) or *E. coli* produced monovalent antibodies (MetMAb, Jin *et al.*, 2008) that do not induce cellular cytotoxicity. Dilution series of bi-specific aptamers bsA17 and bsA22 indicate a half-effective concentration in the 10 - 50 nM range (Figure 33 and Figure 34). This is comparable to antibody-mediated cytotoxicity to GTL-16 cells determined to be half maximal effective at 60 nM concentrations when two synergistical antibodies are applied (van der Horst *et al.*, 2009). Approved therapeutic antibodies targeting other surface proteins have been optimised to elicit enhanced ADCC and exhibit EC_{50} values in a low ng/ml range translating to low picomolar concentrations (Lazar *et al.*, 2006). Since ADCC is dependent on the target protein, its internalisation (Thie *et al.*, in preparation) and to some extent even on the bound epitope on the target protein (as indicated by different target protein variants in Bluemel *et al.*, 2010), targeting other tumour-associated surface proteins such as EGFR could potentially yield stronger aptamer-dependent cytotoxicity as well. CD16α targeting bi-specific constructs in scFv formats that are comparable to bi-specific aptamers described herein show half

maximum effective doses at low nanomolar (Kipriyanov *et al.*, 2002) to three-digit picomolar concentrations (Bruenke *et al.*, 2004; Kugler *et al.*, 2010), while similar constructs as tri-specific triplebodies (sctb) mediate ADCC with low picomolar EC_{50} values (Kellner *et al.*, 2008; Singer *et al.*, 2010). Finally, CD3 specific T cell recruiting BiTEs (e.g. MT103 and MT110) and similar constructs exhibit half maximum effective doses below 1 ng/ml which equals low picomolar to femtomolar concentrations (Mack *et al.*, 1995; Brischwein *et al.*, 2006). Due to target protein dependency of ADCC, direct comparison of bi-specific aptamers is only feasible to c-Met antibodies applied to GTL-16 cells that only synergistically show a potency similar to effective bi-specific aptamers alone (as discussed above and in van der Horst *et al.*, 2009).

Aptamer mediated cellular cytotoxicity was dependent on the concentration of bi-specific aptamers and the amount of applied effector cells. Blocking of aptamer binding to effector cells via the competing monoclonal antibody 3G8 reduced specific cell lysis which provided proof for the suggested mode of action. Specific cytotoxicity was demonstrated for independent human gastric and lung cancer cell lines and determined 3-6 times in independent experiments applying effector cell of different blood donors. Taken together, these results validate that bi-specific aptamers can mediate specific cellular cytotoxicity.

6.4 Perspective

The aim of the project presented herein was the specific re-localisation of NK cells to tumours by aptamers bi-specific for CD16α expressed on NK cells and tumour specific antigen c-Met to elicit "aptamer-dependent cellular cytotoxicity". This was proven in functional cellular ADCC assays. Bi-specific aptamers exhibit affinities similar to certain BiTEs with three-digit picomolar to low nanomolar TSA binding (to c-Met, in comparison to 10^{-9} M affinity to CD19 in BiTE MT103, Baeuerle *et al.*, 2003) and medium affinity ESA binding (15 - 197 nM to CD16α, in comparison to 10^{-7} M CD3 affinity in MT103, Baeuerle *et al.*, 2003). These similar characteristics point out that bi-specific aptamers could induce serial killing of NK cells (cf. Hoffmann *et al.*, 2005). Counterintuitively, a decreased CD3 affinity increased effective T cell targeting of BiTEs (Bortoletto *et al.*, 2002). Therefore, facile adjustment of CD16α affinities of cytolytic-active bi-specific aptamers based on minimisation studies (chapter 5.3.7) could similarily enable optimisation of NK cell recruitment and potentially further increase the potency of bi-specific aptamers. However, as discussed above, the efficacy of BiTEs clearly superseeds that of first-generation bi-specific aptamers reported

herein. Re-localisation of CTLs instead of NK cells by targeting CD3 instead of CD16 could potentially increase the efficacy of bi-specific aptamers. Furthermore, targeting other tumour markers, the establishment of tri-specific aptamers sharing avidity as well as a precise fine tuning of linker lengths could enhance their potency. Additionally, the efficacy could be evaluated further by examining other c-Met tumour cell lines although positive results with two independent tumour types already provided clear evidence that the cytolytic effect is assignable to other c-Met overexpressing tumour cell lines as well.

Future work could focus on *in vivo* evaluations using xenograft mouse models (chapter 2.8). Transgenic mouse models expressing human CD16 receptors could be used with human xenograft c-Met overexpressing tumours. Secondary effects through engagement of the murine immune system can not be excluded, although minimal binding of bi-specific aptamers to murine CD16 is anticipated (chapter 5.3.1). Despite this challenge, issues of serum stability and poor pharmacokinetics remain to be solved. Stability can be further improved by usage of modified nucleotides with substituted 2' residues (chapter 2.4.1). Modifications can be inserted into the already selected DNA aptamers or via an additional SELEX, applying pools with the appropriate compositions. Suitable mRfY aptamers, sharing all essential characteristics with successfully employed DNA aptamer CLN0020, are already available (unpublished results). Renal clearance could be reduced by antibody-approved approaches as PEGylation (Pendergrast *et al.*, 2005), HESylation, PASylation, polysialylation or other glycosylation (reviewed in Table I in Kontermann, 2009; and Constantinou *et al.*, 2010). FcRn-mediated recycling of antibodies (Roopenian and Akilesh, 2007) could be mimicked and converted into an aptamer-format as well. Aptamers binding to the neonatal Fc receptor FcRn at pH 6 but not at pH 7.4 (Ralf Günther, unpublished results) could be additionally linked and would enable half life extension by FcRn-mediated retention in monocytes and endothelial cells. Independently of these approaches, the molecular mass of bi-specific aptamers could be sufficient even without further coupling. The half-life of a PEG-linked aptamer of a molecular mass of 47 kDa was determined to be 23 h in mice (Burmeister *et al.*, 2005). An evaluation whether, for instance, bsA17 with a molecular mass of 39.1 kDa would yield a similarily suitable half-life would be a first step in further evaluation *in vivo*.

Bi-specific aptamers, generated in this work to simultaneously bind to tumour and effector cells, represent a suitable starting concept for the development of stable, nucleotide based therapeutics to mediate lysis of c-Met positive tumours. Their application range could be broadened by facile exchange of the tumour-specific portion with further anti-tumour

aptamers targeting e.g. CD52, HER2/neu or EGFR as seen in current major antibody-based therapies (Table 1 in Das *et al.*, 2009). Tumour-specific cell surface targets are often overexpressed receptors on which binding of therapeutics should either act by inhibiting or at least not activating through multimerisation. In contrast to antibodies, aptamers as single binding entities possess the property of binding tumour-specific surface receptors without the risk of activation (Pacchiana *et al.*, 2010) but can serve as inhibitors (chapter 2.2 and below). Conferring a second function by linkage of CD16α specific aptamers to such nucleotide based inhibitors would broaden their functionality to multiple modes of action. Such constructs could mimic most eligible features of comparable therapeutic antibody approaches, but exceed them, for example, with uniform and cost-effective synthesis as well as no to low immunogenicity (White *et al.*, 2000; Kaur *et al.*, 2008).

Internalisation was not evaluated for c-Met or CD16α specific aptamers. In case of possible internalisation upon high affinity binding, these aptamers could be used as well in further bi-valent constructs for the delivery of cytotoxic substances. Other cancer target specific aptamers have been selected among others against MUC-1, PSMA, EGFR, CTL-A4, PDGF-R and VEGF as single binding entities only (Kaur *et al.*, 2008; Table 2 in Das *et al.*, 2009). Internalising target molecules were also addressed to specifically deliver fused payloads, e.g. as siRNA or cis-platin to target cells (Chu *et al.*, 2006; Dhar *et al.*, 2008; Zhou *et al.*, 2009a). Most other linkage of aptamers aimed at an affinity increase by avidity (Santulli-Marotto *et al.*, 2003; Muller *et al.*, 2007; Kim *et al.*, 2008). Müller and colleagues coupled aptamers to increase enzyme inhibition (Muller *et al.*, 2008, and chapter 2.2). Furthermore, two copies of a receptor specific RNA aptamer were assembled on an olignucleotide-based scaffold to induce multimerisation of target receptors. This proved that linkage can convert single binders into receptor-activating aptamers (Dollins *et al.*, 2008). In a similar approach, McNamara and co-workers hybridised two copies of an aptamer targeting a T cell receptor that induced co-stimulation of these effector cells and led to tumour growth inhibition in mice (McNamara *et al.*, 2008). To the author's knowledge, the work presented herein describes for the first time a gain of tumour-effective function of two distinct binding entities by linkage into a bi-specific aptamer mediating tumour cell lysis.

7 REFERENCES

7.1 Publications derived of the presented work

Achim Boltz, Lars Toleikis, Ralf Günther, Björn Hock (Dec 10th 2010) Bispecific aptamers mediating tumour cell lysis. *Patent application.* Application no. EP10015522.5

Achim Boltz, Angelika-Nicole Helfrich, Ralf Günther, Björn Hock and Lars Toleikis (April 27th 2010) Aptamer Dependent Cellular Cytotoxicity. *Poster at R&D Day, Merck, Darmstadt, Germany*

Achim Boltz, Lars Toleikis, Ralf Günther, Harald Kolmar and Björn Hock (Dec 15th 2010) Aptamer Dependent Cellular Cytotoxicity. *Poster at Doktorandenworkshop, TU Darmstadt, Darmstadt, Germany*

7.2 Literature

Andermarcher E, Surani MA, and Gherardi E (1996) Co-expression of the HGF/SF and c-met genes during early mouse embryogenesis precedes reciprocal expression in adjacent tissues during organogenesis. *Dev Genet,* **18,** 254-266.

Anderson CL, Looney RJ, Culp DJ, Ryan DH, Fleit HB, Utell MJ, Frampton MW, Manganiello PD, and Guyre PM (1990) Alveolar and peritoneal macrophages bear three distinct classes of Fc receptors for IgG. *J Immunol,* **145,** 196-201.

Arndt MA, Krauss J, Kipriyanov SM, Pfreundschuh M, and Little M (1999) A bispecific diabody that mediates natural killer cell cytotoxicity against xenotransplantated human Hodgkin's tumors. *Blood,* **94,** 2562-2568.

Baeuerle PA, Kufer P, and Lutterbuse R (2003) Bispecific antibodies for polyclonal T-cell engagement. *Curr Opin Mol Ther,* **5,** 413-419.

Baeuerle PA and Reinhardt C (2009) Bispecific T-cell engaging antibodies for cancer therapy. *Cancer Res,* **69,** 4941-4944.

Baldrich E, Restrepo A, and O'Sullivan CK (2004) Aptasensor development: elucidation of critical parameters for optimal aptamer performance. *Anal Chem,* **76,** 7053-7063.

Bates PJ, Choi EW, and Nayak LV (2009) G-rich oligonucleotides for cancer treatment. *Methods Mol Biol,* **542,** 379-392.

Birchmeier C, Birchmeier W, Gherardi E, and Vande Woude GF (2003) Met, metastasis, motility and more. *Nat Rev Mol Cell Biol,* **4,** 915-925.

Bladt F, Riethmacher D, Isenmann S, Aguzzi A, and Birchmeier C (1995) Essential role for the c-met receptor in the migration of myogenic precursor cells into the limb bud. *Nature,* **376,** 768-771.

Blank M, Weinschenk T, Priemer M, and Schluesener H (2001) Systematic evolution of a DNA aptamer binding to rat brain tumor microvessels. selective targeting of endothelial regulatory protein pigpen. *J Biol Chem,* **276,** 16464-16468.

Bluemel C, Hausmann S, Fluhr P, Sriskandarajah M, Stallcup WB, Baeuerle PA, and Kufer P (2010) Epitope distance to the target cell membrane and antigen size determine the potency of T cell-mediated lysis by BiTE antibodies specific for a large melanoma surface antigen. *Cancer Immunol Immunother,* **59,** 1197-1209.

Bock LC, Griffin LC, Latham JA, Vermaas EH, and Toole JJ (1992) Selection of single-stranded DNA molecules that bind and inhibit human thrombin. *Nature,* **355,** 564-566.

Bortoletto N, Scotet E, Myamoto Y, D'Oro U, and Lanzavecchia A (2002) Optimizing anti-CD3 affinity for effective T cell targeting against tumor cells. *Eur J Immunol,* **32,** 3102-3107.

Bossi G and Griffiths GM (2005) CTL secretory lysosomes: biogenesis and secretion of a harmful organelle. *Semin Immunol,* **17,** 87-94.

Boyum A (1968) Isolation of leucocytes from human blood. A two-phase system for removal of red cells with methylcellulose as erythrocyte-aggregating agent. *Scand J Clin Lab Invest Suppl,* **97,** 9-29.

Brischwein K, Schlereth B, Guller B, Steiger C, Wolf A, Lutterbuese R, Offner S, Locher M, Urbig T, Raum T, Kleindienst P, Wimberger P, Kimmig R, Fichtner I, Kufer P, Hofmeister R, da Silva AJ, and Baeuerle PA (2006) MT110: a novel bispecific single-chain antibody construct with high efficacy in eradicating established tumors. *Mol Immunol,* **43,** 1129-1143.

Bruenke J, Barbin K, Kunert S, Lang P, Pfeiffer M, Stieglmaier K, Niethammer D, Stockmeyer B, Peipp M, Repp R, Valerius T, and Fey GH (2005) Effective lysis of lymphoma cells with a stabilised bispecific single-chain Fv antibody against CD19 and FcgammaRIII (CD16). *Br J Haematol,* **130,** 218-228.

Bruenke J, Fischer B, Barbin K, Schreiter K, Wachter Y, Mahr K, Titgemeyer F, Niederweis M, Peipp M, Zunino SJ, Repp R, Valerius T, and Fey GH (2004) A recombinant bispecific single-chain Fv antibody against HLA class II and FcgammaRIII (CD16) triggers effective lysis of lymphoma cells. *Br J Haematol,* **125,** 167-179.

Bruhns P, Iannascoli B, England P, Mancardi DA, Fernandez N, Jorieux S, and Daeron M (2008) Specificity and affinity of human Fc{gamma} receptors and their polymorphic variants for human IgG subclasses. *Blood.*

Bryceson YT, March ME, Ljunggren HG, and Long EO (2006a) Activation, coactivation, and costimulation of resting human natural killer cells. *Immunol Rev,* **214,** 73-91.

Bryceson YT, March ME, Ljunggren HG, and Long EO (2006b) Synergy among receptors on resting NK cells for the activation of natural cytotoxicity and cytokine secretion. *Blood,* **107,** 159-166.

Burke DH and Nickens DG (2002) Expressing RNA aptamers inside cells to reveal proteome and ribonome function. *Brief Funct Genomic Proteomic,* **1,** 169-188.

Burmeister PE, Lewis SD, Silva RF, Preiss JR, Horwitz LR, Pendergrast PS, McCauley TG, Kurz JC, Epstein DM, Wilson C, and Keefe AD (2005) Direct in vitro selection of a 2'-O-methyl aptamer to VEGF. *Chem Biol,* **12,** 25-33.

Burmeister PE, Wang C, Killough JR, Lewis SD, Horwitz LR, Ferguson A, Thompson KM, Pendergrast PS, McCauley TG, Kurz M, Diener J, Cload ST, Wilson C, and Keefe AD (2006) 2'-Deoxy purine, 2'-O-methyl pyrimidine (dRmY) aptamers as candidate therapeutics. *Oligonucleotides,* **16,** 337-351.

Carson WE, Parihar R, Lindemann MJ, Personeni N, Dierksheide J, Meropol NJ, Baselga J, and Caligiuri MA (2001) Interleukin-2 enhances the natural killer cell response to Herceptin-coated Her2/neu-positive breast cancer cells. *Eur J Immunol,* **31,** 3016-3025.

Cartron G, Dacheux L, Salles G, Solal-Celigny P, Bardos P, Colombat P, and Watier H (2002) Therapeutic activity of humanized anti-CD20 monoclonal antibody and polymorphism in IgG Fc receptor FcgammaRIIIa gene. *Blood,* **99,** 754-758.

Cerchia L, Hamm J, Libri D, Tavitian B, and de Franciscis V (2002) Nucleic acid aptamers in cancer medicine. *FEBS Lett,* **528,** 12-16.

Cerchia L, Pan W, Giangrande PH, McNamara JO, and de Franciscis V (2009). Cell-Specific Aptamers for Targeted Therapies. In Mayer,G. (Ed.), *Nucleic Acid and Peptide Aptamers: Methods and Protocols*, ., pp. 59-77.

Chames P and Baty D (2009) Bispecific antibodies for cancer therapy: the light at the end of the tunnel? *MAbs,* **1,** 539-547.

Chan MY, Cohen MG, Dyke CK, Myles SK, Aberle LG, Lin M, Walder J, Steinhubl SR, Gilchrist IC, Kleiman NS, Vorchheimer DA, Chronos N, Melloni C, Alexander JH, Harrington RA, Tonkens RM, Becker RC, and Rusconi CP (2008) Phase 1b randomized study of antidote-controlled modulation of factor IXa activity in patients with stable coronary artery disease. *Circulation,* **117,** 2865-2874.

Chao G, Lau WL, Hackel BJ, Sazinsky SL, Lippow SM, and Wittrup KD (2006) Isolating and engineering human antibodies using yeast surface display. *Nat Protoc,* **1,** 755-768.

Chen CH, Chernis GA, Hoang VQ, and Landgraf R (2003) Inhibition of heregulin signaling by an aptamer that preferentially binds to the oligomeric form of human epidermal growth factor receptor-3. *Proc Natl Acad Sci U S A,* **100,** 9226-9231.

Choi EW, Nayak LV, and Bates PJ (2010) Cancer-selective antiproliferative activity is a general property of some G-rich oligodeoxynucleotides. *Nucleic Acids Res,* **38,** 1623-1635.

Christensen JG, Burrows J, and Salgia R (2005) c-Met as a target for human cancer and characterization of inhibitors for therapeutic intervention. *Cancer Lett,* **225,** 1-26.

Chu TC, Twu KY, Ellington AD, and Levy M (2006) Aptamer mediated siRNA delivery. *Nucleic Acids Res,* **34,** e73.

Cipriani NA, Abidoye OO, Vokes E, and Salgia R (2009) MET as a target for treatment of chest tumors. *Lung Cancer,* **63,** 169-179.

Comoglio PM, Giordano S, and Trusolino L (2008) Drug development of MET inhibitors: targeting oncogene addiction and expedience. *Nat Rev Drug Discov,* **7,** 504-516.

Constantinou A, Chen C, and Deonarain MP (2010) Modulating the pharmacokinetics of therapeutic antibodies. *Biotechnol Lett.*

Cowperthwaite MC and Ellington AD (2008) Bioinformatic analysis of the contribution of primer sequences to aptamer structures. *J Mol Evol,* **67,** 95-102.

Cui Z, Willingham MC, Hicks AM, exander-Miller MA, Howard TD, Hawkins GA, Miller MS, Weir HM, Du W, and DeLong CJ (2003) Spontaneous regression of advanced cancer: identification of a unique genetically determined, age-dependent trait in mice. *Proc Natl Acad Sci U S A,* **100,** 6682-6687.

Cullen BR and Greene WC (1989) Regulatory pathways governing HIV-1 replication. *Cell,* **58,** 423-426.

Das M, Mohanty C, and Sahoo SK (2009) Ligand-based targeted therapy for cancer tissue. *Expert Opin Drug Deliv,* **6,** 285-304.

Dassie JP, Liu XY, Thomas GS, Whitaker RM, Thiel KW, Stockdale KR, Meyerholz DK, McCaffrey AP, McNamara JO, and Giangrande PH (2009) Systemic administration of optimized aptamer-siRNA chimeras promotes regression of PSMA-expressing tumors. *Nat Biotechnol,* **27,** 839-849.

De HM, Kleijer M, Minchinton RM, Roos D, and von dem Borne AE (1994) Soluble Fc gamma RIIIa is present in plasma and is derived from natural killer cells. *J Immunol,* **152,** 900-907.

Desjarlais JR, Lazar GA, Zhukovsky EA, and Chu SY (2007) Optimizing engagement of the immune system by anti-tumor antibodies: an engineer's perspective. *Drug Discov Today,* **12,** 898-910.

Dhar S, Gu FX, Langer R, Farokhzad OC, and Lippard SJ (2008) Targeted delivery of cisplatin to prostate cancer cells by aptamer functionalized Pt(IV) prodrug-PLGA-PEG nanoparticles. *Proc Natl Acad Sci U S A,* **105,** 17356-17361.

Di Giusto DA and King GC (2004) Construction, stability, and activity of multivalent circular anticoagulant aptamers. *J Biol Chem,* **279,** 46483-46489.

Di Giusto DA, Knox SM, Lai Y, Tyrelle GD, Aung MT, and King GC (2006) Multitasking by multivalent circular DNA aptamers. *Chembiochem,* **7,** 535-544.

Dollins CM, Nair S, Boczkowski D, Lee J, Layzer JM, Gilboa E, and Sullenger BA (2008) Assembling OX40 aptamers on a molecular scaffold to create a receptor-activating aptamer. *Chem Biol,* **15,** 675-682.

Dollins CM, Nair S, Boczkowski D, Lee J, Layzer JM, Gilboa E, and Sullenger BA (2008) Assembling OX40 aptamers on a molecular scaffold to create a receptor-activating aptamer. *Chem Biol,* **15,** 675-682.

Dorner BG, Smith HR, French AR, Kim S, Poursine-Laurent J, Beckman DL, Pingel JT, Kroczek RA, and Yokoyama WM (2004) Coordinate expression of cytokines and chemokines by NK cells during murine cytomegalovirus infection. *J Immunol,* **172,** 3119-3131.

Edberg JC, Barinsky M, Redecha PB, Salmon JE, and Kimberly RP (1990) Fc gamma RIII expressed on cultured monocytes is a N-glycosylated transmembrane protein distinct from Fc gamma RIII expressed on natural killer cells. *J Immunol,* **144,** 4729-4734.

Edberg JC and Kimberly RP (1997) Cell type-specific glycoforms of Fc gamma RIIIa (CD16): differential ligand binding. *J Immunol,* **159,** 3849-3857.

Eder JP, Vande Woude GF, Boerner SA, and LoRusso PM (2009) Novel therapeutic inhibitors of the c-Met signaling pathway in cancer. *Clin Cancer Res,* **15,** 2207-2214.

Ellington AD and Szostak JW (1990) In vitro selection of RNA molecules that bind specific ligands. *Nature,* **346,** 818-822.

Fauriat C, Long EO, Ljunggren HG, and Bryceson YT (2009) Regulation of human NK cell cytokine and chemokine productionby target cell recognition. *Blood.*

Fehniger TA, Shah MH, Turner MJ, VanDeusen JB, Whitman SP, Cooper MA, Suzuki K, Wechser M, Goodsaid F, and Caligiuri MA (1999) Differential cytokine and chemokine gene expression by human NK cells following activation with IL-18 or IL-15 in combination with IL-12: implications for the innate immune response. *J Immunol,* **162,** 4511-4520.

Ferreira CS, Cheung MC, Missailidis S, Bisland S, and Gariepy J (2009) Phototoxic aptamers selectively enter and kill epithelial cancer cells. *Nucleic Acids Res,* **37,** 866-876.

Ferreira CS, Papamichael K, Guilbault G, Schwarzacher T, Gariepy J, and Missailidis S (2008) DNA aptamers against the MUC1 tumour marker: design of aptamer-antibody sandwich ELISA for the early diagnosis of epithelial tumours. *Anal Bioanal Chem,* **390,** 1039-1050.

Gentile A, Trusolino L, and Comoglio PM (2008) The Met tyrosine kinase receptor in development and cancer. *Cancer Metastasis Rev,* **27,** 85-94.

Habicht G and Siegemund M. (2002) Konstruktion einer vollsynthetischen *Camelidae*-VHH-Antikörper-Bibliothek optimierter Qualität und deren Expression in *Escherichia coli*. Dissertation

Harrison D, Phillips JH, and Lanier LL (1991) Involvement of a metalloprotease in spontaneous and phorbol ester-induced release of natural killer cell-associated Fc gamma RIII (CD16-II). *J Immunol,* **147,** 3459-3465.

Healy JM, Lewis SD, Kurz M, Boomer RM, Thompson KM, Wilson C, and McCauley TG (2004) Pharmacokinetics and biodistribution of novel aptamer compositions. *Pharm Res,* **21,** 2234-2246.

Hedrick JA, Saylor V, Figueroa D, Mizoue L, Xu Y, Menon S, Abrams J, Handel T, and Zlotnik A (1997) Lymphotactin is produced by NK cells and attracts both NK cells and T cells in vivo. *J Immunol,* **158,** 1533-1540.

Hermann T and Patel DJ (2000) Adaptive recognition by nucleic acid aptamers. *Science,* **287,** 820-825.

Hicke BJ, Stephens AW, Gould T, Chang YF, Lynott CK, Heil J, Borkowski S, Hilger CS, Cook G, Warren S, and Schmidt PG (2006) Tumor targeting by an aptamer. *J Nucl Med,* **47,** 668-678.

Hoffmann P, Hofmeister R, Brischwein K, Brandl C, Crommer S, Bargou R, Itin C, Prang N, and Baeuerle PA (2005) Serial killing of tumor cells by cytotoxic T cells redirected with a CD19-/CD3-bispecific single-chain antibody construct. *Int J Cancer,* **115,** 98-104.

Homann M and Goringer HU (1999) Combinatorial selection of high affinity RNA ligands to live African trypanosomes. *Nucleic Acids Res,* **27,** 2006-2014.

Huang YF, Shangguan D, Liu H, Phillips JA, Zhang X, Chen Y, and Tan W (2009) Molecular assembly of an aptamer-drug conjugate for targeted drug delivery to tumor cells. *Chembiochem,* **10,** 862-868.

Huizinga TW, De HM, van Oers MH, Kleijer M, Vile H, van der Wouw PA, Moulijn A, van WH, Roos D, and von dem Borne AE (1994) The plasma concentration of soluble Fc-gamma RIII is related to production of neutrophils. *Br J Haematol,* **87,** 459-463.

Jenison RD, Gill SC, Pardi A, and Polisky B (1994) High-resolution molecular discrimination by RNA. *Science,* **263,** 1425-1429.

Jin H, Yang R, Zheng Z, Romero M, Ross J, Bou-Reslan H, Carano RA, Kasman I, Mai E, Young J, Zha J, Zhang Z, Ross S, Schwall R, Colbern G, and Merchant M (2008) MetMAb, the one-armed 5D5 anti-c-Met antibody, inhibits orthotopic pancreatic tumor growth and improves survival. *Cancer Res,* **68,** 4360-4368.

Kasahara Y, Kitadume S, Morihiro K, Kuwahara M, Ozaki H, Sawai H, Imanishi T, and Obika S (2010) Effect of 3'-end capping of aptamer with various 2',4'-bridged nucleotides: Enzymatic post-modification toward a practical use of polyclonal aptamers. *Bioorg Med Chem Lett,* **20,** 1626-1629.

Kaur G and Roy I (2008) Therapeutic applications of aptamers. *Expert Opin Investig Drugs,* **17,** 43-60.

Kawazoe N, Ito Y, and Imanishi Y (1996) Patterned staining by fluorescein-labeled oligonucleotides obtained by in vitro selection. *Anal Chem,* **68,** 4309-4311.

Keefe AD and Cload ST (2008) SELEX with modified nucleotides. *Curr Opin Chem Biol,* **12,** 448-456.

Keefe AD, Pai S, and Ellington A (2010) Aptamers as therapeutics. *Nat Rev Drug Discov,* **9,** 537-550.

Kellner C, Bruenke J, Stieglmaier J, Schwemmlein M, Schwenkert M, Singer H, Mentz K, Peipp M, Lang P, Oduncu F, Stockmeyer B, and Fey GH (2008) A novel CD19-directed recombinant bispecific antibody derivative with enhanced immune effector functions for human leukemic cells. *J Immunother,* **31,** 871-884.

Kim D, Jeong YY, and Jon S (2010) A Drug-Loaded Aptamer-Gold Nanoparticle Bioconjugate for Combined CT Imaging and Therapy of Prostate Cancer. *ACS Nano,* **4,** 3689-3696.

Kim MK, Huang ZY, Hwang PH, Jones BA, Sato N, Hunter S, Kim-Han TH, Worth RG, Indik ZK, and Schreiber AD (2003) Fcgamma receptor transmembrane domains: role in cell surface expression, gamma chain interaction, and phagocytosis. *Blood,* **101,** 4479-4484.

Kim S, Iizuka K, Aguila HL, Weissman IL, and Yokoyama WM (2000) In vivo natural killer cell activities revealed by natural killer cell-deficient mice. *Proc Natl Acad Sci U S A,* **97,** 2731-2736.

Kim Y, Cao Z, and Tan W (2008) Molecular assembly for high-performance bivalent nucleic acid inhibitor. *Proc Natl Acad Sci U S A,* **105,** 5664-5669.

Kipriyanov SM, Cochlovius B, Schafer HJ, Moldenhauer G, Bahre A, Le GF, Knackmuss S, and Little M (2002) Synergistic antitumor effect of bispecific CD19 x CD3 and CD19 x CD16 diabodies in a preclinical model of non-Hodgkin's lymphoma. *J Immunol,* **169,** 137-144.

Klussmann S (2006). *The Aptamer Handbook.* Wiley-VCH, Weinheim, Germany.

Kontermann RE (2005) Recombinant bispecific antibodies for cancer therapy. *Acta Pharmacol Sin,* **26,** 1-9.

Kontermann RE (2009) Strategies to extend plasma half-lives of recombinant antibodies. *BioDrugs,* **23,** 93-109.

Kugler M, Stein C, Kellner C, Mentz K, Saul D, Schwenkert M, Schubert I, Singer H, Oduncu F, Stockmeyer B, Mackensen A, and Fey GH (2010) A recombinant trispecific single-chain Fv derivative directed against CD123 and CD33 mediates effective elimination of acute myeloid leukaemia cells by dual targeting. *Br J Haematol,* **150,** 574-586.

Kulbachinskiy AV (2007) Methods for selection of aptamers to protein targets. *Biochemistry (Mosc),* **72,** 1505-1518.

Lai AZ, Abella JV, and Park M (2009) Crosstalk in Met receptor oncogenesis. *Trends Cell Biol,* **19,** 542-551.

Lanier LL, Le AM, Civin CI, Loken MR, and Phillips JH (1986) The relationship of CD16 (Leu-11) and Leu-19 (NKH-1) antigen expression on human peripheral blood NK cells and cytotoxic T lymphocytes. *J Immunol,* **136,** 4480-4486.

Lanier LL, Yu G, and Phillips JH (1989) Co-association of CD3 zeta with a receptor (CD16) for IgG Fc on human natural killer cells. *Nature,* **342,** 803-805.

Lazar GA, Dang W, Karki S, Vafa O, Peng JS, Hyun L, Chan C, Chung HS, Eivazi A, Yoder SC, Vielmetter J, Carmichael DF, Hayes RJ, and Dahiyat BI (2006) Engineered antibody Fc variants with enhanced effector function. *Proc Natl Acad Sci U S A,* **103,** 4005-4010.

Lee JF, Stovall GM, and Ellington AD (2006) Aptamer therapeutics advance. *Curr Opin Chem Biol,* **10,** 282-289.

Li M, Wirthmueller U, and Ravetch JV (1996) Reconstitution of human Fc gamma RIII cell type specificity in transgenic mice. *J Exp Med,* **183,** 1259-1263.

Li N, Ebright JN, Stovall GM, Chen X, Nguyen HH, Singh A, Syrett A, and Ellington AD (2009) Technical and biological issues relevant to cell typing with aptamers. *J Proteome Res,* **8,** 2438-2448.

Li P, Jiang N, Nagarajan S, Wohlhueter R, Selvaraj P, and Zhu C (2007) Affinity and kinetic analysis of Fcgamma receptor IIIa (CD16a) binding to IgG ligands. *J Biol Chem,* **282,** 6210-6221.

Loffler A, Kufer P, Lutterbuse R, Zettl F, Daniel PT, Schwenkenbecher JM, Riethmuller G, Dorken B, and Bargou RC (2000) A recombinant bispecific single-chain antibody, CD19 x CD3, induces rapid and high lymphoma-directed cytotoxicity by unstimulated T lymphocytes. *Blood,* **95,** 2098-2103.

Longati P, Bardelli A, Ponzetto C, Naldini L, and Comoglio PM (1994) Tyrosines1234-1235 are critical for activation of the tyrosine kinase encoded by the MET proto-oncogene (HGF receptor). *Oncogene,* **9,** 49-57.

Lopez-Albaitero A, Lee SC, Morgan S, Grandis JR, Gooding WE, Ferrone S, and Ferris RL (2009) Role of polymorphic Fc gamma receptor IIIa and EGFR expression level in cetuximab mediated, NK cell dependent in vitro cytotoxicity of head and neck squamous cell carcinoma cells. *Cancer Immunol Immunother,* **58,** 1853-1864.

Mack M, Riethmuller G, and Kufer P (1995) A small bispecific antibody construct expressed as a functional single-chain molecule with high tumor cell cytotoxicity. *Proc Natl Acad Sci U S A,* **92,** 7021-7025.

Mallikaratchy P, Liu H, Huang YF, Wang H, Lopez-Colon D, and Tan W (2009) Using aptamers evolved from cell-SELEX to engineer a molecular delivery platform. *Chem Commun (Camb),* 3056-3058.

Mani A, Roda J, Young D, Caligiuri M, Fleming G, Kaufman P, Brufsky A, Ottman S, Carson W, and Shapiro C (2009) A phase II trial of trastuzumab in combination with low-dose interleukin-2 (IL-2) in patients (PTS) with metastatic breast cancer (MBC) who have previously failed trastuzumab. *Breast Cancer Research and Treatment,* **117,** 83-89.

Mayer G (2009) The chemical biology of aptamers. *Angew Chem Int Ed Engl,* **48,** 2672-2689.

Mayer G, Ahmed MS, Dolf A, Endl E, Knolle PA, and Famulok M (2010) Fluorescence-activated cell sorting for aptamer SELEX with cell mixtures. *Nat Protoc,* **5,** 1993-2004.

McCall AM, Adams GP, Amoroso AR, Nielsen UB, Zhang L, Horak E, Simmons H, Schier R, Marks JD, and Weiner LM (1999) Isolation and characterization of an anti-CD16 single-chain Fv fragment and construction of an anti-HER2/neu/anti-CD16 bispecific scFv that triggers CD16-dependent tumor cytolysis. *Mol Immunol,* **36,** 433-445.

McNamara JO, Andrechek ER, Wang Y, Viles KD, Rempel RE, Gilboa E, Sullenger BA, and Giangrande PH (2006) Cell type-specific delivery of siRNAs with aptamer-siRNA chimeras. *Nat Biotechnol,* **24,** 1005-1015.

McNamara JO, Kolonias D, Pastor F, Mittler RS, Chen L, Giangrande PH, Sullenger B, and Gilboa E (2008) Multivalent 4-1BB binding aptamers costimulate CD8+ T cells and inhibit tumor growth in mice. *J Clin Invest,* **118,** 376-386.

Michalowski D, Chitima-Matsiga R, Held DM, and Burke DH (2008) Novel bimodular DNA aptamers with guanosine quadruplexes inhibit phylogenetically diverse HIV-1 reverse transcriptases. *Nucleic Acids Res,* **36,** 7124-7135.

Muller J, Freitag D, Mayer G, and Potzsch B (2008) Anticoagulant characteristics of HD1-22, a bivalent aptamer that specifically inhibits thrombin and prothrombinase. *J Thromb Haemost,* **6,** 2105-2112.

Muller J, Wulffen B, Potzsch B, and Mayer G (2007) Multidomain targeting generates a high-affinity thrombin-inhibiting bivalent aptamer. *Chembiochem,* **8,** 2223-2226.

Mullis K, Faloona F, Scharf S, Saiki R, Horn G, and Erlich H (1986) Specific enzymatic amplification of DNA in vitro: the polymerase chain reaction. *Cold Spring Harb Symp Quant Biol,* **51 Pt 1,** 263-273.

Murphy K, Travers P, and Walport M (2008). *Janeway's Immunobiology.* 7th ed. Garland Science, New York, USA.

Nakamura A, Kubo T, and Takai T (2008) Fc receptor targeting in the treatment of allergy, autoimmune diseases and cancer. *Adv Exp Med Biol,* **640,** 220-233.

Nimjee SM, Rusconi CP, and Sullenger BA (2005) Aptamers: an emerging class of therapeutics. *Annu Rev Med,* **56,** 555-583.

Nimmerjahn F and Ravetch JV (2006) Fcgamma receptors: old friends and new family members. *Immunity,* **24,** 19-28.

Nimmerjahn F and Ravetch JV (2008) Fcgamma receptors as regulators of immune responses. *Nat Rev Immunol,* **8,** 34-47.

Oney S, Nimjee SM, Layzer J, Que-Gewirth N, Ginsburg D, Becker RC, Arepally G, and Sullenger BA (2007) Antidote-controlled platelet inhibition targeting von Willebrand factor with aptamers. *Oligonucleotides,* **17,** 265-274.

Orava EW, Cicmil N, and Gariepy J (2010) Delivering cargoes into cancer cells using DNA aptamers targeting internalized surface portals. *Biochim Biophys Acta.*

Pacchiana G, Chiriaco C, Stella MC, Petronzelli F, De SR, Galluzzo M, Carminati P, Comoglio PM, Michieli P, and Vigna E (2010) Monovalency unleashes the full therapeutic potential of the DN-30 anti-Met antibody. *J Biol Chem,* **285,** 36149-36157.

Padmanabhan K, Padmanabhan KP, Ferrara JD, Sadler JE, and Tulinsky A (1993) The structure of alpha-thrombin inhibited by a 15-mer single-stranded DNA aptamer. *J Biol Chem,* **268,** 17651-17654.

Patel DJ, Suri AK, Jiang F, Jiang L, Fan P, Kumar RA, and Nonin S (1997) Structure, recognition and adaptive binding in RNA aptamer complexes. *J Mol Biol,* **272,** 645-664.

Pendergrast PS, Marsh HN, Grate D, Healy JM, and Stanton M (2005) Nucleic acid aptamers for target validation and therapeutic applications. *J Biomol Tech,* **16,** 224-234.

Peng CG and Damha MJ (2007) G-quadruplex induced stabilization by 2'-deoxy-2'-fluoro-D-arabinonucleic acids (2'F-ANA). *Nucleic Acids Res,* **35,** 4977-4988.

Powell MS and Hogarth PM (2008) Fc receptors. *Adv Exp Med Biol,* **640,** 22-34.

Que-Gewirth NS and Sullenger BA (2007) Gene therapy progress and prospects: RNA aptamers. *Gene Ther,* **14,** 283-291.

Radaev S, Motyka S, Fridman WH, Sautes-Fridman C, and Sun PD (2001) The structure of a human type III Fcgamma receptor in complex with Fc. *J Biol Chem,* **276,** 16469-16477.

Radaev S and Sun PD (2001) Recognition of IgG by Fcgamma receptor. The role of Fc glycosylation and the binding of peptide inhibitors. *J Biol Chem,* **276,** 16478-16483.

Raddatz MS, Dolf A, Endl E, Knolle P, Famulok M, and Mayer G (2008) Enrichment of cell-targeting and population-specific aptamers by fluorescence-activated cell sorting. *Angew Chem Int Ed Engl,* **47,** 5190-5193.

Ravetch JV and Perussia B (1989) Alternative membrane forms of Fc gamma RIII(CD16) on human natural killer cells and neutrophils. Cell type-specific expression of two genes that differ in single nucleotide substitutions. *J Exp Med,* **170,** 481-497.

Reali E, Guiliani AL, Spisani S, Moretti S, Gavioli R, Masucci G, Gambari R, and Traniello S (1994) Interferon-gamma enhances monoclonal antibody 17-1A-dependent neutrophil cytotoxicity toward colorectal carcinoma cell line SW11-16. *Clin Immunol Immunopathol,* **71,** 105-112.

Rimmele M (2003) Nucleic acid aptamers as tools and drugs: recent developments. *Chembiochem,* **4,** 963-971.

Robertson DL and Joyce GF (1990) Selection in vitro of an RNA enzyme that specifically cleaves single-stranded DNA. *Nature,* **344,** 467-468.

Roda JM, Parihar R, Magro C, Nuovo GJ, Tridandapani S, and Carson WE, III (2006) Natural killer cells produce T cell-recruiting chemokines in response to antibody-coated tumor cells. *Cancer Res,* **66,** 517-526.

Roda JM, Joshi T, Butchar JP, McAlees JW, Lehman A, Tridandapani S, and Carson WE (2007) The Activation of Natural Killer Cell Effector Functions by Cetuximab-Coated, Epidermal Growth Factor ReceptorΓÇôPositive Tumor Cells is Enhanced By Cytokines. *Clinical Cancer Research,* **13,** 6419-6428.

Roopenian DC and Akilesh S (2007) FcRn: the neonatal Fc receptor comes of age. *Nat Rev Immunol,* **7,** 715-725.

Rusconi CP, Scardino E, Layzer J, Pitoc GA, Ortel TL, Monroe D, and Sullenger BA (2002) RNA aptamers as reversible antagonists of coagulation factor IXa. *Nature,* **419,** 90-94.

Santulli-Marotto S, Nair SK, Rusconi C, Sullenger B, and Gilboa E (2003) Multivalent RNA aptamers that inhibit CTLA-4 and enhance tumor immunity. *Cancer Res,* **63,** 7483-7489.

Sayer NM, Cubin M, Rhie A, Bullock M, Tahiri-Alaoui A, and James W (2004) Structural determinants of conformationally selective, prion-binding aptamers. *J Biol Chem,* **279,** 13102-13109.

Sazani PL, Larralde R, and Szostak JW (2004) A small aptamer with strong and specific recognition of the triphosphate of ATP. *J Am Chem Soc,* **126,** 8370-8371.

Scherer L, Rossi JJ, and Weinberg MS (2007) Progress and prospects: RNA-based therapies for treatment of HIV infection. *Gene Ther,* **14,** 1057-1064.

Schmidt KS, Borkowski S, Kurreck J, Stephens AW, Bald R, Hecht M, Friebe M, Dinkelborg L, and Erdmann VA (2004) Application of locked nucleic acids to improve aptamer in vivo stability and targeting function. *Nucleic Acids Res,* **32,** 5757-5765.

Schrama D, Reisfeld RA, and Becker JC (2006) Antibody targeted drugs as cancer therapeutics. *Nat Rev Drug Discov,* **5,** 147-159.

Sefah K, Shangguan D, Xiong X, O'Donoghue MB, and Tan W (2010) Development of DNA aptamers using Cell-SELEX. *Nat Protocols,* **5,** 1169-1185.

Sen D (2008) The use of light to investigate and modulate DNA and RNA conformations. *Nucleic Acids Symp Ser (Oxf),* 11-12.

Shamah SM, Healy JM, and Cload ST (2008) Complex target SELEX. *Acc Chem Res,* **41,** 130-138.

Shangguan D, Li Y, Tang Z, Cao ZC, Chen HW, Mallikaratchy P, Sefah K, Yang CJ, and Tan W (2006) Aptamers evolved from live cells as effective molecular probes for cancer study. *Proc Natl Acad Sci U S A,* **103,** 11838-11843.

Shaw BR, Moussa L, Sharaf M, Cheek M, and Dobrikov M (2008) Boranophosphate siRNA-aptamer chimeras for tumor-specific downregulation of cancer receptors and modulators. *Nucleic Acids Symp Ser (Oxf),* **52,** 655-656.

Shaw JP, Fishback JA, Cundy KC, and Lee WA (1995) A novel oligodeoxynucleotide inhibitor of thrombin. I. In vitro metabolic stability in plasma and serum. *Pharm Res,* **12,** 1937-1942.

Shaw JP, Kent K, Bird J, Fishback J, and Froehler B (1991) Modified deoxyoligonucleotides stable to exonuclease degradation in serum. *Nucleic Acids Res,* **19,** 747-750.

Shibuya A (2003) Development and functions of natural killer cells. *Int J Hematol,* **78,** 1-6.

Singer H, Kellner C, Lanig H, Aigner M, Stockmeyer B, Oduncu F, Schwemmlein M, Stein C, Mentz K, Mackensen A, and Fey GH (2010) Effective elimination of acute myeloid leukemic cells by recombinant bispecific antibody derivatives directed against CD33 and CD16. *J Immunother,* **33,** 599-608.

Sliwkowski MX, Lofgren JA, Lewis GD, Hotaling TE, Fendly BM, and Fox JA (1999) Nonclinical studies addressing the mechanism of action of trastuzumab (Herceptin). *Semin Oncol,* **26,** 60-70.

Smyth MJ, Takeda K, Hayakawa Y, Peschon JJ, van den Brink MR, and Yagita H (2003) Nature's TRAIL--on a path to cancer immunotherapy. *Immunity,* **18,** 1-6.

Smyth MJ and Trapani JA (1995) Granzymes: exogenous proteinases that induce target cell apoptosis. *Immunol Today,* **16,** 202-206.

Somersalo K, Carpen O, and Saksela E (1994) Stimulated natural killer cells secrete factors with chemotactic activity, including NAP-1/IL-8, which supports VLA-4- and VLA-5-mediated migration of T lymphocytes. *Eur J Immunol,* **24,** 2957-2965.

Stellrecht CM and Gandhi V (2009) MET receptor tyrosine kinase as a therapeutic anticancer target. *Cancer Lett,* **280,** 1-14.

Stoltenburg R, Reinemann C, and Strehlitz B (2007) SELEX--a (r)evolutionary method to generate high-affinity nucleic acid ligands. *Biomol Eng,* **24,** 381-403.

Suzuki H, Ando T, Umekage S, Tanaka T, and Kikuchi Y (2010) Extracellular production of an RNA aptamer by ribonuclease-free marine bacteria harboring engineered plasmids: a proposal for industrial RNA drug production. *Appl Environ Microbiol,* **76,** 786-793.

Tabrizi MA and Roskos LK (2007) Preclinical and clinical safety of monoclonal antibodies. *Drug Discov Today,* **12,** 540-547.

Tahiri-Alaoui A, Frigotto L, Manville N, Ibrahim J, Romby P, and James W (2002) High affinity nucleic acid aptamers for streptavidin incorporated into bi-specific capture ligands. *Nucleic Acids Res,* **30,** e45.

Takayama H, La Rochelle WJ, Anver M, Bockman DE, and Merlino G (1996) Scatter factor/hepatocyte growth factor as a regulator of skeletal muscle and neural crest development. *Proc Natl Acad Sci U S A,* **93,** 5866-5871.

Takayama H, LaRochelle WJ, Sharp R, Otsuka T, Kriebel P, Anver M, Aaronson SA, and Merlino G (1997) Diverse tumorigenesis associated with aberrant development in mice overexpressing hepatocyte growth factor/scatter factor. *Proc Natl Acad Sci U S A,* **94,** 701-706.

Taub DD, Proost P, Murphy WJ, Anver M, Longo DL, van DJ, and Oppenheim JJ (1995) Monocyte chemotactic protein-1 (MCP-1), -2, and -3 are chemotactic for human T lymphocytes. *J Clin Invest,* **95,** 1370-1376.

Tavitian B, Duconge F, Boisgard R, and Dolle F (2009) In vivo imaging of oligonucleotidic aptamers. *Methods Mol Biol,* **535,** 241-259.

Taylor RJ, Chan SL, Wood A, Voskens CJ, Wolf JS, Lin W, Chapoval A, Schulze DH, Tian G, and Strome SE (2008) FcgammaRIIIa polymorphisms and cetuximab induced cytotoxicity in squamous cell carcinoma of the head and neck. *Cancer Immunol Immunother.*

Terunuma H, Deng X, Dewan Z, Fujimoto S, and Yamamoto N (2008) Potential role of NK cells in the induction of immune responses: implications for NK cell-based immunotherapy for cancers and viral infections. *Int Rev Immunol,* **27,** 93-110.

Toschi L and Janne PA (2008) Single-agent and combination therapeutic strategies to inhibit hepatocyte growth factor/MET signaling in cancer. *Clin Cancer Res,* **14,** 5941-5946.

Trapani JA and Smyth MJ (2002) Functional significance of the perforin/granzyme cell death pathway. *Nat Rev Immunol,* **2,** 735-747.

Tsang J and Joyce GF (1996) Specialization of the DNA-cleaving activity of a group I ribozyme through in vitro evolution. *J Mol Biol,* **262,** 31-42.

Tsarfaty I, Rong S, Resau JH, Rulong S, da Silva PP, and Vande Woude GF (1994) The Met proto-oncogene mesenchymal to epithelial cell conversion. *Science,* **263,** 98-101.

Tucker CE, Chen LS, Judkins MB, Farmer JA, Gill SC, and Drolet DW (1999) Detection and plasma pharmacokinetics of an anti-vascular endothelial growth factor oligonucleotide-aptamer (NX1838) in rhesus monkeys. *J Chromatogr B Biomed Sci Appl,* **732,** 203-212.

Tuerk C and Gold L (1990) Systematic evolution of ligands by exponential enrichment: RNA ligands to bacteriophage T4 DNA polymerase. *Science,* **249,** 505-510.

Ulevitch RJ (2004) Therapeutics targeting the innate immune system. *Nat Rev Immunol,* **4,** 512-520.

Umekage S and Kikuchi Y (2006) Production of circular form of streptavidin RNA aptamer in vitro. *Nucleic Acids Symp Ser (Oxf),* 323-324.

Valitutti S and Lanzavecchia A (1997) Serial triggering of TCRs: a basis for the sensitivity and specificity of antigen recognition. *Immunol Today,* **18,** 299-304.

van der Horst EH, Chinn L, Wang M, Velilla T, Tran H, Madrona Y, Lam A, Ji M, Hoey TC, and Sato AK (2009) Discovery of fully human anti-MET monoclonal antibodies with antitumor activity against colon cancer tumor models in vivo. *Neoplasia,* **11,** 355-364.

van Sorge NM, van der Pol WL, and van de Winkel JG (2003) FcgammaR polymorphisms: Implications for function, disease susceptibility and immunotherapy. *Tissue Antigens,* **61,** 189-202.

Vance BA, Huizinga TW, Wardwell K, and Guyre PM (1993) Binding of monomeric human IgG defines an expression polymorphism of Fc gamma RIII on large granular lymphocyte/natural killer cells. *J Immunol,* **151,** 6429-6439.

Vivier E, Nunes JA, and Vely F (2004) Natural Killer Cell Signaling Pathways. *Science,* **306,** 1517-1519.

Wallace ME and Smyth MJ (2005) The role of natural killer cells in tumor control--effectors and regulators of adaptive immunity. *Springer Semin Immunopathol,* **27,** 49-64.

White RR, Sullenger BA, and Rusconi CP (2000) Developing aptamers into therapeutics. *J Clin Invest,* **106,** 929-934.

Wolf E, Hofmeister R, Kufer P, Schlereth B, and Baeuerle PA (2005) BiTEs: bispecific antibody constructs with unique anti-tumor activity. *Drug Discov Today,* **10,** 1237-1244.

Wu J, Edberg JC, Redecha PB, Bansal V, Guyre PM, Coleman K, Salmon JE, and Kimberly RP (1997) A novel polymorphism of FcgammaRIIIa (CD16) alters receptor function and predisposes to autoimmune disease. *J Clin Invest,* **100,** 1059-1070.

Yarus M and Berg P (1970) On the properties and utility of a membrane filter assay in the study of isoleucyl-tRNA synthetase. *Anal Biochem,* **35,** 450-465.

Zhang YW, Su Y, Volpert OV, and Vande Woude GF (2003) Hepatocyte growth factor/scatter factor mediates angiogenesis through positive VEGF and negative thrombospondin 1 regulation. *Proc Natl Acad Sci U S A,* **100,** 12718-12723.

Zhou J, Soontornworajit B, Snipes MP, and Wang Y (2009a) Development of a novel pretargeting system with bifunctional nucleic acid molecules. *Biochem Biophys Res Commun,* **386,** 521-525.

Zhou J, Swiderski P, Li H, Zhang J, Neff CP, Akkina R, and Rossi JJ (2009b) Selection, characterization and application of new RNA HIV gp 120 aptamers for facile delivery of Dicer substrate siRNAs into HIV infected cells. *Nucleic Acids Res,* **37,** 3094-3109.

Zinnen SP, Domenico K, Wilson M, Dickinson BA, Beaudry A, Mokler V, Daniher AT, Burgin A, and Beigelman L (2002) Selection, design, and characterization of a new potentially therapeutic ribozyme. *RNA,* **8,** 214-228.

Zompi S and Colucci F (2005) Anatomy of a murder--signal transduction pathways leading to activation of natural killer cells. *Immunol Lett,* **97,** 31-39.

Zuker M (2003) Mfold web server for nucleic acid folding and hybridization prediction. *Nucleic Acids Research,* **31,** 3406-3415.

8 APPENDIX

8.1 Supporting information

Table 4: Specifications of CD16 DNA SELEX.

Target protein was CD16α-6His while CD16β-10His was applied for counterselection, tRNA served as unspecific competitor. PCR cycles needed to re-amplify a certain amount of aptamers were monitored and are highlighted. MTP, microtiter plate.

	DNA filter SELEX 01.09						*DNA filter SELEX 02.09*					
Round	*DNA conc. (µM)*	*Protein conc. (µM)*	*Neg. sel.*	*Counter sel. (µM)*	*tRNA (mg/ml)*	*No. of PCR cycles*	*DNA conc. (µM)*	*Protein conc. (µM)*	*Neg. sel.*	*Counter sel. (µM)*	*tRNA (mg/ml)*	*No. of PCR cycles*
1	1.66	1	none	0	0	**10**	1.66	1	none	0	0	**10**
2	0.62	1	filter	0	0	**15**	0.83	0.96	filter	1	0	**18**
3	1	1	filter	0	0	**20**	1	1	filter	1	0	**20**
4	1	1	filter	0	0.1	**17**	0.75	1	filter	1	0	**28**
5	1	0.8	filter	0	0.1	**20**	1	1	filter	1	0.1	**20**
6	1	0.8	filter	0	0.1	**10**	1	0.8	filter	0.8	0.1	**9**
7	0.62	0.6	filter	0	0.1	**10**	0.69	0.6	filter	0.6	0.1	**11**
8	0.69	0.6	filter	0	0.1	**7**	0.96	0.6	filter	0.6	0.1	**8**
9	0.55	0.6	filter	0	1	**10**	0.56	0.6	filter	0.6	1	**10**
	DNA MTP SELEX 01.09						*DNA MTP SELEX 02.09*					
10	0.7	0.2	none	1	0	**14**	0.7	0.2	none	1	0	**14**
11	0.5	0.2	none	1	0	**21**	0.6	0.2	none	1	0	**18**
12	1	0.2	filter	0	1	**11**	1	0.6	filter	0	1	**11**

Table 5: Specifications of CD16 DNA cell SELEX

Aptamers were selected alternating against recombinant Jurkat CD16α V158 or F158 cells with counterselection with maternal Jurkat E6.1 cells from the second round on and at least as many cells as for positive selection. tRNA served as unspecific competitor. PCR cycles needed to re-amplify a certain amount of aptamers were monitored and are highlighted.

	DNA cell SELEX 01.09						*DNA cell SELEX 02.09*					
Round	*DNA conc. (µM)*	*Cells ($x10^7$)*	*Allo-type*	*E6.1 cells ($x10^7$)*	*tRNA (mg/ml)*	*No. of PCR cycles*	*DNA conc. (µM)*	*Cells ($x10^7$)*	*Allo-type*	*E6.1 cells ($x10^7$)*	*tRNA (mg/ml)*	*No. of PCR cycles*
4	1	0.36	V158	0	0	**20**						
5	1	0.75	F158	0.75	0	**19**						
6	1	0.2	V158	0.85	0.1	**18**	1	0.36	V158	0	0	**20**
7	1	0.4	F158	0.75	0.1	**15**	1	0.75	F158	0.75	0	**17**
8	1	0.3	V158	0.75	1	**16**	1	0.2	V158	0.85	0.1	**16**
9	1	0.3	F158	0.3	1	**16**	1	0.4	F158	0.75	0.1	**15**
10							1	0.3	V158	0.75	1	**16**
11							1	0.3	F158	0.3	1	**16**

Table 6: Overview of the frequency of all selected CD16 DNA aptamers in all analysed pools.

Filter and MTP SELEX pools 01.09 and 02.09 analysed jointly

	Frequency of aptamers in the respective SELEX pool (%)							
Code	***filter R3***	***filter R5***	***filter R9***	***MTP R12***	***cell 01.09 R7***	***cell 01.09 R9***	***cell 02.09 R9***	***cell 02.09 R11***
single seq.	100	79	14	39	18	3	19	6
CLN0015	0	5	31	15	4	2	4	3
CLN0016	0	0	10	3	0	0	0	0
CLN0017	0	0	9	4	0	0	0	0
CLN0018	0	0	10	4	0	0	0	0
CLN0019	0	3	5	14	0	0	0	0
CLN0020	0	0	4	0	0	0	8	2
CLN0021	0	3	3	4	33	40	20	24
CLN0022	0	4	6	1	38	39	21	2
CLN0023	0	0	2	0	0	0	0	0
CLN0024	0	4	3	0	0	0	0	0
CLN0025	0	0	1	0	0	0	0	0
CLN0026	0	2	1	0	0	0	0	0
CLN0027	0	0	1	2	0	0	0	0
CLN0028	0	0	0	6	4	6	0	2
CLN0029	0	0	0	3	0	0	0	0
CLN0030	0	0	0	2	0	0	0	0
CLN0031	0	0	0	2	0	0	0	0
CLN0032	0	0	0	1	0	0	4	3
CLN0118	0	0	0	0	2	9	3	27
CLN0119	0	0	0	0	0	0	4	1
CLN0120	0	0	0	0	0	0	3	6
CLN0121	0	0	0	0	0	0	2	2
CLN0122	0	0	0	0	0	0	2	2
CLN0123	0	0	0	0	0	1	2	2
CLN0124	0	0	0	0	0	0	2	1
CLN0125	0	0	0	0	0	0	2	0
CLN0126	0	0	0	0	0	0	0	9
CLN0127	0	0	0	0	0	0	1	3
CLN0128	0	0	0	0	0	0	1	3

8.2 Abbreviations

A	Nucleotide adenosine
aa	Amino acid
ADCC	Antibody-dependent cellular cytotoxicity
Amp	Ampicillin
APS	Ammoniumpersulfate
BID	BH3-interacting domain death agonist protein
bp	Base pair
BSA	Bovine serum albumin

C	Nucleotide Cytidine
CAD	Caspase-activated deoxyribonuclease
CD	Cluster of differentiation
CD16	Fc γ receptor III
CRP	C-reactive protein
CTL	Cytotoxic T lymphocyte, T cell
(k)Da	(kilo-)Dalton
dH_2O	Distilled water
DNA	Deoxyribonucleic acid
dNTPs	Desoxyribonucleotide triphosphate
ECD	Extracellular domain
FACS	Fluorescence-activated cell sorting
FcγRIII	Fc γ receptor III or CD16
FcR	Fc receptor
FcRn	Neonatal Fc receptor
FCS	Fetal calf serum
G	Nucleotide Guanosine
GM-CSF	Granulocyte-macrophage colony stimulating factor
GPI	Glycosylphosphatidyl inositol
HGF / SF	Hepatocyte growth factor / scatter factor
HGFR / c-Met	HGF receptor
His	Histidin
HPLC	High performance liquid chromatography
iCAD	Inhibitor of caspase-activated deoxyribonuclease
ICAM-1	Intercellular adhesion molecule 1
IEF	Isoelectrical focussing
IFNγ	Interferon γ
IgG	Immunoglobuline G
IL-8/NAP-1	Interleukin 8
IP-10	IFN induced protein 10
ITAM	Immunoreceptor tyrosine-based activating motif
ITIM	Immunoreceptor tyrosine-based inhibitory motif
LB medium	Luria-Bertani medium
LFA-1	Lymphocyte function-associated antigen 1

LTN/ATAC	Lymphotactin
MCS	Multiple cloning site
MDC	Macrophage-derived chemokine
MIG	Monokine induced IFNγ
MIP-1α/β	Macrophage-inflammatory protein 1
NC	Nitrocellulose
NK cells	Natural killer cells
nt	nucleotide, length of single stranded oligonucleotide chain
OD	Optical density
PAGE	Polyacrylamide gel electrophoresis
PBMCs	Peripheral blood mononuclear cells (MNCs)
PCR	Polymerase chain reaction
PE	R-phycoerythrin
PI	Propidiumiodid
pI	Isoelectrical point
PVDF	Polyvinylidene fluoride
RANTES	Regulated on activation, normal T cell expressed and secreted
RNA	Ribonucleic acid
RT	Room temperature, ambient temperature
RTK	Receptor tyrosine kinase
rpm	Revolutions per minute
SA-PE	Streptavidin-R-phycoerythrin conjugate
sctb	Single chain triabody
SELEX	Systematic evolution of ligands by exponential enrichment
SDS	Sodium dodecylsulfate
T	Nucleotide Thymidine
tBID	Truncated BH3-interacting domain death agonist protein
TEMED	N,N,N,N'-Tetramethylendiamine
TNFα	Tumor necrosis factor α
Tris	Tris(hydroxymethyl)aminomethane
v/v	Volume per volume
w/v	Weight per volumen
ZAP-70	Z-associated protein of 70 kDa

8.3 List of figures

8.4 List of tables

8.5 Curriculum vitae

04/2011	PhD: *summa cum laude*
04/2008 – 04/2011	Doctorate at Merck KGaA and Technical University Darmstadt in Prof. Dr. Kolmar's group, Darmstadt, Germany
10/2005 - 03/2008	Master of Science in Molecular Biotechnology, Ruprecht-Karls University Heidelberg, Germany, major subject drug design, final grade 1.0 (A)
04/2007 - 12/2007	- Master thesis: protein interaction studies *in vivo* via fluorescense microscopy, grade 1.0 (A)
02/2006 - 07/2006	- Semester abroad at the University of Queensland, Institute of Molecular Biosciences, Brisbane, Australia. Internships: Tumour mutation screening & microarray analyses, grades 1.2 (A) & 1.0 (A)
10/2002 - 09/2005	Bachelor of Science in Molecular Biotechnology, Ruprecht-Karls University Heidelberg, Germany, final grade 1.3 (A)
03/2005 - 05/2005	- Project work „Parameter Estimation for Quantitative Analysis of the NF-kB Signal Transduction Pathway", grade 1.0 (A)
08/2001 - 05/2002	Community service, High school for blind people, Marburg, Germany
08/1992 - 07/2001	High school Gymnasium Philippinum, Marburg, Germany - Graduation (Abitur), final grade 1.5 (A) - Karl-von-Frisch award for excellent achievements in biology

8.6 Affirmations

Achim Boltz
Höhenstraße 14
60385 Frankfurt am Main

_____

Eidesstattliche Erklärung

Ich erkläre hiermit an Eides Statt, dass ich meine Dissertations selbstständig und nur mit den angegebenen Hilfsmitteln angefertigt habe.

_____

Achim Boltz
Höhenstraße 14
60385 Frankfurt am Main

_____

Erklärung

Ich erkläre hiermit, noch keinen Promotionsversuch unternommen zu haben.

_____

8.7 Acknowledgements

DANKSAGUNG

Mein erster Dank gilt Prof. Dr. Harald Kolmar für die Betreuung meiner Promotion an der TU Darmstadt sowie die enge und unkomplizierte Anbindung an die akademische Forschungslandschaft. Genauso danke ich Dr. Björn Hock für die stete Unterstützung bei Merck Serono, für Führung durch die Promotion und die optimalen Bedingungen.

Prof. Dr. H. Ulrich Göringer danke ich für die Übernahme des Zweitgutachtens.

Dr. Lars Toleikis und Ralf Günther danke ich für die durchweg gute Betreuung und Stimmung in ihren Laboren.

Ein herzlicher Dank geht auch an Birgit Piater, Laura Rhiel und Tan-Thanh Huynh für das Meistern aller gemeinsamen Aufgaben, Stefan Becker und Nils Bahl für Hilfe bei eigentlich allen Fragen und die gute Musik, Anja Lamack und Konstanze Waurisch für Hilfe auch über die Zellkultur hinaus, Angelika Helfrich für die c-Met Aptamere und ELISAs, Jürgen Schmidt für FACS Assistenz, beiden letzteren und der werksärztlichen Abteilung für Blutspenden, Christof Reusch und Frank Jährling für ADCC Assay Ansichten und Austausch, Jessica Dawson für Korrekturen sowie allen Kollegen bei Merck für das super Arbeitsklima und den vielen Spaß innerhalb und außerhalb des Labors.

An der TU Darmstadt gilt mein Dank Matin Daneschdar für Einführung in fortéBio Messungen, Barbara Diestelmann für organisatorische Hilfe aller Art, Martin Empting für Hilfe mit Origin sowie ganz besonders Janine Fritz, Gernot Habicht und allen anderen für fachlichen Austausch, Kino, Kicken, Kickern und co.

Meinen Eltern und Großeltern danke ich für die Unterstützung bis hierhin und das Mitfiebern außerhalb des Labors.

Ruth Doerner danke ich für ihren Rückhalt, alle Unterstützung und ihre Energie, die mir immer sehr geholfen hat.